SEMMELWEIS EGYETEM

DOKTORI ISKOLA

Ph.D. értekezések

3248.

TIAGO CHAVES DO CARMO

Neuroendokrinológia

című program

Programvezető: Dr. Fekete Csaba, tudományos főmunkatárs

Témavezető: Dr. Zelena Dóra, egyetemi tanár

Konzulens: Dr. Varga Viktor, tudományos főmunkatárs

REGULATORY EFFECTS OF MEDIAN RAPHE GABAERGIC AND DOPAMINERGIC NEURONS ON SOCIAL BEHAVIOR AND REINFORCEMENT- BASED LEARNING

PhD Thesis in Neuroscience

Tiago Chaves do Carmo

János Szentágothai Neurosciences Division

Semmelweis University

Supervisor:	Dóra Zelena, D.Sc
Consultant:	Viktor Varga, Ph.D
Official reviewers:	Gergely Zachar, Ph.D Petra Varró, Ph.D
Head of the Complex Examination Committee:	Gábor Varga, D.Sc
Members of the Complex Examination Committee:	Zsuzsanna Helyes, D.Sc Krisztina Káldi, D.Sc

Budapest

2025

Table of Contents

List of Abbreviations

5-HT: 5-hydroxytryptamine (serotonin)

AADC: Aromatic L-amino acid decarboxylase

AAV: Adeno-associated virus (also AAVs)

AAV2: Adeno-associated virus serotype 2

AAV8: Adeno-associated virus serotype 8

ABC: Avidin-biotin complex

ANOVA: Analysis of variance

AP: Anteroposterior (coordinates)

Aq: Cerebral aqueduct

ARRIVE: Animal Research: Reporting of In Vivo Experiments

B1-B9: Serotonergic clusters (e.g., B5, B8)

BIS: Behavioral inhibition system

bp: Base pair (product size unit)

BSA: Bovine serum albumin

CA2: Cornu Ammonis 2 (region of the hippocampus)

cDNA: Complementary DNA

ChR: Channelrhodopsin (mentioned as example)

CNO: Clozapine-N-oxide

Cre: Cyclization recombination enzyme

Ctx: Cortex

D1, D2, D3, D4, D5: Dopamine receptor subtypes

DA: Dopamine

DAB: 3,3'-Diaminobenzidine

DAT: Dopamine transporter

DAT-Cre: Dopamine transporter Cre recombinase driver line

DBH: Dopamine beta-hydroxylase

dHC: Dorsal hippocampus

Di: Diencephalon

DIO: Double-floxed inverted open reading frame

DREADD: Designer receptor exclusively activated by designer drugs (also DREADDs)

DRN: Dorsal raphe nucleus

DV: Dorsoventral (coordinates)

EDFS: Escape during footshock

EDST: Escape during stimulus

EDTA: Ethylenediaminetetraacetic acid

EPM: Elevated plus maze

ESFL: Escape failure

GABA: Gamma-aminobutyric acid

GAD67: Glutamate decarboxylase 67

GAPDH: Glyceraldehyde 3-phosphate dehydrogenase

GC/ml: Genome copies per milliliter

GPCRs: G-protein coupled receptors

HC: Hippocampus

hDAT: Human dopamine transporter

Hind: Hindbrain

hM3Dq: Excitatory DREADD receptor (human muscarinic M3 DREADD Gq-coupled)

hM4Di: Inhibitory DREADD receptor (human muscarinic M4 DREADD Gi-coupled)

hSyn: Human synapsin promoter

HTO: Hippocampal theta oscillation (also HTOs)

Hz: Hertz

i.p.: Intraperitoneal

IHC:Immunohistochemistry

IPN: Interpeduncular nucleus

ITI: Intertrial interval

LHA: Lateral hypothalamic area

LHb: Lateral habenula

LPO: Lateral preoptic area

loxP: Locus of X-over P1 (DNA sequence recognized by Cre recombinase)

LSD: Fisher's Least Significant Difference (post-hoc test)

mA: Milliamperes

ME: Median eminence

MDMA: 3,4-methylenedioxymeth-amphetamine, ecstasy

mg/kg: Milligrams per kilogram (dose unit)

Mid: Midbrain

ML: Mediolateral

mm: Millimeters

mPFC: Medial prefrontal cortex

MR: Median raphe

mRNA: messenger Ribonucleic Acid

MRN: Median raphe nucleus

MRR: Median raphe region

MS: Medial septal nucleus

mVTA: Medial ventral tegmental area

NAcc: Nucleus accumbens

NDB: Nucleus of the diagonal band

NGS: Normal goat serum

Ni-DAB: Nickel-enhanced 3,3'-diaminobenzidine

nl: Nanoliters

nM: Nanomolar (concentration unit)

OF: Open field

PAG: Periaqueductal gray

PBS: Phosphate-buffered saline

PCR: Polymerase chain reaction

PFA: Paraformaldehyde

PI: Prosocial Index

PRN: Paramedian raphe nucleus / Pontine reticular nucleus (Note context dependency)

PSTH: Peri-Stimulus Time Histogram

PVN: Paraventricular nucleus of the hypothalamus

PVT: Paraventricular nucleus of the thalamus

rAAV: Recombinant adeno-associated virus

REM: Rapid eye movement

RFP: Red fluorescent protein

RIT: Resident-intruder test

RNA: Ribonucleic acid

RT-PCR: Reverse transcription polymerase chain reaction

SAP: Stretched attend posture

SD: Social discrimination index / Standard deviation (Note context dependency)

SDT: Social discrimination test

SEM: Standard error of the mean

SI: Social preference index

SIT: Social interaction test

SNc: Substantia nigra pars compacta

SSRI: Selective serotonin reuptake inhibitor (also SSRIs)

Str: Striatum

SWR: Sharp-wave ripple (also SWRs)

TAE: Tris-acetate-EDTA buffer

TH: Tyrosine hydroxylase

TPH: Tryptophan hydroxylase

TXT: Triton X-100 (detergent)

μm: Micrometers

VGAT: Vesicular GABA transporter

VGAT-Cre: Vesicular GABA transporter Cre recombinase driver line

VGluT2: Vesicular glutamate transporter 2

VGluT3: Vesicular glutamate transporter 3

VTA: Ventral tegmental area

ZsGreen: Green fluorescent protein variant

1 Introduction

Mental illnesses constitute a major factor in disability worldwide, significantly impacting well-being and placing a substantial burden on societies (Arias, Saxena, & Verguet, 2022). Despite decades of extensive research, progress in uncovering innovative therapeutic mechanisms has been slow, partly due to the intricate nature of neuropsychiatric disorders (Shemesh & Chen, 2023). These conditions exhibit a wide spectrum of symptoms, ranging from mild manifestations to severe disruptions in everyday life. Complicating matters further, the classification of these disorders proves challenging as symptoms frequently overlap, making it difficult to delineate clear boundaries between distinct diseases.

This complexity is primarily attributed to the wide variety of neurotransmitters affected in each disorder. Serving as chemical messengers, neurotransmitters play an important role in information processing throughout the nervous system. They facilitate and enhance signaling between nerves and various cell types, influencing diverse functions such as movements, sleep patterns, memories, thoughts and emotions (Teleanu et al., 2022). Neuronal communication relies on distinct neurotransmitter systems-including cholinergic (attention and memory), glutamatergic (excitatory signaling), gamma-aminobutyric acid (GABA) containing (inhibitory signaling), dopaminergic (reward and motor control), serotonergic (mood and sleep), and histaminergic (arousal) pathways-each mediating unique physiological functions within the nervous system (Purves D., 2018).

One crucial element in this neurochemical balance is serotonin (5-hydroxytryptamine, 5-HT), a monoamine neurotransmitter synthesized from the amino acid tryptophan. Serotonin plays a crucial role in regulating mood, anxiety, sleep-wake cycles, and other behaviors (Kulikova & Kulikov, 2019). However, its influence is mediated through a remarkably diverse family of at least 14 receptor subtypes, allowing for functional specificity, and involves extensive interactions with other major neurotransmitter systems, creating a complex signaling landscape (Barnes & Sharp, 1999; Celada, Puig, & Artigas, 2013). Dysregulation of the serotonergic system has been strongly implicated in various psychiatric disorders, including depression and anxiety (Kulikova & Kulikov, 2019).

Complementing the modulatory role of serotonin, GABA (gamma-aminobutyric acid) is the primary inhibitory neurotransmitter in the mammalian brain (de Leon & Tadi, 2025). GABAergic neurons release GABA, which binds to GABAA and GABAB receptors on postsynaptic neurons (Sharma et al., 2023). GABAA receptors are ionotropic receptors that mediate fast inhibitory responses by increasing chloride conductance, while GABAB receptors are metabotropic receptors that couple to G proteins (GPCR) and modulate neuronal activity through slower intracellular signaling pathways (Allan & Harris, 1986; Sharma et al., 2023). GABAergic neurotransmission is essential for maintaining the balance between excitation and inhibition in the brain, and dysfunction in this system has been linked to anxiety disorders, epilepsy, and other neurological conditions (Lydiard, 2003; Treiman, 2001; Wong, Bottiglieri, & Snead, 2003).

In contrast to the inhibitory influence of GABA, dopamine (DA), a catecholamine neurotransmitter synthesized from the amino acid tyrosine, plays a critical role in reward, motivation, and motor control (Klein et al., 2019). The major dopaminergic pathways in the brain include the nigrostriatal pathway, crucial for motor control; the mesolimbic pathway, implicated in reward and motivation; and the mesocortical pathway, which plays a role in cognitive functions (Klein et al., 2019; Luo & Huang, 2016). However, overall impact of DA likely arises from its integrated activity across both these major pathways and other crucial regions, such as brainstem modulatory centers. DA exerts its effects by binding to a family of GPCRs, classified into D1-like (D1 and D5) and D2-like (D2, D3, and D4) receptors (Jaber et al., 1996; Klein et al., 2019). These receptors have distinct signaling mechanisms and are differentially distributed throughout the brain. Dysregulation of DA signaling has been strongly implicated in various neurological and psychiatric disorders, including Parkinson's disease, schizophrenia, and addiction (Klein et al., 2019).

While numerous brain regions contribute to these neurological and psychiatric conditions, the median raphe region (MRR) is emerging as a particularly crucial hub. Although historically less studied than areas like the prefrontal cortex (PFC) or amygdala, its importance is increasingly recognized. Indeed, very recent work underscores its crucial role, proposing the MRR functions as a 'subcortical switchboard' that orchestrates transitions between fundamental behavioral states like perseveration, exploration, and

disengagement, highlighting the coordinated action of its serotonergic, GABAergic, and glutamatergic populations (Ahmadlou et al., 2025). This newly proposed framework reinforces the significance of understanding the complex role of MRR in regulating behaviors relevant to neuropsychiatric disorders. While often primarily associated with serotonergic function, the MRR contains diverse neuronal populations, including significant GABAergic and glutamatergic populations as well as dopaminergic neurons – the latter two being the focus of this dissertation. This work, initiated prior to the publication of the switchboard model, investigates the roles of GABAergic and dopaminergic neurons within the MRR. We examine, using various behavioral paradigms, the effects of manipulating these specific populations on anxiety-related behaviors, social interactions, spatial learning and memory, and reward-based learning. Our aim is to expand the understanding of the MRR beyond its classical serotonergic role and elucidate, how these distinct non-serotonergic populations contribute to the neural circuits underlying complex behaviors, findings that may now be viewed through the lens of behavioral state regulation.

1.1 The median raphe region (MRR)

The MRR plays an integral role in various cognitive and behavioral functions (Hensler, 2006; Vertes & Kocsis, 1997), including memory consolidation (Wang et al., 2015) and stress response (Andrade, Zangrossi, & Graeff, 2013; Graeff et al., 1996). Although the MRR is often associated with its dense population of serotonergic neurons (Andrade, Zangrossi, & Graeff, 2013), it is crucial to recognize the diversity of its neuronal populations. Beyond serotonergic cells, the MRR encompasses a spectrum of other neuron types (Sos et al., 2017), whose specific contributions to behavior remain largely unexplored.

Furthermore, it is noteworthy that the dorsal raphe nucleus (DRN) contains a larger population of serotonergic neurons, making it the primary source of serotonergic neurons in the brain (Andrade & Haj-Dahmane, 2013; Pollak Dorocic et al., 2014; Vertes, Fortin, & Crane, 1999). Consequently, the DRN was considered primarily responsible for integrating limbic-cortical information to regulate mood, reward valuation, and stress adaptation. In contrast, the MRR shows functional specialization; while often linked to modulating hippocampal-dependent memory and phasic behavioral responses (Balazsfi

et al., 2018; Commons, Connolley, & Valentino, 2003; Kawai et al., 2022; Wang et al., 2023), its crucial to recognize its distinct roles, exemplified by the fact that the suprachiasmatic nucleus receives its serotonergic input almost exclusively from the MRR, thereby positioning the MRR as a key modulator of circadian phase-shifting in response to external influences (Glass et al., 2003; Morin, 1999).

1.1.1 Anatomy of the median raphe region

The median raphe nucleus (MRN), also known as the nucleus centralis superior in humans, is situated within the ponto-mesencephalic tegmentum, specifically spanning the border between the rostral pons and midbrain, just caudal to the decussation of the superior cerebellar peduncle (Hornung, 2003). Due to the narrow nature of the nucleus, the paramedial raphe region (PMR) is often co-manipulated during experiments (Paxinos G., 2007). Therefore, it is more correct to speak of the MRR, which includes the nucleus and its surrounding areas (Sos et al., 2017). It is a complex structure with a heterogeneous neuronal population. Apart from the serotonergic neurons (mostly in the central, MRN part), the MRR is now known to also contain significant numbers of GABAergic, glutamatergic, and even a small population of dopaminergic neurons. This neurochemical diversity suggests a multifaceted role for the MRR in regulating brain function, extending beyond its well-established serotonergic functions.

Based on the anatomical description provided by Dahlstroem and Fuxe (1964), the MRN is classified as serotonergic clusters B5 and B8. This structure, alongside the DRN, the caudal linear nucleus, and the oral pontine nucleus, collectively forms the rostral serotonergic system (Tork, 1990) (Fig.1).

The central core contains densely packed small neurons with relatively short dendrites, many oriented parallel to the midsagittal plane. Conversely, the PMR contains more dispersed neurons lacking a specific orientation (Tork, 1990).

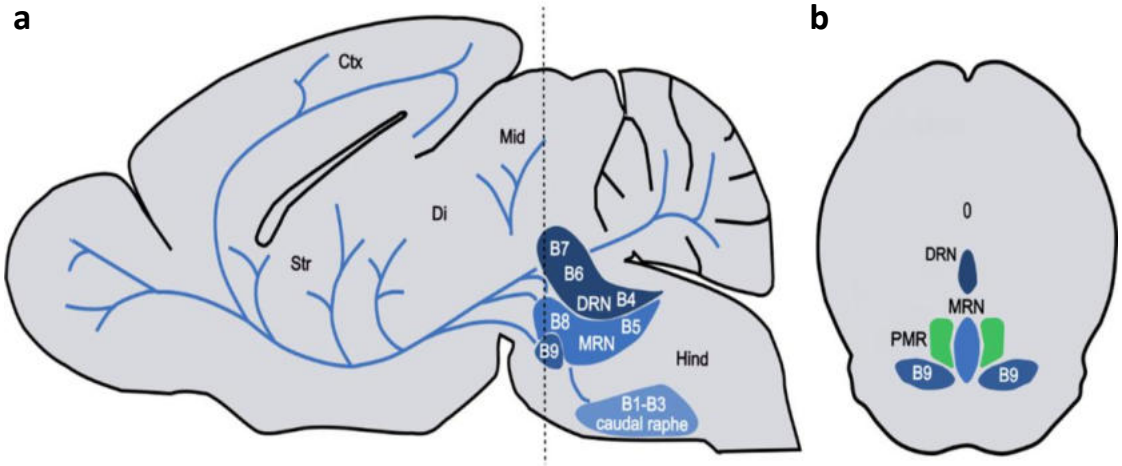

Figure 1 - Anatomy of brainstem raphe nuclei in mouse: (a) Sagittal schematic of the mouse brain depicting serotonergic raphe nuclei (B1-B9) and projections to the forebrain. (b) A coronal schematic corresponding to the dotted line in A is shown with B8 and B9 labeled. DRN, dorsal raphe nucleus (dark blue); MRN, median raphe nucleus (blue); PMR: paramedian raphe region (green); caudal raphe, raphe pallidus (B1), raphe obscurus (B2); raphe magnus (B3); raphe obscurus, dorsolateral part (B4); median raphe nucleus, caudal part (B5); dorsal raphe nucleus, caudal part (B6); dorsal raphe nucleus principal, rostral part (B7); caudal linear nucleus (B8); the supralemniscal serotonergic cell group (B9); Di, diencephalon; Mid, midbrain; Hind, hindbrain; Ctx, cortex; Str, striatum. Schematic representation adapted from (Niederkofler, Asher, & Dymecki, 2015) and extracted from (Tork, 1990).

1.1.2 Neuronal Composition of the Median Raphe Region

While historically the focus has been on serotonergic neurons, recent studies have revealed a much more diverse and complex neuronal composition of MRR (Sos et al., 2017), characterized by the expression of specific neurotransmitters and transporters, and corresponding to multifaceted functionality.

Serotonergic neurons, long considered the primary population in the MRR, actually constitute only a small percentage (approximately 8.5%) of the total MRR population (Sos et al., 2017). These neurons synthesize and release 5-HT, a monoamine neurotransmitter involved in regulating mood, appetite, sleep, and numerous other physiological and psychological processes. Despite their relatively small numbers, these serotonergic neurons have extensive projections throughout the brain, allowing them to exert widespread modulatory effects.

The majority of MRR neurons are GABAergic (approximately 61%) (Sos et al., 2017). These neurons utilize GABA, the primary inhibitory neurotransmitter in the

mammalian central nervous system. The high proportion of GABAergic neurons suggests that inhibitory signaling plays a crucial role in MRR function, potentially modulating the activity of local neurons as well as distant targets through direct, long-term projections.

A significant portion of MRR neurons express vesicular glutamate transporters, which are required for the packaging and release of glutamate, the main excitatory neurotransmitter in the brain. Interestingly, the MRR contains neurons expressing either vesicular glutamate transporter 2 or 3 (VGluT2 or VGluT3) (Sos et al., 2017; Szonyi et al., 2019; Xu et al., 2021), two distinct subtypes of these transporters. The presence of these glutamatergic neurons adds another layer of complexity to MRR circuitry and function.

The neurochemical complexity of the MRR is further increased by colocalization between these different markers. VGluT2 and GABAergic neurons do not colocalize, representing entirely separate populations. Similarly, VGluT2-positive neurons do not colocalize with serotonergic neurons (Xu et al., 2021). However, VGluT3-positive neurons can colocalize with serotonergic (5-HT positive) neurons (Amilhon et al., 2010; Sos et al., 2017), suggesting the potential for glutamate co-release from some serotonergic projections. This colocalization indicates that these neurons can utilize both serotonin and glutamate as signaling molecules, allowing for more complex and nuanced modulation of their target regions. Conversely, neurons co-expressing GABAergic markers (like glutamate decarboxylase (GAD) a rate limiting synthesis enzyme; or VGAT, packing the neurotransmitter into vesicles) and serotonin are extremely rare within the midbrain raphe nuclei, including the MRR, according to dual-labeling studies (Stamp & Semba, 1995).

Adding to this already diverse neuronal composition, a small population (around 1%) of dopaminergic neurons has also been identified within the MRR (Jahanshahi, Steinbusch, & Temel, 2013). The presence and production of DA in the rat MRR has been consistently demonstrated across multiple studies (Jahanshahi, Steinbusch, & Temel, 2013; Kocabicak et al., 2015; Loullis, Felten, & Shea, 1979; Ochi & Shimizu, 1978; Saavedra, Grobecker, & Zivin, 1976; Trulson, Cannon, & Raese, 1985), including evidence of glial DA uptake (Liesi et al., 1981). The presence of dopaminergic neurons in the MRR is particularly noteworthy as DA systems are typically associated with specific nuclei such as the substantia nigra pars compacta (SNc) and ventral tegmental

area (VTA). While the existence of this MRR population is confirmed, our understanding of the functional roles of raphe DA neurons largely stems from research on the adjacent DRN. Studies focusing on the DRN have established these neurons as critically involved in modulating affective states and behaviors, particularly in response to social isolation and interaction (Matthews GA, 2021; Matthews et al., 2016). Consequently, the specific contribution of the MRR DA population remains largely unexplored.

1.1.3 Afferent and Efferent Connections of MRR Neuronal Populations

The diverse neuronal populations within the MRR form complex patterns of connectivity with numerous brain regions, allowing the MRR to influence and be influenced by multiple neural systems. These connections vary depending on the specific neuronal type, creating parallel, yet distinct circuits that serve different functions.

1.1.3.1 Connectivity of Serotonergic Neurons: Inputs and Outputs

MRR serotonergic neurons receive afferent input from various regions, including cortical areas like the cingulate cortex, as well as subcortical structures in the forebrain and hypothalamus (Azmitia & Segal, 1978; Behzadi et al., 1990). Regulatory inputs to these serotonergic neurons arise from the lateral habenula (LHb) and the interpeduncular nucleus, notably via excitatory amino acid pathways (Behzadi et al., 1990). More recent whole-brain mapping confirmed direct monosynaptic inputs to MRR serotonergic neurons from various regions, including the PFC, LHb, and hypothalamus (Pollak Dorocic et al., 2014). These inputs are particularly relevant because the LHb has been implicated in aversive processing and mood regulation, while the interpeduncular nucleus is involved in stress responses.

Regarding efferent projections, the MRR contributes to ascending serotonergic pathways projecting to limbic brain regions, which are crucial for regulating emotional behaviors (Beck et al., 2004; Paul & Lowry, 2013). The MRR projections are located primarily in the medial aspects of the brainstem, forebrain, and select cortical areas (Azmitia & Segal, 1978; Vertes, Fortin, & Crane, 1999).

Two primary types of serotonergic axons have been identified: thin axons with small varicosities, and thicker axons with large, rounded or oval varicosities (Kosofsky & Molliver, 1987; Mamounas & Molliver, 1988; Tork, 1990). While both axon types may

innervate the same brain regions, their distribution and synaptic density can vary considerably. For example, both types are present in the cerebral cortex, but the dentate gyrus receives a particularly high concentration of fibers with large varicosities originating from the MRR, forming "basket fibers" around granule cells (Kosofsky & Molliver, 1987; Mamounas & Molliver, 1988; Tork, 1990). Importantly, these morphologically distinct axon types show differential vulnerability to neurotoxic amphetamines like 3,4-methylenedioxymethamphetamine (MDMA or ecstasy) and fenfluramine (Mamounas & Molliver, 1988; Mamounas et al., 1991; Molliver et al., 1990). These drugs function as serotonin releasers by disrupting terminal handling: they inhibit the vesicular monoamine transporter, increasing cytosolic serotonin, and reverse the serotonin transporter, causing non-vesicular release (Brown & Molliver, 2000; Molliver et al., 1990). This mechanism explains why thin axons are more susceptible to the neurotoxicity, while thicker, large-varicosity axons are more resistant (Mamounas & Molliver, 1988; Mamounas et al., 1991).

The MRR contributes significantly to the mesolimbic serotonergic pathway, projecting to the septum and hippocampus (HC), unlike the DRN, which primarily projects to the amygdala, nucleus accumbens (NAcc), and ventral pallidum (Commons, 2016). Extensive research has focused on this pathway, revealing the involvement of the MRR in anxiety, depression, and the regulation of circadian rhythms; this regulatory process is understood to be directly modulated by the MRR, partly through its known influence on hippocampal theta rhythm generation (Andrade & Graeff, 2001; Andrews et al., 1997; Bland, Bland, & MacIver, 2016; Ciarleglio, Resuehr, & McMahon, 2011; Dos Santos, de Andrade, & Zangrossi, 2005; Leander, Vrang, & Moller, 1998; Lopez Hill et al., 2013; Morin, 2013; Numasawa et al., 2017; Ohmura et al., 2014).

1.1.3.2 Glutamatergic and GABAergic Connections

GABAergic and glutamatergic MRR neurons receive inputs from overlapping regions, including the LHb, periaqueductal gray (PAG), pons, and the MRR itself. However, the relative strength and functional significance of these inputs differ. Xu et al. (2021) found that glutamatergic neurons receive stronger inputs from the pontine reticular nucleus (PRN) and pons, while GABAergic neurons receive proportionally more inputs from the LHb. Conversely, Szonyi et al. (2019) showed that the LHb provides the majority (~40%) of monosynaptic inputs to VGluT2+ glutamatergic neurons. These

differences likely stem from methodological variations: Xu et al. (2021) quantified input proportions across all regions, while Szőnyi et al. focused on absolute input density from specific regions. Thus, while LHb input is substantial for both populations, it is the dominant source for VGluT2+ neurons.

Furthermore, GABAergic MRR neurons receive inputs from distinct LHb subregions that participate in processing diverse motivational signals (Hikosaka, 2010; Proulx, Hikosaka, & Malinow, 2014) (Fig.2). While the LHb integrates information related to aversive experiences, its subregions show marked functional heterogeneity (Congiu et al., 2019; Hikosaka, 2010; Proulx, Hikosaka, & Malinow, 2014) (It is important to note that while this diagram highlights overlapping regions, many of these connections are not strictly reciprocal, with significant input/output biases for specific pathways (Xu et al., 2021)).

Recent studies demonstrated that approximately 10% of LHb neurons actually exhibit inhibitory responses to aversive stimuli, particularly those clustered in the medial division (Congiu et al., 2019). This functional diversity is further supported by evidence that LHb receives convergent inputs from multiple systems, including reward-related dopaminergic/serotonergic projections from midbrain structures (Hikosaka, 2010; Proulx, Hikosaka, & Malinow, 2014) and glutamatergic inputs from the lateral hypothalamus linked to motivational and homeostatic states (Poller et al., 2013). The LHb subregions differentially connect with downstream targets, forming parallel circuits that process both aversive and rewarding information in a context-dependent manner (Hikosaka, 2010; Proulx, Hikosaka, & Malinow, 2014). Rather than simply encoding aversion, GABAergic MRR neurons likely participate in orchestrating responses to behaviorally significant stimuli based on their valence, motivational relevance, and contextual factors. This complexity suggests these neurons may contribute to adaptive behavioral flexibility rather than serving a unidimensional role in aversive processing.

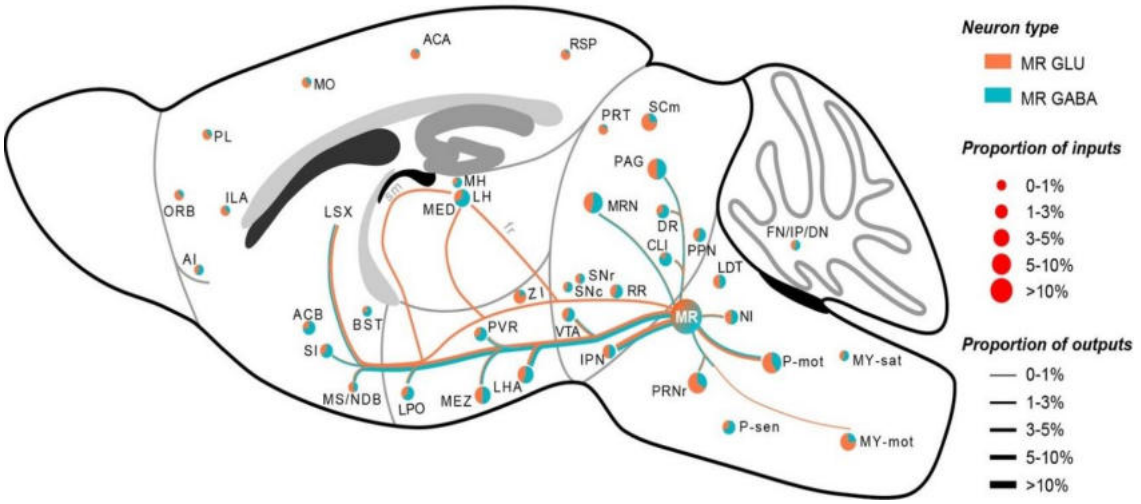

Figure 2 - Diagram illustrating the input and output connections of glutamatergic and GABAergic median raphe (MR) neurons in the mouse brain. Pie charts illustrate the inputs within various brain regions, with colors representing postsynaptic neuron types and size indicating proportion values. The lines symbolize the outputs within each brain region, with variations in color denoting different neuron types, while the thickness of the lines corresponds to the relative proportion. Figure extracted and adapted from Xu et al., 2021, where the meaning of abbreviations can be also found.

Regarding the outputs of glutamatergic and GABAergic MRR neurons, Xu et al. (2021) identified ascending projections to the forebrain and midbrain, as well as varying degrees of descending projections to the pons and medulla. These neurons predominantly target midline structures such as the paraventricular nucleus of the thalamus (PVT), median eminence (ME), lateral hypothalamic area (LHA), and lateral preoptic area (LPO). They also project to forebrain regions like the lateral septal complex, medial septal nucleus (MS), nucleus of the diagonal band (NDB), and LHb, with dense projections to the hypothalamus and midbrain, including the LHA and VTA.

Xu et al. (2021) found that GABAergic MRR neurons preferentially target neighboring regions, with the interpeduncular nucleus (IPN) identified as the most prominent recipient, receiving nearly 30% of their total output. However, their projections are not limited to these areas. This more extensive projection pattern suggests that they might have broader influences than initially thought, potentially contributing to inhibitory control across multiple brain regions.

1.1.3.3 Dopaminergic Neurons: A Poorly Understood Population

Little is known about the connectivity of dopaminergic neurons due to their sparse distribution within the MRR. However, it is believed that they may receive inputs from the VTA or the medial aspect of the SNc (Kitahama et al., 2000; Ogawa et al., 2014). The output targets of these dopaminergic MRR neurons remain largely unexplored, representing a significant gap in our understanding of MRR circuitry. The presence of this small, but distinct dopaminergic population raises intriguing questions about their functional role and their potential interactions with the more abundant, local serotonergic, GABAergic, and glutamatergic neurons. While classical dopamine systems are well-known for their roles in reward processing, motor control, and motivation, the specific contribution of MRR dopaminergic neurons to behavior and physiological functions is currently unknown.

1.1.4 Functional aspects

Building on the established role of MRR in arousal, attention, stress responses, and emotional regulation, this section will delve into the specific functional contributions of its diverse neuronal populations. The recent conceptualization of the MRR as a 'subcortical switchboard' governing perseverative, exploratory, and disengaged states (Ahmadlou et al., 2025) provides a compelling new framework for integrating these diverse functions and emphasizes the need to understand how different MRR cell types contribute to behavioral control.

1.1.4.1 Modulation of Locomotion

Among the pioneering studies that explored the functional significance of the MRR, key findings revealed that its inactivation through electrolytic lesions resulted in increased locomotor activity and responsiveness to environmental changes (Geyer et al., 1976; Jacobs & Cohen, 1976; Jacobs, Wise, & Taylor, 1974; Srebro & Lorens, 1975; Wirtshafter & Asin, 1982). While the hyperactive effect does not seem to arise from the destruction of serotonergic neurons, as it cannot be replicated by serotonin-depleting drugs, it is believed that the nonserotonergic transmission is associated with this hyperactive effect (Shim, Stratford, & Wirtshafter, 2014; Wirtshafter, Klitenick, & Asin, 1988). Microinjection of GABAA receptor agonists (muscimol or baclofen) or the metabotropic glutamate receptor antagonist pBB-PZDA directly into the MRR also

increased locomotor activity, accompanied by increased DA metabolism in the NAcc. Interestingly, while the D2 receptor blockade with haloperidol suppressed DA-mediated locomotor activity (induced by drugs like amphetamine), it does not affect the hyperlocomotion induced by GABAergic or glutamatergic modulation within the MRR. This is because the D2 receptors are primarily located on dopaminergic neurons and within the dopaminergic pathways, while the GABAergic and glutamatergic manipulations within the MRR are acting through separate, non-dopaminergic pathways to influence locomotor activity. This suggests that the MRR may regulate locomotion through multiple, potentially independent, pathways or mechanisms (Shim, Stratford, & Wirtshafter, 2014).

1.1.4.2 Modulation of Aversive Behavior

Intermittent optogenetic stimulation of the dorso-central area of the MRR at a 50 Hz theta-burst frequency induced agitated behavior in a conditioning paradigm. The authors interpreted this agitation as an aversive response, as it was associated with stimulation-induced running (a characteristic behavior observed in mice after electric shocks (Haller et al., 2014)) as well as activation of the paraventricular nucleus (PVN) and PAG, both regions associated with the processing of aversive responses (Balazsfi et al., 2017). Interestingly, this aversive experience did not elicit an immediate, but rather a delayed fear memory, as evidenced by the absence of freezing behavior (a characteristic of contextual fear) when the animals were re-exposed to the conditioning cage one day, but presence of freezing seven days after the optogenetic stimulation (Balazsfi et al., 2017). This may reflect the time required for consolidation of aversive memory traces. The initial MRR stimulation likely induced neural plasticity in downstream structures, such as the HC and amygdala, that are crucial for contextual fear learning. These plastic changes, potentially involving alterations in gene expression or synaptic strength, may require several days to fully manifest and reach the threshold necessary for overt behavioral expression of fear (freezing). Alternatively, the initial aversive experience may have been subthreshold for immediate freezing, but created a latent fear memory that was strengthened over time. Another possibility is that it is a state-dependent memory that is only triggered by a specific physiological state.

A later study by Szonyi et al. (2019) expanded these findings by demonstrating that VGluT2-positive neurons in the MRR directly innervate DA cells in the medial VTA

(mVTA) which is associated with negative rewards predictions. This research utilized simultaneous viral injections of tracers into the MRR and LHb, another region that regulates aversion via its projections to the mVTA. The analysis revealed that both MRR and LHb VGluT2 neurons specifically targeted mVTA DA cells. Additionally, VGluT2-positive terminals from the MRR were found to form synaptic contacts with mVTA DA neurons that project to brain areas involved in processing negative predictions, further supporting the role of the MRR in modulating aversive behaviors through its glutamatergic influences on mVTA DA signaling.

1.1.4.3 Modulation of Memory and Learning

The HC plays a central role in learning and memory, particularly in the encoding and consolidation of spatial information. This region is characterized by specialized "place cells," neurons that exhibit location-specific firing patterns, enabling the brain to create internal maps of the environment (Burgess, Maguire, & O'Keefe, 2002). Furthermore, the HC exhibits distinct oscillatory activity patterns, including theta and ripple oscillations, which are prominently observed during different sleep stages and have been implicated in memory consolidation processes (Buzsaki, 2002). While the complexity of HC function and its regulation are still being elucidated, recent research has begun to shed light on the significant influence of the MRR, highlighting its critical role not only in aversive behavior but also in memory consolidation. Electrophysiological studies have revealed a complex interplay between MRR activity and HC oscillations. Wang et al. (2015) observed an inverse relationship between non-selective MRR activity and HC sharp-wave ripples (SWRs): stimulating all MRR neurons suppressed SWRs, while inhibiting all MRR neurons increased SWR activity. Importantly, in the same study it has also been shown that not the serotonergic, rather other neurons are responsible for this phenomenon. Further research has investigated the influence of MRR on hippocampal theta oscillations (HTOs) during rapid eye movement (REM) sleep, another state crucial for memory processing. The ability of the MRR to modulate HTOs was already demonstrated in previous studies (Maru, Takahashi, & Iwahara, 1979; Varga et al., 2002; Vertes & Kocsis, 1997). Build upon this, Huang, Ikemoto and Wang (2022), showed that optogenetic stimulation of all MRR neurons at theta frequency amplified HTO amplitude. Interestingly, different MRR neuronal subpopulations exhibited distinct activity patterns during HTOs. Moreover, even describing a homogenous behavior for

MRR-GABA and MRR-VGluT3 is an oversimplification. While some GABAergic neurons increased their firing rate, and some VGluT3 neurons decreased their firing, phase-locked to the HC theta rhythm, others displayed more diverse patterns (Jelitai et al., 2021). Though GABAergic MRR neurons do not project directly to the HC, their influence on HTOs is likely mediated indirectly, via local circuits involving, among others, VGluT3 containing and serotonergic neurons.

Prior studies have generally suggested that MRR exerts an inhibitory influence on HC activity, as lesions or pharmacological inhibition of the MRR lead to increased HC neuronal activity and enhanced theta oscillations (Bland, Bland, & MacIver, 2016; Crooks, Jackson, & Bland, 2012; Maru, Takahashi, & Iwahara, 1979; Varga et al., 2002; Vinogradova et al., 1999). However, the influence of MRR is likely more complex. Domonkos et al. (2016) demonstrated that MRR neurons exhibit diverse firing patterns and complex interactions with HC oscillations, suggesting a multifaceted role. The findings of Wang et al. (2015) and Huang, Ikemoto and Wang (2022), combined with the cell-type-specific data from Jelitai et al. (2021), point to a model where different MRR neuronal populations exert distinct, potentially opposing, influences on hippocampal circuits, allowing for fine-grained control of HC activity and its role in memory processing.

1.1.4.4 Regulation of Social and Aggressive Behavior

Social behavior, which includes interactions such as cooperation and bonding, along with aggressive behavior, involving actions like threat displays and attacks, are fundamental aspects of animal life, including humans (Chen & Hong, 2018; Hashikawa et al., 2018). These behaviors are not simply opposing forces; they are intricately orchestrated by a complex interplay of brain regions and neural circuits. Key areas within the limbic system - a collection of structures deeply involved in emotions and memory - are essential for regulating these behaviors. For instance, the amygdala is essential for processing the emotional significance of social stimuli, helping us recognize and respond to threats or friendly cues (Gothard & Fuglevand, 2022). The HC, crucial for memory formation, contributes to social recognition, allowing us to remember individuals and our past interactions with them (Wang & Zhan, 2022). Notably, specific sub regions within the HC, like area CA2, have been implicated in encoding social memories (Wang & Zhan, 2022). Beyond the limbic system, cortical regions like the PFC, particularly its medial

portion (mPFC) in rodents, are heavily involved in higher-order cognitive functions that contribute to social behavior, such as decision-making and impulse control (Kim & Lee, 2011). Understanding how these different brain regions interact and how their activity is modulated by neurotransmitters is vital for addressing dysfunctions in social and aggressive behavior, which can manifest in various psychiatric disorders (e.g., autism, schizophrenia (Cowen, 2008; Kroeze & Roth, 1998; Mann, 2003)).

One crucial area implicated in regulating aggression is the midbrain raphe nuclei, specifically the MRR and the DRN. These regions are the primary sources of serotonin in the brain, heavily implicated in mood regulation. Early research pointed towards a clear role for serotonin in suppressing aggression. Lesions of the raphe nuclei, particularly the DRN, were shown to increase aggression in mice (Kostowski et al., 1975). Furthermore, depleting serotonin levels pharmacologically with drugs like fenclonine induced aggressive behaviors in rats (Miczek et al., 1975). In line with this, it was shown that social dominance is positively correlated with increased activity of 5-HT neurons (Kim et al., 2015; Kiser et al., 2012), while reduced serotonin levels are associated with social withdrawal (Higley et al., 1996). Conversely, enhanced serotonin activity has been linked to increased social cooperation and contact (Anstey et al., 2009; Paula et al., 2015), as well as affiliative behaviors (aan het Rot et al., 2006; Tse & Bond, 2002). This suppressive effect of serotonin on aggression is also observed in humans, where low serotonin levels are associated with increased aggression, and serotonin-enhancing drugs can reduce such behaviors (Greenberg & Coleman, 1976).

Despite the evidence linking serotonin to aggression, the specific role of the MRR remains debated. While some studies have shown that lesions of the MRR do not affect aggression (Jacobs & Cohen, 1976), others suggest a more nuanced role. For instance, stimulating the DRN, but not the MRR, inhibited aggressive behavior in rats (Pucilowski & Kostowski, 1981). Adding to the complexity, stimulating the entire MRR by optogenetics decreased aggression (Balazsfi et al., 2018). However, this research did not distinguish the roles of specific MRR neuronal populations, highlighting the need for future studies using cell-type-specific manipulations to clarify their individual contributions to aggression regulation.

1.1.4.5 Emotional Behavior

Emotions play a critical role in shaping behavior, and their underlying neural mechanisms involve complex interactions between neurotransmitters and brain regions. Serotonin, in particular, is heavily implicated in mood regulation, and disruptions in serotonergic signaling are linked to mood disorders like depression. This understanding led to the development of selective serotonin reuptake inhibitors (SSRIs), which increase serotonin levels and effectively alleviate depressive symptoms in many individuals (Blier, de Montigny, & Chaput, 1990; Nutt, 2005). However, the precise mechanisms by which specific neural pathways, particularly those originating from heterogeneous regions like the MRR, influence emotional behaviors remain an active area of investigation.

Studies employing various techniques, including lesions, pharmacological manipulations, and optogenetics, have consistently demonstrated that MRR inactivation produces anxiolytic effects, while its activation enhances anxiety-like behaviors (Abela et al., 2020; Andrade, Zangrossi, & Graeff, 2013; Teissier et al., 2015). Notably, these effects appear to be specific to generalized anxiety-like behaviors, as opposed to panic-like responses, and are often observed in tasks involving approach-avoidance conflict, supporting Gray's "behavioral inhibition system" (BIS) theory (Gray, 1982; McNaughton & Gray, 2002). The BIS, according to Gray, is a neuropsychological system that responds to conditioned stimuli associated with punishment, non-reward, or novelty. It is proposed to mediate behavioral inhibition, increase arousal, and heighten attention, particularly to threatening or unexpected stimuli. Activity of BIS is hypothesized to be the core psychological component of anxiety (Gray, 1982; McNaughton & Gray, 2002). Understanding how the diverse cell types within the MRR contribute to this system is therefore critical.

Ohmura et al. (2014) provided compelling evidence for the direct, causal link between MRR, serotonin and anxiety. Using optogenetic stimulation of MRR 5-HT neurons in transgenic mice, they observed a rapid increase in anxiety-like behavior, directly challenging the traditional view of acute SSRI-induced 5-HT release as purely anxiolytic (den Boer et al., 1987). Their findings also pinpoint the ventral HC as a crucial target for anxiogenic effects of MRR, demonstrated increased HC 5-HT levels upon MRR stimulation. Subsequent research from the same group further validated these findings, reinforcing the role of MRR 5-HT neurons in anxiety regulation (Ohmura et al., 2020).

While their findings highlight the prominent role of MRR in acute anxiety via its serotonergic output, they acknowledge that DRN likely contributes to other anxiety-related processes, potentially involving learned fear or social contexts (Challis et al., 2013; Maier, Grahn, & Watkins, 1995). Furthermore, these studies raise the question of how the non-serotonergic populations of MRR might contribute – independently or in interaction with 5-HT containing neurons - to anxiety regulation.

Further supporting the role of the serotonergic MRR-HC connection in anxiety, Abela et al. (2020) employed optogenetics to manipulate serotoninergic MRR axonterminals in HC of female mice. This stimulation mimicked the anxiogenic effects of MRR stimulation across multiple tests. Their work emphasizes the specificity of this projection in mediating the influence of MRR on anxiety, particularly in contexts involving approach-avoidance conflict. While the MRR is the main source of 5-HT to the dorsal HC (dHC) (Vertes, Fortin, & Crane, 1999), the DRN also contributes some 5-HT input to this region. Thus, it is not surprising that changes in DRN 5-HT activity are also known to impact anxiety-like behavior, however, mostly in the opposite direction as the MRR-dHC connection (File & Gonzalez, 1996; File, Hyde, & MacLeod, 1979; Ohmura et al., 2014). The precise nature of the raphe-HC modulation may depend on the balance and interaction between these two serotonergic inputs, as well as potential modulation by local or projecting GABAergic and dopaminergic elements within the raphe itself, rather than the independent action of either pathway alone (Abela et al., 2020).

MRR is also implicated in broader mood regulation, including mania, a key feature of bipolar disorder. Building on previous research in rats suggesting a link between MRR inactivation and manic-like symptoms (Andrade & Graeff, 2001; Asin & Fibiger, 1983; Giambalvo & Snodgrass, 1978; Wirtshafter, Montana, & Asin, 1986), Pezzato et al. (2015) conducted MRR lesions in mice and observed increased locomotor activity, stereotyped circling, and risk-taking behaviors, reminiscent of mania. Importantly, they demonstrated that chronic lithium treatment, a standard treatment for mania, specifically attenuated hyperactivity and circling, without impacting risk-taking. This aligns with the idea that the therapeutic effects of lithium in mania might involve modulation of both excitatory and inhibitory systems, potentially restoring balance between hyperactive DA pathways and hypoactive serotonergic systems disrupted by MRR inactivation (Giambalvo & Snodgrass, 1978; Yamamoto & Ueki, 1978). While

acknowledging that MRR lesions affect non-serotonergic fibers, the authors highlighted the translational relevance of this model and potential for investigating the complex neurobiology underlying mania and its treatment (Pezzato et al., 2015).

Given the established role of MRR in emotional behavior, largely attributed to its serotonergic component, understanding the contributions of its other neuronal populations becomes crucial, especially considering the intricacies of serotonin signaling itself. Serotonin exerts its diverse effects through a multitude of receptor subtypes (at least 14) located on different cell types and in different brain regions (Barnes et al., 2021; Stiedl et al., 2015). These receptors can have opposing effects on neuronal activity (e.g., excitatory vs. inhibitory) and engage distinct intracellular signaling pathways (Barnes et al., 2021; Stiedl et al., 2015). Therefore, simply increasing or decreasing overall serotonin levels (as with SSRIs) does not fully capture the nuanced and often localized actions of this neurotransmitter (Stahl, 1998). Furthermore, serotonin can act through both synaptic transmission (direct, point-to-point communication at synapses) and volume transmission (diffuse release affecting wider area) (Gianni & Pasqualetti, 2023; Ozcete, Banerjee, & Kaeser, 2024; Zhang et al., 2025). Structurally, the potential for volume signaling is supported by observations that many serotonin-releasing axons have swellings along their length, rather than typical synapses, a feature particularly noted in areas like the DRN nucleus (Gianni & Pasqualetti, 2023; Ozcete, Banerjee, & Kaeser, 2024). Functionally, the transmission mode can dynamically switch: while lower frequency firing tends to confine serotonin near the synapse via transporter action, high-frequency or synchronized activity allows serotonin to 'spill over' and act diffusely through volume transmission (Zhang et al., 2025). This contrasts with the predominantly fast, spatially precise synaptic actions typical of GABAergic and glutamatergic neurons (Gianni & Pasqualetti, 2023; Ozcete, Banerjee, & Kaeser, 2024).

Thus, the MRR, with its diverse neuronal populations and projection targets, likely exerts a context-dependent and multifaceted influence on emotional behavior, using both serotonergic and non-serotonergic mechanisms (Abela et al., 2020; Andrade, Zangrossi, & Graeff, 2013; Szonyi et al., 2019).

1.2 Technics to investigate specific neuron populations in vivo: the Cre-loxP System

Several advanced methods have been developed to manipulate targeted cell populations within the living brain. The Cre-loxP system emerging as a particularly powerful approach (Fig.3). Originally discovered in P1 bacteriophages (Sternberg & Hamilton, 1981), this genetic technique centers on the Cre (cyclization recombination) enzyme, which recognizes and acts upon specific DNA sequences called loxP sites. By catalyzing precise recombination between these sites, researchers can achieve controlled genetic modifications with unprecedented specificity.

The effectiveness of the system relies on two primary components: transgenic animals and viral vectors. Researchers generate transgenic mouse lines that express Cre recombinase under cell type-specific promoters, which restricts enzymatic activity to particular neuronal populations (Lakso et al., 1992). This strategic design ensures that subsequent genetic manipulations occur exclusively within targeted neuronal subtypes.

Adeno-associated viruses (AAVs) are commonly used viral vectors for delivering genetic material to specific brain regions (Challis et al., 2022; Deverman et al., 2016). These vectors can be engineered to carry gene sequences flanked by loxP sites, typically in an inverted orientation. After stereotaxic injection into the brain, AAVs infect neurons in the target area. In Cre-expressing neurons, Cre recombinase enzyme inverts the gene sequence between the loxP sites, promoting the expression of the delivered gene specifically in the targeted neuronal subtype (Sauer & Henderson, 1988).

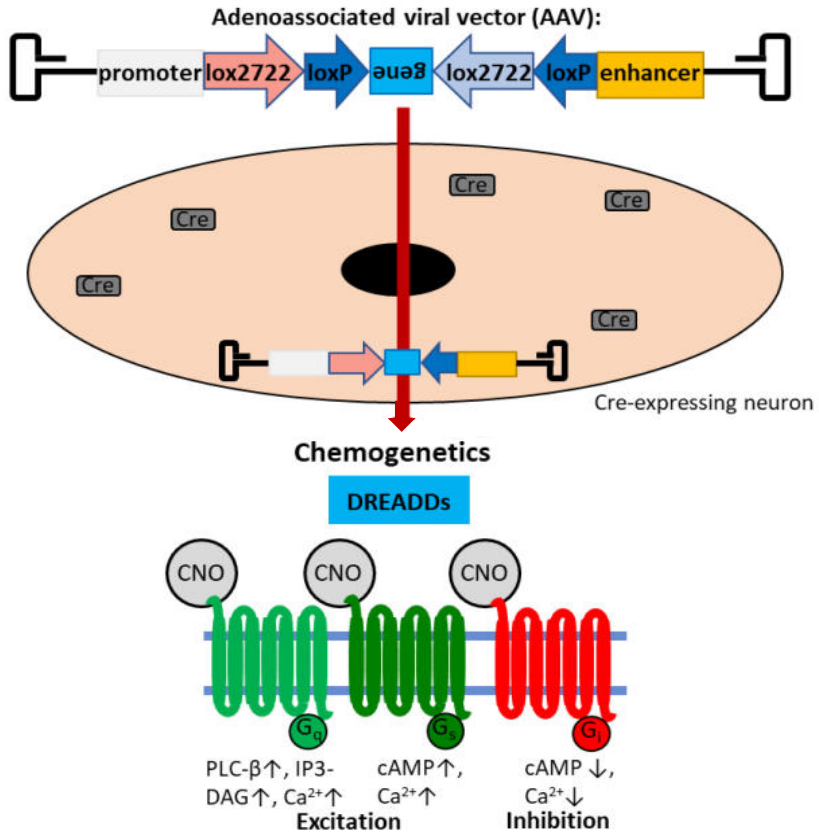

Figure 3 - Schematic representation of Cre-mediated AAV expression for chemogenetics: In the AAV construct, the double-floxed gene (flanked by loxP sites) can be transcribed only in cells expressing the Cre recombinase enzyme. This allows for cell-type-specific expression of the introduced gene. For chemogenetic manipulation, the introduced gene encodes a DREADD. Following the administration and binding of an artificial ligand, such as clozapine-N-oxide (CNO), these engineered G-protein coupled receptors induce different intracellular signaling pathways to modulate neuronal activity. Excitatory DREADDs typically couple to Gq (activating the IP3-DAG pathway) or Gs (stimulating cAMP production, though Gq is more prevalent for hM3Dq). Inhibitory DREADDs primarily couple to Gi, which inhibits cAMP production. Abbreviations: AAV, Adeno-associated virus; cAMP, cyclic adenosine monophosphate; CNO, clozapine-N-oxide; Cre, causes recombination (Cre recombinase); DREADD, Designer Receptor Exclusively Activated by Designer Drug; Gi, inhibitory G-protein; Gq, Gq G-protein; Gs, stimulatory G-protein; IP3-DAG, inositol trisphosphate-diacylglycerol; loxP, Cre-recognized recombination sites. Figure designed by the author.

The use of Cre-driver mouse lines combined with Cre-dependent viral vectors (e.g., designer receptor exclusively activated by designer drugs (DREADDs) (Armbruster et al., 2007) or channelrhodopsin (ChR) (Boyden et al., 2005)) allows for precise, cell-type-specific manipulation of neuronal activity within the MRR. This is achieved because

the Cre recombinase enzyme, expressed only in the targeted cell type, activates the gene of interest (e.g., DREADD or ChR) carried by the virus, which is otherwise inactive due to the loxP-flanked inverted sequence (Atasoy et al., 2008)..

This approach enables us to establish causal relationships between the activity of specific MRR neuronal populations (GABAergic, dopaminergic) and the observed behavioral and physiological changes (Deisseroth, 2015; Wess, Nakajima, & Jain, 2013). Furthermore, these viral tools, when used in combination, allow us to trace monosynaptic (Kim et al., 2016) and polysynaptic connections (Schwarz et al., 2015), providing unprecedented details in circuit mapping.

1.2.1 Manipulation of neuronal activity

Building upon the precise genetic control offered by the Cre-loxP system, neuroscientists have developed advanced techniques for manipulating neuronal activity in behaving animals. Among these, both optogenetics (Boyden et al., 2005) and chemogenetics (Armbruster et al., 2007) have emerged as powerful approaches, leveraging cell-type-specific, Cre-dependent gene expression to introduce tools for modulating neural function with high precision. Optogenetics uses light-sensitive proteins (e.g., ChR) to rapidly activate or inhibit neurons with millisecond precision (Deisseroth, 2015). Chemogenetics, on the other hand, employs engineered receptors that are activated by specific, otherwise inert, ligands, allowing for more sustained modulation of neuronal activity (Urban & Roth, 2015). Because we aimed to observe behavior, which lasts several minutes, we were using a more prolonged manipulation by DREADDs. This technique will be described in detail below.

Chemogenetics employs DREADDs, which are engineered G-protein coupled receptors (GPCRs) derived from human muscarinic acetylcholine receptors. These artificial receptors can be designed to either excite or inhibit host cells, primarily through the Gq and Gi signaling pathways, respectively (Armbruster et al., 2007; Vardy et al., 2015). DREADDs are typically introduced into target neurons via AAVs, allowing for localized expression in specific brain regions (Deverman et al., 2016).

Traditionally, DREADDs have been activated by clozapine-N-oxide (CNO). While alternative DREADD ligands, such as compound 21, perlapine and deschloroclozapine (Chen et al., 2015; Nagai et al., 2020; Thompson et al., 2018), have been developed for more selective activation, CNO remains a valuable tool when used with appropriate controls and dosing. Despite the potential of CNO conversion to clozapine, an antipsychotic with known off-target effects, carefully chosen doses can effectively activate DREADDs while minimizing these confounds (Mahler et al., 2014; Thompson et al., 2018). The studies in this dissertation employed CNO at 1 mg/kg and included CNO-treated control animals not expressing DREADDs to account for any nonspecific effects.

A key feature of chemogenetic manipulation is its temporal profile. Following CNO administration, DREADD-mediated effects typically onset within 15 minutes and can persist for up-to 6 hours (Roth, 2016; Smith et al., 2016). While this temporal resolution is lower compared to optogenetics, it provides a suitable timeframe for studying the sustained effects of neuronal modulation on behavior. The combination of chemogenetics with transgenic animal models, using Cre-dependent AAVs in Cre-driver mouse lines (e.g., DAT-Cre for dopaminergic neurons (Backman et al., 2006), VGAT-Cre for GABAergic neurons (Vong et al., 2011)), allows for precise cell-type specificity. Overall, chemogenetics, with its ability to modulate defined neural circuits, facilitates establishing causal relationships between neuronal activity and behavior (Krashes et al., 2011).

2 Objectives

We investigated the distinct roles of GABAergic (marked with vesicular GABA transporter (VGAT)) and dopaminergic neurons (marked with dopamine transporter (DAT)) within the MRR in modulating behaviors relevant to neuropsychiatric disorders. Using chemogenetics, behavioral testing, and anatomical/molecular techniques, this work aimed to:

Project I.: Determine the role of VGAT-MRR neurons in reinforcement-based learning

Experiment 1.: Nonspecific whole-MRR manipulation

Experiment 2.: Targeted GABAergic neuron manipulation to assess learning, reversal learning, and impulsiveness.

Project II.: Investigate VGAT-MRR neuron influence on social and emotional behaviors through:

a) Targeted chemogenetic manipulation (Cre-dependent DREADDs in AAVs into the MRR of VGAT-Cre mice)
b) Behavioral testing (social behavior, locomotion, anxiety, memory).
c) Examining neuronal activation (c-Fos) patterns in VGAT-MRR neurons following specific social tasks.

Project III.: Characterize and investigate DAT-MRR neuron function, through:

a) Confirming their presence and localization
b) Targeted chemogenetic manipulation (Cre-dependent DREADDs in AAVs into the MRR of DAT-Cre mice)
c) Behavioral testing (social behavior, locomotion, anxiety, memory).

This research aimed to elucidate the functional role of these MRR neuronal populations and their implications in neuropsychiatric disorders.

3 Materials and methods

All experiments were conducted in accordance with relevant ethical guidelines (see Ethical Approval section for details).

3.1 Animals

All mice had C57BL/6J background and were obtained from the Institute of Experimental Medicine, Budapest, Hungary and originated from The Jackson Laboratory. The animals were maintained under standard laboratory conditions (21 ± 1°C, 12-hour light/dark cycle, lights on 21:00h) with ad libitum access to standard laboratory chow (Charles River, Hungary) and water. Behavioral testing was conducted during the early dark (active) phase under red light. Project-specific details are as follows:

Project I.: Adult male VGAT-Cre mice (Jackson Laboratory, #016962) homozygous for Cre recombinase, and C57BL/6J wild-type mice, aged 14-15 weeks, were group-housed (2-3 mice/cage) in Makrolon type III cages.

Project II.: Adult male VGAT-Cre mice (Jackson Laboratory, #016962), homozygous for Cre recombinase, aged 8-10 weeks, were initially group-housed (2-3 mice/cage) in Makrolon type III cages and then singly housed following the first CNO injection to prevent potential manipulation-induced aggression between cage mates and standardize social conditions prior to interaction tests. For some experiments, VGAT-Cre mice were crossed with ZsGreen reporter mice (Jackson Laboratory, #007906). This reporter line expresses the bright fluorescent protein ZsGreen, originally isolated from reef corals, upon Cre-mediated recombination, allowing for clear, genetically-defined visualization of the targeted GABAergic neurons. ZsGreen has superior brightness and photostability compared to other fluorescent proteins (Heddle & Mazaleyrat, 2007; Lopez-Yrigoyen et al., 2018; Wenck et al., 2003). This bright fluorescence allows for extended imaging sessions, and excellent signal-to-noise ratio, which is critical for in vivo imaging studies (Lopez-Yrigoyen et al., 2018). This strategy was employed to facilitate the identification and analysis of neuronal activation (via c-Fos staining) specifically within the VGAT-MRR population following behavioral testing. Male juvenile C57BL/6J mice (30–45 days old) served as stimulus animals in social behavior tests. Behavioral testing was conducted during the early dark phase.

Project III.: Adult male DAT-Cre mice (Jackson Laboratory, #006660), heterozygous for Cre recombinase, were used. These mice were offspring of C57BL/6J mothers. They were group-housed (2–3 mice/cage) until behavioral testing began, at which point they were individually housed. Male juvenile C57BL/6J mice (30–45 days old) were used as stimulus animals, and adult male C57BL/6J mice were used for reverse transcription polymerase chain reaction (RT-PCR).

3.2 Ethical Approval

All experiments were approved by the Workplace Animal Welfare Committee of the Institute of Experimental Medicine and the National Scientific Ethical Committee on Animal Experimentation of Hungary (PEI/001/33-4/2013, PE/EA/254-7/2019) and performed according to the European Communities Council Directive recommendations for the care and use of laboratory animals (2010/63/EU). The authors complied with the ARRIVE guidelines.

3.3 Stereotaxic Surgery and Viral Vector Delivery

Animals in all three projects underwent stereotaxic surgery for viral vector delivery into the MRR. Mice were anesthetized via intraperitoneal (i.p.) injection of a ketamine/xylazine solution at a volume of 10 mL/kg. The anesthetic mixture was prepared by combining 0.5 mL ketamine (100 mg/mL), 0.1 mL xylazine (20 mg/mL), and 2.4 mL sterile saline. This formulation delivers approximately 167 mg/kg ketamine and 6.7 mg/kg xylazine, providing a surgical level of anesthesia. Post-surgical analgesia was provided via subcutaneous buprenorphine injections (0.1 mg/kg; Bupaq, Gedeon Richter Plc.) at the time of surgery and for the two following days. All surgical procedures were performed using a stereotaxic frame (David Kopf Instruments). Across all experiments targeting the MRR, the same stereotaxic coordinates were used (relative to Bregma): AP: -4.1 mm, ML: 0 mm, and DV: -4.6 mm (Fig. 4a). A glass capillary (20-30 μm tip diameter) attached to a Nanoject II precision microinjector (Drummond) was used for all AAV infusions, typically at a rate of 100 nL/minute followed by a 3-minute pause before capillary withdrawal. Animals were allowed to recover for 4 weeks (28 days) post-surgery to allow for DREADD expression and acclimation to a reversed light/dark cycle.

The initial study involved nonspecific MRR stimulation using a non-Cre-dependent AAV2-hSyn-hM3Dq-mCherry (3.0e12 GC/mL titer; Addgene #50474) to express the stimulatory DREADD (hM3Dq) and mCherry (also called red fluorescent protein, RFP) under a neuron specific Synapsin promoter (10 nL injected); AAV2 was chosen for its broad neuronal tropism suitable for this nonspecific manipulation (Castle et al., 2016; Haery et al., 2019). Subsequent experiments focused on Cre-dependent targeting. For the manipulation of VGAT-MRR neurons (in VGAT-Cre mice) animals received 20 nL injections of viruses encoding either control (AAV8-hSyn::DIO-mCherry, 4.1e12 GC/mL titer; Addgene #50459), stimulatory (AAV8-hSyn::DIO-hM3Dq-mCherry, 4.0e12 GC/mL titer; Addgene #44361), or inhibitory (AAV8-hSyn::DIO-hM4Di-mCherry, 1.9e13 GC/mL titer; Addgene #44362) constructs in Cre-dependent way. AAV8 was selected for these Cre-dependent studies due to its efficient and widespread neuronal transduction capabilities, ensuring robust DREADD expression within the targeted cell populations (Botterill et al., 2021; Zhao et al., 2024). Project II also targeted GABAergic neurons using these same constructs and 20 nL injections. Project III targeted dopaminergic neurons (in DAT-Cre mice) using the same control, stimulatory, and inhibitory constructs with 20 nL injections.

Following the 4-week expression period and completion of behavioral testing, injection accuracy was histologically verified for all animals. Targeting was confirmed by visualizing the fluorescent protein signal (RFP) or via immunohistochemical (IHC) enhancement (Fig.4b). Animals exhibiting inaccurate targeting, such as significant viral spread outside the MRR or missed target (Figure 4c), were excluded from all subsequent analyses.

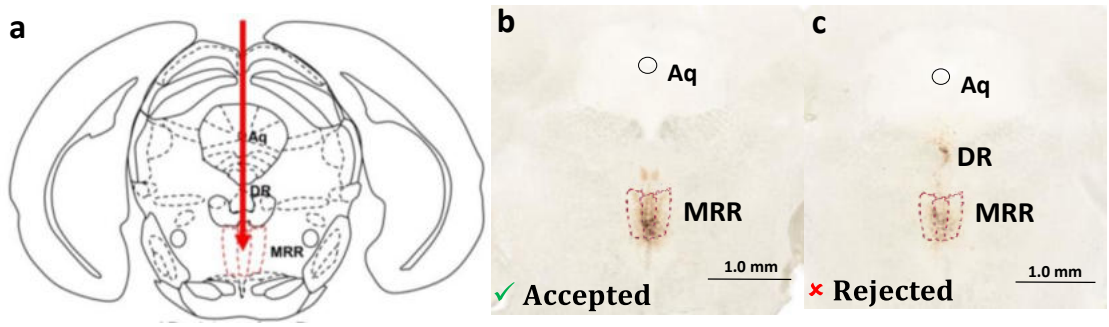

Figure 4 - Virus injection details: (a) Coronal schematic of the mouse MRR adapted from Paxinos and Watson (2007). The targeted injection site is indicated. (b) Representative image of accurate viral targeting

in the MRR of a DAT-Cre mouse, visualized by nickel-enhanced DAB staining against RFP, six weeks after injection of 20 nL rAAV8/hSyn-DIO-HM4D(Gi)-mCherry (Addgene, #44362). (c) Representative image of an excluded injection due to off-target staining in both the dorsal and median raphe region (DR and MRR. Aq: cerebral aqueduct. Injection coordinates relative to bregma: AP: -4.1 mm, ML: 0 mm, DV: -4.6 mm. Figure reproduced from Chaves et al., 2024.

3.4 Drug Administration

In all projects, the DREADD receptors were activated by an intraperitoneal (i.p.) injection of its specific ligand, Clozapine-N-oxide (CNO). CNO was administered at a dose of 1 mg/kg, delivered in a saline vehicle at a volume of 10 mL/kg. CNO was administrated 30 minutes before each behavioral test, with the exception of the social discrimination test (SDT), in which CNO was not administered. This was to ensure that the SDT specifically assessed social recognition memory formed during the prior sociability test (when CNO was given), without the confounding influence of acute DREADD manipulation on memory retrieval or general behavior during the SDT itself. Some control animals in Project I. - Experiment 1., received saline injections instead of CNO. This saline control group was included to establish a baseline performance and to account for any potential non-specific effects of the injection procedure. All other animals, including control virus injected ones in other experiments, received CNO to control for nonspecific drug effects.

3.5 Behavioral experiments

Mice underwent a battery of tests to evaluate reinforcement-based learning, social behavior, anxiety, and memory. The experimental design and specific tests employed varied slightly between projects, as detailed below.

Reinforcement-based learning is a type of learning where behavior is shaped by its consequences; actions leading to positive outcomes are more likely to be repeated, while those leading to negative outcomes are avoided. We have chosen operant conditioning as positive reinforcement learning and active avoidance as negative valence, because they are well suited to study functions the MRR is believed to regulate, such as cognitive flexibility and reward-related behavior; they also offer quantifiable outcomes and have well-established literature.

3.5.1 Operant conditioning

To increase motivation, mice were food-restricted for 72 hours before testing (Fazekas et al., 2019) and subsequently maintained at approximately 80% of their initial free-feeding body weight through controlled daily food access during the training period. The test was conducted in an automated operant chamber using 45-mg food pellets (Bio-Serv Dustless Precision Rodent Pellet, Bilaney Consultants GmbH, Germany) as reward (Aliczki et al., 2014). Each day, 30 minutes after CNO injection animals were placed in the chamber for 30 minutes and allowed to freely explore. One nose hole was designated as the "rewarded" one, as its activation by nose poke resulted in immediate reward delivery followed by a 25-second timeout period, during which the chamber light was illuminated. An incorrect nose poke also triggered a 25-second timeout, serving as a time-based penalty for errors. Responses during the timeout were recorded but not rewarded and served as a measure of impulsivity (Wenger, Schmidt, & Davisson, 2004). During the reversal learning phase or cognitive flexibility the location of the rewarded nose poke was switched.

Reward preference (the ratio of responses on the rewarded nose poke) was calculated as follows:

$$Reward\ preference = \frac{correct\ nose\ poke}{incorrect + correct\ nose\ pokes} \times 100$$

The total number of responses (correct + incorrect) was also recorded.

3.5.2 Active avoidance (shuttle-box) test

A classical automated shuttle-box apparatus was used, consisting of two identical compartments equipped with photobeam sensors, stimulus lights, a tone generator, a stainless-steel grid floor, and a guillotine door (Otrokocsi, Kittel, & Sperlagh, 2017). Mice were placed in either the left or right compartment of the apparatus for 10 days. After a 1-minute habituation period, 40 trials (30 seconds each) commenced. In each trial, the light and tone (conditioning stimuli) were initiated 20 seconds after trial onset, and the guillotine door opened. During the final five seconds of each trial, an electric footshock (0.15 mA, unconditioned stimulus) was applied to the grid floor of one compartment. At the end of each trial, all stimuli were terminated, the guillotine door

closed, and a 5-second intertrial interval (ITI) began before the next trial. During the reversal learning phase, shocks were delivered to the opposite compartment and the mice had to learn to suppress the previously learned escape response. An avoidance response was recorded if the animal avoided the shock by moving to the other compartment (or remaining in the same compartment during the reversal phase) during the presentation of the conditioning stimuli (escape during stimulus, EDST) or during the footshock itself (escape during footshock, EDFS). Escape failure (ESFL) was recorded if the animal remained in the compartment and received the footshock (or moved to the other compartment during the reversal phase). Average escape latencies were also calculated as a potential indicator of impulsivity. During the reversal learning phase, the correct adaptive behavior is to inhibit the previously learned escape response. Therefore, an increase in ESFL during this phase serves as the operational measure of successful reversal learning.

3.5.3 Sociability and Social Discrimination Tests

It allows for precise measurement of social approach motivation without the confound of reciprocal interaction. Previous research has implicated serotonergic transmission in social approach (Dolen et al., 2013), but the upstream GABAergic regulation of this system remained undefined. Additionally, this paradigm is widely used in models of autism and similar paradigms are also employed in research on other neurodevelopmental disorders, making our findings potentially relevant for understanding the neurobiological basis of social deficits in these conditions (Moy et al., 2004).

The sociability test consisted of four, 5-minute phases, the first 3 in consecutive order, and the 4. followed 24 hours later. 30 minutes before the first phase CNO was administered.

Phase I.: Open Field (OF)

This test assesses locomotor activity and anxiety-like behavior. Animals were placed in an empty white plastic box (40 cm × 36 cm × 15 cm). Four animals were tested simultaneously in separate boxes arranged in a 2 × 2 grid. "Distance moved" was analyzed using EthoVision XT 15 software as a measure of mobility. The arena was virtually

divided into peripheral and central zones (the central zone comprising 75% of the arena). Time spent in each zone and the frequency of entries into the central zone were recorded as measures of anxiety-like behavior.

Phase II.: Side Preference

Two identical weighted wire cages were placed in the boxes to assess object and place preference. The cages were designated as "left" or "right" based on their location, and the frequency and time spent investigating each was recorded**.**

Phase III.: Sociability

An unfamiliar juvenile male mouse was placed under one of the wire cages consistently towards the center of the overall 4-arena setup. This procedure systematically varied the absolute spatial location (left/right) of the social stimulus across the simultaneously tested animals. Animals could not physically interact but could see, smell, and hear each other. Time spent investigating the cage with the conspecific versus the empty cage was recorded. A social preference index (SI) was calculated as follows:

$$SI = \frac{t_{mouse}}{t_{mouse}+t_{cage}} \times 100,$$

where t_{mouse} stands for the time spent investigating the cage containing the juvenile mouse, and t_{cage} stands for the time spent investigating the empty cage. This index provides a measure of relative social preference. Typically, a group average SI significantly above 50% (chance level) indicates social preference, and this index is primarily used for comparing the degree of social investigation between experimental groups.

Phase IV.: Social Discrimination Test (SDT)

The SDT is considered the most ethologically relevant paradigm for assessing social memory (Engelmann, Wotjak, & Landgraf, 1995).

Twenty-four hours after the sociability test an SDT was performed without CNO administration. Two weighted wire cages were placed in the empty box, each containing a juvenile male mouse. One mouse was an unfamiliar, novel conspecific (J1, novel mouse). The other mouse was the same conspecific that the test animal had encountered during the sociability phase 24 hours prior (J2, familiar mouse). Time spent investigating

each mouse was recorded, and a social discrimination index (SD) was calculated as follows:

$$SD = \frac{t_{J1}}{t_{J1}+t_{J2}} \times 100,$$

where t_{J1} is the time spent investigating the novel mouse, and t_{J2} is the time spent investigating the familiar mouse.

For this score, performance at 50% indicates chance level (no preference). Values significantly above 50% indicate a preference for the novel mouse and thus, intact social recognition memory.

3.5.4 Social interaction test (SIT)

Mice are naturally nocturnal, exhibiting peak social activity during the dark phase (Arakawa, Blanchard, & Blanchard, 2007). While ideally, social behavioral testing would occur during this active period, practical considerations often necessitate light phase assessments. Critically, research has demonstrated that SIT measures, particularly in standardized laboratory settings, remain remarkably consistent across light and dark cycles (Yang, Weber, & Crawley, 2008). Therefore, the present SIT was conducted under bright light (120 lx) (although during the dark, active circadian phase of the animals), leveraging this translatability to induce anxiety-like behavior and investigate its modulatory effects on social interaction. Specifically, the day before the test, animals were individually placed in a transparent Plexiglas aquarium (35 cm × 20 cm × 25 cm) within the experimental room, furnished with bedding, for two 15-minute habituation sessions spaced 4 hours apart. During the test, two animals from the same experimental group (e.g., control vs. control, inhibitory vs. inhibitory) with similar weights were placed together in the aquarium. Similar body weights were sought to ensure hierarchical equality and minimize the likelihood of unilateral territorial aggression. Mice were allowed to interact freely for 10 minutes.

Social (e.g., sniffing), aggressive (e.g., biting, aggressive dominance, chasing), and defensive behaviors were analyzed (frequencies and duration) for both animals. All other behaviors were categorized as "other." A Prosocial Index (PI) was calculated as follows:

$$PI = \frac{t_{social}}{t_{social} + t_{aggressive}} \times 100$$

3.5.5 Resident intruder (RIT)

The RIT assesses territorial aggression in mice, a distinct aspect of social behavior from the general sociability and social interaction. Resident mice were individually housed for one week without cage cleaning to establish territoriality via olfactory cues (Koolhaas et al., 2013). Following this isolation period, a smaller, unfamiliar, adult male mouse (intruder) was introduced into the home cage of the resident test mice. This size difference promoted submissiveness in the intruder, allowing for a clearer assessment of the territorial aggression of the resident. The 10-minute interaction was recorded, and the behavior of the resident was analyzed using the same ethological categories as the SIT, focusing on aggressive displays.

3.5.6 Elevated-plus maze (EPM)

The EPM assesses anxiety-like behavior in mice. Each animal was placed in the central zone of the EPM apparatus (67 cm × 7 cm × 30 cm), which consists of two open and two enclosed arms. While mice generally prefer the safety of the enclosed arms, exploratory drive motivates ventures into the open arms. Under bright light (120 lx), which further enhances anxiety-related behaviors, mice were allowed to freely explore the maze for 5 minutes. The number of entries into, and time spent in each arm was recorded and analyzed. To control for variations in overall activity, an open arm preference index, independent of total arm entries, was calculated:

$$Open\ Arm\ Preference\ Index = \frac{number\ of\ open\ arm\ entries}{sum\ of\ open + closed\ arm\ entries} \times 100$$

Additionally, the frequency of risk assessment behaviors (head dipping, stretched attend postures, rearing) and grooming were also analyzed.

3.5.7 Y-maze

The Y-maze was selected for its capacity to probe hippocampal-dependent spatial working memory, a process influenced by VGAT-MRR neurons through their modulation of hippocampal network dynamics and cognitive flexibility (Jelitai et al.,

2021). VGAT-MRR cells regulate theta rhythm coordination between the MRR and HC, which is critical for spatial navigation and memory consolidation (Jelitai et al., 2021).

The apparatus consists of three arms (A, B, and C; 25 cm × 5 cm × 21 cm) at 120° angles, joined by a central zone. Mice, initially placed at the end of arm A, were allowed to freely explore for 5 minutes. A higher rate of alternating arm entries (e.g., ABC, BCA, CAB) reflects better spatial working memory. Spontaneous alternation was calculated as:

$$Spontaneous\ alternation = \frac{'correct'alternation}{sum\ of\ all\ arm\ entries - 2} \times 100.$$

A "correct" alternation is defined as entering all three arms on consecutive choices, excluding repeated visits to the same arm (Fazekas et al., 2019).

3.5.8 Behavioural Analysis

Project I.: Data acquisition for the operant conditioning and shuttle box tests was performed automatically using Med-PC IV software (Med Associates). Six animals were tested per run, with each run including animals from each experimental group. For operant conditioning, the following parameters were analyzed: total responses, reward preference, and timeout responses. For the shuttle box (active avoidance), the analyzed parameters were: EDST, EDFS, ESFL and average escape latency.

Projects II. and III.: Behavior was recorded using a digital camera (Samsung SNB 7000) and analyzed by an experimenter blind to the treatment groups. Videos were subsequently analyzed using two approaches: manual scoring of defined behaviors with computer-based event recorders (H77, Solomon Coder), and automated analysis of parameters such as locomotion and zone preference using Noldus EthoVision XT 15 software. OF data were analyzed using EthoVision XT 15 to assess distance traveled and time spent in the center zone. EPM data were also analyzed using EthoVision XT 15 to measure time spent in open/closed arms, open arm entry ratio, and latency to enter open arms. SIT and RIT tests were scored using Solomon Coder to assess the frequency and duration of specific social behaviors (e.g., sniffing, aggression, etc.). Time spent with the stimulus mice, and with an empty cage, as well as the social preference index were also investigated during sociability test. Y-maze performance was evaluated by calculating the percentage of spontaneous alternations. Social discrimination was analyzed by

calculating a discrimination index, which represents the ability to discriminate between familiar and unfamiliar stimulus mice. To ensure CNO clearance, tests in Projects II. and III. were separated by 48–72 hours, except for the SDT, which was conducted 24 hours after the sociability test and without CNO administration.

3.6 Immunohistochemistry (IHC)

A range of IHC techniques were employed to assess correctness of viral targeting, confirm neuronal phenotypes, and measure neuronal activation.

3.6.1 Tissue Processing

Upon completion of behavioral testing (or specific time points post-CNO injection or behavioral tests for c-Fos studies), mice were deeply anesthetized (ketamine/xylazine solution, i.p.) and transcardially perfused with ice-cold phosphate-buffered saline (PBS), followed by ice-cold 4% paraformaldehyde (PFA) in PBS. Brains were extracted, post-fixed in 4% PFA for 24 hours at 4°C, and then cryoprotected in a sucrose-based (30% sucrose with sodium azide in PBS) or glucose-based (20% glucose in PBS) solution for at least 24 hours at 4°C. Coronal sections (30 µm thick) were cut using a sliding microtome and stored in a cryoprotectant solution (containing 20% glycerol and 30% ethylene glycol in PBS) at -20°C until staining.

3.6.2 Verification of Viral Targeting and Expression

To confirm accurate AAV injection targeting, the expression of the RFP reporter in the MRR was confirmed in all experiments by nickel-enhanced 3,3'-diaminobenzidine (Ni-DAB) staining (Biro et al., 2017). Briefly, free-floating sections were washed in PBS (3 × 10 min), permeabilized with 0.5% Triton X-100 (TXT) and 0.3% H_2O_2 in PBS, and blocked with 2% bovine serum albumin (BSA) in PBS for 1 hour. Sections were incubated with a rabbit anti-RFP primary antibody (1:4000; Rockland, #600-401-379) diluted in 2% BSA/0.1% TXT/PBS for 48 hours at 4°C. Following PBS washes, sections were incubated with a biotinylated anti-rabbit secondary antibody (i.e., Biotin-SP Donkey Anti-Rabbit IgG, 1:1000, Jackson ImmunoResearch, #711-065-152) in 2% BSA/PBS for 1-2 hours. After washes in PBS and Tris buffer, sections were incubated with an avidin-biotin complex (ABC; e.g., Vectastain ABC Kit, Vector Laboratories) diluted 1:1000 in Tris buffer for 1 hour. The peroxidase reaction was developed using DAB (0.2-0.3 mg/mL) and 0.1-0.2% nickel ammonium sulfate in Tris buffer, initiated by adding

0.003% H_2O_2. After precipitation, sections were washed by Tris buffer, mounted onto gelatin-coated slides, dehydrated through graded alcohols and xylene, and coverslipped with DPX mounting medium (Sigma-Aldrich).

RFP-stained sections were imaged using a light microscope (i.e., Olympus DP70 with 4× objective). The extent of viral expression was examined across relevant anteroposterior coordinates (approx. -4.04 to -5.20 mm from Bregma). Animals were excluded from analysis if (1) RFP staining was absent in the MRR, (2) staining was predominantly unilateral, or (3) significant off-target staining was observed in adjacent regions (e.g., DRN). (Example exclusion rate: In the VGAT-Cre experiments for social behavior, 31 out of 58 injected mice showed accurate targeting (53%)).

3.6.3 Neuronal Phenotype Characterization

Identification of Transduced Cell Types (Nonspecific AAV): To identify cell types transduced by the non-Cre-dependent AAV (AAV2-hSyn-hM3Dq-mCherry), double or triple immunofluorescent staining was performed. Sections were washed in PBS, blocked (i.e., 5% normal goat serum (NGS) / 0.2% TXT in PBS), and incubated for 48 hours at 4°C with cocktails of primary antibodies including rabbit anti-RFP (1:1000, Rockland #600-401-379) combined with either rabbit anti-GABA (1:500, Sigma #A2052), or a combination of mouse anti-tryptophan hydroxylase (TPH, rate limiting enzyme for serotonin synthesis) (1:500, Sigma #T0678) and rabbit anti-VGluT3 (1:500, Synaptic Systems #135203). As these three neuron-types were known in the MRR at the beginning of our experiments (see (Sos et al., 2017)), we were concentrating only on them. Primary antibodies were detected using appropriate Alexa Fluor-conjugated secondary antibodies (i.e., anti-rabbit Alexa 488 or 594; anti-mouse Alexa 488 or 594). Sections were mounted with Mowiol and visualized using a Nikon C2 confocal laser-scanning microscope (20× objective).

Validation of GABAergic Target in VGAT-Cre mice: Triple immunofluorescent staining confirmed the expression of RFP (from different AAV8-hSyn::DIO...) in the VGAT-MRR neurons, thus, the validity of the mice strain. As the GABAergic cell bodies are not easy to detect, we combined two antibodies (GAD67 and VGAT) for their visualization. Sections were washed in PBS (4 × 10 min) and incubated for 48 hours at 4°C in a primary antibody solution containing rat anti-RFP (1:1000;

ChromoTek, #5f8-100), mouse anti-GAD67 (1:200; Merck Millipore, #MAB5406), and rabbit anti-GABA (1:500; Sigma-Aldrich, #A2052) diluted in PBS with 0.5% BSA and 0.25% TXT. After PBS washes (3 × 10 min), sections were incubated for 1.5 hours in a secondary antibody solution containing goat anti-rat Alexa 594 (1:200; Abcam, #ab150160), goat anti-mouse Alexa 488 (1:200; Invitrogen, #A11029), and goat anti-rabbit Alexa 488 (1:200; Jackson ImmunoResearch, #111-545-003) diluted in PBS. Sections were mounted with Mowiol and imaged using a Nikon C2 confocal laser-scanning microscope (20× objective, NA 0.75). This allowed visualization of virally transduced cells (RFP, red) and confirmation of their GABAergic identity (co-localized GAD67/GABA signal, green).

Validation of Dopaminergic Target in DAT-Cre mice: A key goal was to distinguish true dopaminergic neurons (which are tyrosine hydroxylase positive (TH+) but Dopamine Beta-Hydroxylase negative (DBH-)) from noradrenergic neurons (which are both TH+ and DBH+). Therefore, one method involved staining for RFP alongside TH (1:1000, rabbit; DiaSorin) or DBH (1:1000, rabbit; Invitrogen, #PA1-18314), using biotinylated secondary antibodies (1:1000, goat anti-rabbit; Vector, #BA 1000). Extravidin-peroxidase, and tyramide signal amplification (Fictiramin 488) was used for TH/DBH detection, followed by standard IHC for RFP. A second approach utilized cocktails for triple labeling: sheep anti-RFP (1:100,000; provided by C. Fekete, IEM), mouse anti-TH (1:300; Cell Signaling Technology, #45648), and rabbit anti-DBH (1:2000; Abcam, EPR20385), or sheep anti-RFP and rat anti-DAT (1:1000; Sigma-Aldrich, MAB369). These were detected using a combination of appropriate Alexa Fluor-conjugated secondary antibodies, biotinylated secondaries, streptavidin-conjugated dyes (e.g., Pacific Blue), and Fab fragment blocking (anti-mouse Fab, Jackson ImmunoResearch, #715-007-003), where necessary. Sections were mounted (Mowiol or PBS/glycerol) and imaged using a Nikon C2 confocal laser-scanning microscope (20× and 100× objectives).

3.6.4 Assessment of Neuronal Activation (c-Fos)

Chemogenetically Induced Activation of VGAT-MRR in VGAT-Cre mice: To confirm that our chemogenetic manipulation indeed activated the VGAT-MRR cells 120 min (30 min for CNO effect + 90 min for c-Fos activation) after CNO injection brain

were collected from VGAT-Cre mice (control: n = 4; stimulatory: n = 4), and IHC was performed for c-Fos and RFP. Sections were washed in PBS (3 × 10 min), blocked (10% NGS for 30 min), and incubated overnight at 4°C with primary antibodies: guinea pig anti-c-Fos (1:2000; Synaptic Systems, #226004) and rabbit anti-RFP (1:4000; Rockland, #600-401-379) diluted in 2% NGS / 0.1% TXT / PBS. Primary antibodies were detected using fluorescent secondary antibodies: Alexa 488 donkey anti-guinea pig (1:500; Thermo Fisher Scientific, #S32354) and Alexa 594 goat anti-rabbit (1:500; Abcam, #ab150160). Images were acquired using a Nikon C2 confocal laser-scanning microscope (20× objective, NA 0.75), and colocalization analysis was performed using NIS-Elements software. Three sagittal MRR sections per animal were analyzed. Cell counts were performed using a semi-automated method. Positive nuclei were first identified in NIS-Elements software using an intensity threshold, followed by manual, blinded verification by the experimenter. For each animal, counts were made within a standardized Region of Interest (ROI) encompassing the MRR across three sagittal sections, and these values were then averaged.

Behaviorally Induced Activation (ZsGreen Mice): To assess activation of VGAT-MRR neurons following specific social behaviors, VGAT-Cre x ZsGreen mice were perfused 1.5 hours (for c-Fos activation) after the sociability test or RIT. Sections were washed in PBS (3 x 10 min), permeabilized (0.3% TXT in PBS for 30 min), and blocked (2.5% BSA in PBS for 30 min). Sections were then incubated for 3 days at 4°C with rabbit anti-c-Fos primary antibody (1:1000; Santa Cruz Biotechnology, #sc-52) diluted in 2.5% BSA/PBS. The primary antibody was detected using goat anti-rabbit Alexa 594 secondary antibody (1:500; Abcam, #ab150160). Sections were mounted with Mowiol. Fluorescence signals (c-Fos red, ZsGreen green) were imaged using a Panoramic Digital Slide Scanner (Zeiss, Plan-Apochromat 10×/NA 0.45, 3DHISTECH Pannoramic MIDI II) equipped with an LED light engine (Lumencor SPECTRA X). Colocalization and cell counts were analyzed using NIS-Elements software. Three sagittal MRR sections per animal were analyzed.

3.7 Molecular Biology Methods

To complement the IHC analyses and confirm the presence of dopaminergic markers at the molecular level, RT-PCR was performed to detect mRNA expression in dissected brain regions.

3.7.1 Verification of the Presence of DA in the MRR by RT-PCR

For measurements in mice, wild-type, C57BL6/J animals were sacrificed, and their DRN and MRR region were dissected by punch needles, before being fresh frozen on dry ice. Samples were kept on −80 °C until further preparations for one-step PCR.

In the case of human samples, the study was approved by the Hungarian Medical Research Council—Scientific and Research Ethical Committee (Egészségügyi Tudományos Tanács—Tudományos és Kutatásetikai Bizottság, #40197-2/2019/EKU), in accordance with the Ethical Rules for Using Human Tissues for Medical Research in Hungary (HM 34/1999) and the Code of Ethics of the World Medical Association (Declaration of Helsinki). Post-mortem brain samples were obtained from the Human Brain Tissue Bank, Semmelweis University (Budapest, Hungary). The brains of twelve individuals who died of natural causes were used in the measurement. All RT-PCR experiments used glyceraldehyde 3-phosphate dehydrogenase (GAPDH) as a housekeeping gene for normalization, and product sizes were validated against expected molecular weights (e.g., DAT amplicon matched predicted length).

3.7.2 RNA Extraction and cDNA Synthesis

Frozen samples from mice were thawed and total RNA was processed according to RNeasy® Mini Kit instructions (QIAGEN, Germantown, MD, USA, #74106). Reverse transcription (High-Capacity RNA-to-cDNA™ Kit, Thermo Fisher Scientific, Budapest, Hungary #4387406) and one-step PCR (DreamTaqTM Green PCR Master Mix, Thermo Fisher Scientific, Budapest, Hungary, K1085) were performed by Biometra Tone (Analytik Jena, Jena, Germany). The following primers were designed using Primer-BLAST (NCBI) and were acquired from Integrated DNA Technologies (IDT; Coralwille, Iowa, USA): GAPDH (housekeeping gene), DAT, TH and DBH.

For human samples, post-mortem brain tissue containing the pontine raphe nucleus was obtained from the Human Brain Tissue Bank, Semmelweis University (Budapest, Hungary), with ethical approval from the Hungarian Medical Research Council (#40197-2/2019/EKU) and in accordance with relevant ethical guidelines. Samples were from nine individuals (3 females, 6 males; age range: 27-67 years, mean: 52.4 ± 11.8 years) who died of natural causes, with post-mortem delays ranging from 2 to 10 hours (mean: 5.7 ±

2.3 hours). Causes of death included myocardial infarction, cardiorespiratory insufficiency, pulmonary embolism, pneumonia, and cancer. Total RNA was isolated using the RNeasy® Mini Kit according to the manufacturer's instructions. RNA was diluted into RNase-free water. The quality and quantity of extracted RNA were determined using NanoDrop ND-1000 Spectrophotometer (Thermo Fisher Scientific, Budapest, Hungary), and only those with A260/A280 ratio between 1.8 and 2.1 were used in subsequent experiments. Initial RNA concentrations for these samples ranged from 144.50 ng/µL to 1048.20 ng/µL. The isolated RNA concentration was calculated and normalized with RNase-free water to 1000 ng before reverse transcription into cDNA using a SuperScript II reverse transcriptase kit (Invitrogen, Carlsbad, CA, USA). After 10-fold dilution, 2.5 µL of the resulting cDNA was used as template in PCR. The PCR reactions were performed on CFX-96 C1000 Touch Real-Time System (Bio-Rad Laboratories, Hercules, CA, USA) with iTaq DNA polymerase (Bio-Rad Laboratories, Hercules, CA, USA) in total volumes of 12.5 µL under the following conditions: 95 °C for 3 min, followed by 35 cycles of 95 °C for 0.5 min, 60 °C for 0.5 min and 72 °C for 1 min. All the determinations were conducted in duplicate. The primers used for RT-PCR were synthesized by IDT (Coralville, IA, USA) and used at 300 nM final concentration. Sequences of primers are listed in Table 1.

Table 1. - List of primers for PCR.

Primer ID	**Bases**	**Sequence**	**NCBI reference sequence**	**Product Size (bp)**
hDAT-E-1-F	20	GTC TGT TTG GAT TGA CGC GG	NM_001044.5	205
hDAT-E-1-R	20	ACT GTG CTT CTG TGC CAT GT		

A: adenine; C: cytosine; E: exon-exon junction; F: forward primer; G: guanine hDAT: human dopamine transporter; R: reversed primer; T: thymine.

3.7.3 Agarose Gel Electrophoresis

To verify successful PCR amplification and confirm the expected size and specificity of the amplified DNA products, one-third of each PCR product was loaded onto a 1.2% agarose gel containing EcoSafe nucleic acid staining solution (1:20,000;

Pacific Image Electronics). Electrophoresis was performed in 1× TAE buffer (40 mM Tris-acetate, 1 mM EDTA, pH 8.0) at 100 V. DNA bands were subsequently visualized using UV transillumination and their sizes were compared against expected molecular weights.

3.8 Experimental Design and Project-Specific Procedures

Project I.: The role of the GABAergic cells of the MRR in reinforcement-based learning

Experiment 1. (Nonspecific MRR manipulation): all C57BL/6J mice received injections of a non-Cre-dependent AAV2-hSyn-hM3Dq-mCherry (stimulatory DREADD) into MRR and after 28 days recovery animals underwent an operant conditioning paradigm consisting of 14 days of learning, and seven days of reversal learning. This was followed by four days of recovery and then an active avoidance paradigm consisting of five days of learning and five days of reversal learning. Control animals received saline injections instead of CNO every test day 30 minutes before testing.

After completion IHC was performed to verify viral expression and only mice with correct hits were included in further analysis (MRR-stimulated: n = 9; control: n = 6). To characterize the neurochemical identity of virally transduced cells in the MRR, we performed IHC analyses using fluorescent markers for RFP (infected cells), GABA (GABAergic neurons), VGluT3 (subset of glutamatergic neurons), and TPH (serotonergic neurons). Due to technical constraints with antibody compatibility, the staining was conducted in two separate immunostaining runs. One run used antibodies against RFP and GABA, while the other used antibodies against RFP, VGluT3, and TPH.

To verify that the DREADD is functionally expressed in RFP+ neurons we perfused the animals transcardially 2 hours after a CNO injection for c-Fos and RFP IHC.

Experiment 2. (VGAT-MRR neuron manipulation): VGAT-Cre mice received MRR injections of Cre-dependent viruses encoding control, stimulatory, or inhibitory DREADD constructs. The behavioral procedures followed those of Experiment 1., with the operant conditioning learning phase lasting 10 days and the reversal learning phase seven days. The active avoidance learning phase lasted seven days, and the reversal

learning phase three days. All animals in this experiment received CNO injections. Due to missing data, only the first five days of active avoidance learning are presented for both experiments.

Project II.: VGAT-MRR neurons contribute to social interest in mice

First, similar to Project I. Experiment 1. CNO-induced neuronal activation was studied in VGAT-Cre mice expressing either the stimulatory (hM3Dq-RFP, n = 4) or control (RFP only, n = 4) AAV constructs. Validation of the inhibitory DREADD (hM4Di) via c-Fos was not performed, as detecting inhibition through reduced c-Fos expression is less direct than detecting activation. Only mice with accurate viral injections confined to the MRR, confirmed by RFP fluorescence (Fig.16a), were included. Ninety minutes following an i.p. CNO injection, these animals were deeply anesthetized and transcardially perfused for tissue processing.

Next, another group of VGAT-Cre mice received MRR injections of viruses encoding either stimulatory (hM3Dq-mCherry, n = 9), inhibitory (hM4Di-mCherry, n = 10), or control (mCherry only, n = 12) constructs and manipulated with CNO 30 minutes before each test. We investigated 3 social behaviors: sociability, SIT and RIT. As possible confounder locomotion (OF), anxiety-related behavior (EPM), and short-term memory (SDT, y-maze) were also examined. The use of both OF and EPM tests provided complementary measures of anxiety-like behavior that could reveal subtle phenotypes not captured by a single test (Ramos, 2008). Additionally, GABAergic transmission within the raphe nuclei has been specifically linked to anxiolytic drug effects, making these neurons particularly relevant targets for anxiety assessment (Nunes-de-Souza et al., 2000).

Additionally, to assess the activation of VGAT-MRR neurons in response to social behavior, the previously described VGAT-Cre x ZsGreen double transgenic mice were utilized without stereotaxic surgeries. Two separate cohorts were conducted. The first cohort underwent the sociability test, while the second cohort underwent the RIT. Ninety minutes after each respective test, animals were perfused. This allowed for the measurement of neuronal activation (c-Fos expression by IHC) specifically within the ZsGreen-labeled VGAT-MRR neurons. Control groups (sociability: n=7; RIT: n=5), which did not participate in the behavioral tests, underwent the same perfusion procedure

to establish baseline c-Fos expression. The experimental groups (sociability: n=9; RIT: n=7) were used to determine behaviorally-induced changes in c-Fos expression.

Project III.: The DAT-MRR cells Regulate Social Behavior in Male Mice

First, we confirmed the presence of dopaminergic cells in the MRR and validated the specificity of our approach, which was challenging due to their low abundance and overlapping markers with other catecholaminergic cell types. We used DAT-Cre mice, which express Cre recombinase under the control of the DAT promoter. DAT is a key regulator of dopamine neurotransmission, primarily expressed in dopaminergic neurons, and its localization is critical for understanding dopaminergic circuits (Ciliax et al., 1995). While DAT-Cre models are well-validated for major dopaminergic nuclei, their specificity in atypical regions like the MRR needed confirmation due to reports of potential off-target recombination (Papathanou et al., 2019). To address this, we injected a Cre-dependent AAV vector expressing the reporter protein RFP into the MRR of DAT-Cre mice, followed by IHC analysis for TH, DBH, and DAT.

We confirmed that dopamine was expressed and packed in vesicles within the MRR by using RT-PCR to detect TH, DBH, and DAT mRNA. For translational relevance, we also tested equivalent human postmortem brain samples alongside negative controls from the temporal and frontopolar cortex. To investigate the function of these cells, we then compared the behavior of DAT-Cre mice injected with control, stimulatory, or inhibitory DREADD constructs, using the same test battery as in Project II.

Notably, we had initially considered employing operant conditioning techniques to elucidate the involvement of DAT-MRR neurons in the reward system. Additionally, due to involvement of DA in prolactin secretion regulation, we made attempts to measure this hormone from the blood after DAT-MRR manipulation. However, due to technical difficulties, we did not get reasonable results from both experimental series.

3.9 Statistical Analysis

Data were analyzed by Statistica software (StatSoft, Tulsa, OK, USA; version 13.0 for Projects I. and III., version 13.4 for Project II.). Data are presented as mean ± SEM.

In all projects, a p-value less than 0.05 was considered statistically significant. Statistical significance is represented by asterisks. Dots/Triangles represent individual values.

A combination of statistical tests was used across the projects, including single-sample t-tests, one-way ANOVAs, and repeated-measures ANOVAs, followed by Fisher's LSD post-hoc comparisons where appropriate. Single-sample t-tests were used to compare SI, SD and spontaneous alternation to a chance level of 50%. Repeated-measures ANOVAs were used to analyze the effects of treatment and time on various behavioral measures. The specific within-subjects factors varied across projects and included choice (e.g., left vs. right, familiar vs. novel), time, and specific behavioral measures. One-way ANOVAs were used in Project I. to compare treatment groups, followed by Bonferroni post-hoc comparisons.

4 Results

4.1 Project I. The role of VGAT-MRR cells in reinforcement-based learning

In Experiment 1. we employed nonspecific chemogenetic stimulation of the entire MRR in C57BL/6J mice, while in Experiment 2. we focused on the specific role of VGAT-MRR neurons, utilizing VGAT-Cre mice and Cre-dependent DREADD viral vectors to achieve selective manipulation (Fig.5).

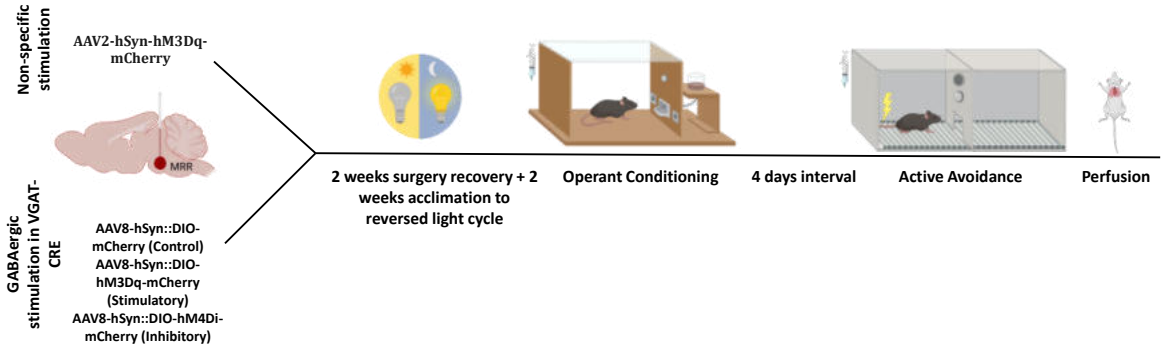

Figure 5 - Experimental outline of Project I.: Mice (C57BL/6J with AAV2-hSyn-hM3Dq-mCherry for nonspecific stimulation; VGAT-Cre for GABAergic stimulation: Control (AAV8-hSyn::DIO-mCherry), Stimulatory (AAV8-hSyn::DIO-hM3Dq-mCherry), or Inhibitory (AAV8-hSyn::DIO-hM4Di-mCherry)) received stereotaxic viral injections into the MRR. Following a 4-week post-surgery recovery period, mice underwent sequential behavioral testing. 1) Operant Conditioning (exp.1.: 14 days + 7 days reversed; exp.2.: 10 days + 7 days reversed), followed by a 4-day recovery interval. 2) Active Avoidance testing (exp.1.: 5 days + 5 days reversed; exp.2.: 7 days + 3 days reversed). In both projects, mice received i.p. injections of CNO (1 mg/kg/10mL, all groups in GABAergic stimulation; or vs. saline control in case of nonspecific stimulation) 30 minutes before each behavioral session. Perfusion for histological analysis was performed 2 hours after the final CNO injection, subsequent to active avoidance testing completion. Figure designed by the author.

4.1.1 Nonspecific MRR Stimulation

In the RFP/GABA immunostaining, 45.34% of RFP+ cells also stained positive for GABA (Fig. 6a-b). In the RFP/VGluT3/TPH IHC, smaller proportions of RFP+ neurons were TPH+ (0.34%), VGluT3+ (6.06%), or co-expressed both VGluT3 and TPH (1.39%) (Fig. 6c-d). A substantial proportion (92.20%) of RFP+ cells in the VGluT3/TPH run did not express detectable levels of either VGluT3 or TPH.

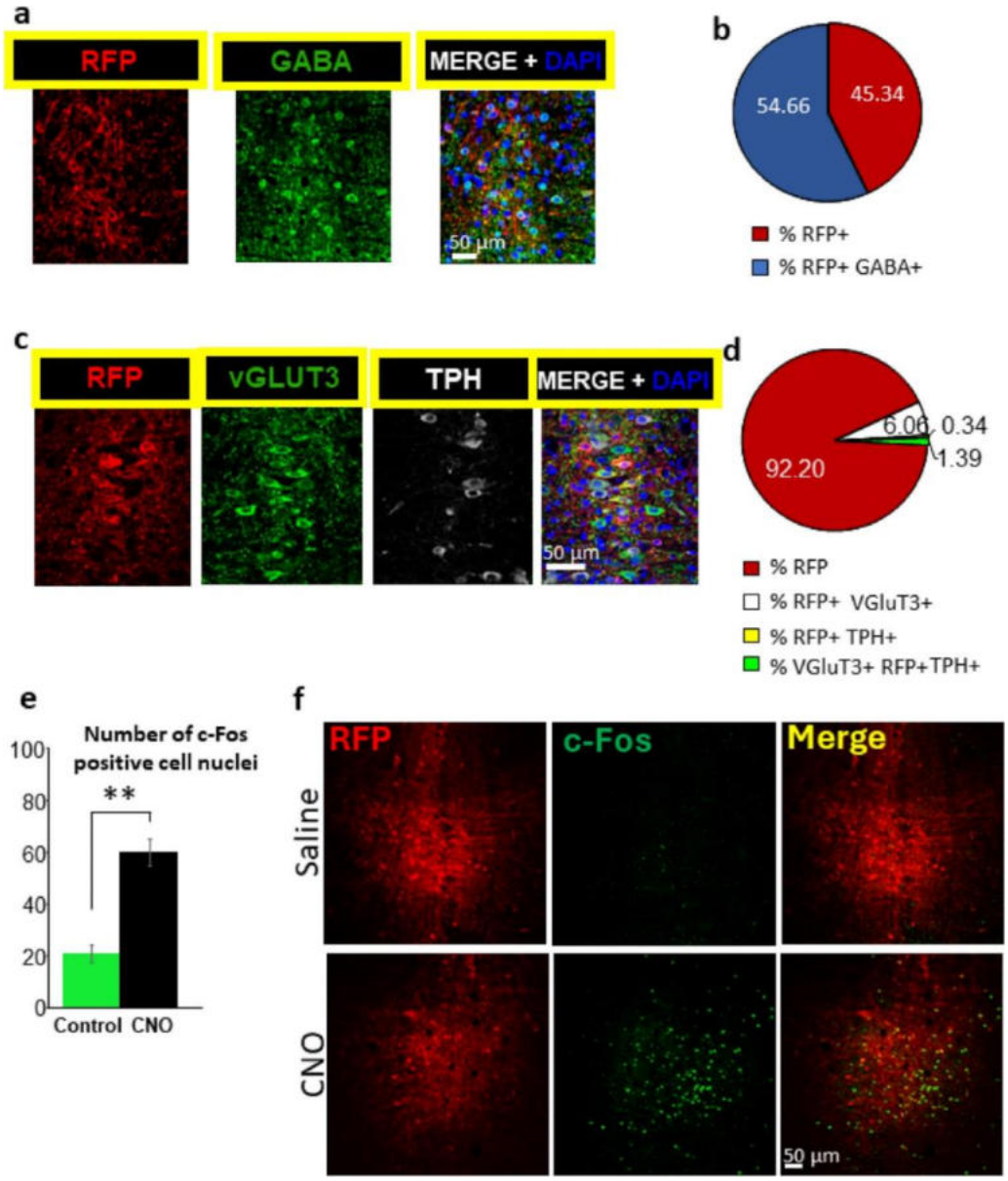

Figure 6 - Colocalization of GABAergic and viral infection (RFP) markers: (a) Representative image of the MRR showing virally transduced cells (RFP, red) and GABAergic neurons (green) (40× magnification). (b) Quantification of colocalization, showing the percentage of RFP-positive cells that are also GABA-positive. (c) Representative image of the MRR showing RFP-positive cells (red), VGluT3-positive neurons (green), TPH-positive neurons (blue) (40× magnification). (d) Percentage of RFP-positive cells expressing each neurotransmitter marker. (e) Quantification of c-Fos-positive nuclei in CNO-injected DREADD-expressing mice and saline-injected controls. ** $p < 0.01$ (t-test) (f). Representative image of neuronal activation visualized by c-Fos (green) and RFP (red) colocalization. Figure reproduced from Chaves et al., 2024.

Because the GABA staining was performed in a separate run from the VGluT3/TPH staining, we could not directly assess the degree of overlap between

GABAergic neurons and the VGluT3/TPH+ populations. Therefore, it is possible that some of those RFP+ cells that did not stain for VGluT3 or TPH were, in fact, GABAergic. 47.9% of cells infected by the virus carrier were stained neither for the GABAergic marker nor for the VGluT3 or TPH, suggesting the presence of other neurochemical phenotypes or technical limitations in detecting these markers.

Further, we confirmed that RFP positivity represented functional DREADD expression, as i.p. CNO injection significantly increased c-Fos expression in the MRR of DREADD-expressing mice compared to saline-injected controls ($p < 0.01$; Fig. 6e-f). While the majority of c-Fos expression was observed in RFP-positive cells, some non-RFP-positive neurons also exhibited c-Fos, suggesting that the chemogenetic stimulation may have engaged local neuronal circuits and indirectly influenced activity in neighboring cells.

4.1.1.1 Operant Conditioning

During the learning phase, one nose poke was rewarded with a food pellet, while the other was unrewarded. During reversal (cognitive flexibility) the active nose poke was switched (Fig.7).

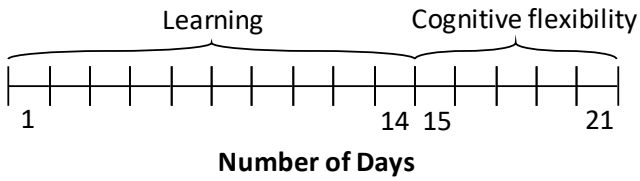

Figure 7 - Schematic timeline of the operant conditioning test. The learning phase consisted of 14 days while the reversal learning phase lasted for 7 days, each with 30-minute training sessions per day and with i.p. saline/CNO 30 min before each section. Figure reproduced from Chaves et al., 2024.

Learning Phase (Days 1-14): During the initial learning phase, both control and MRR-stimulated groups demonstrated engagement with the task, evidenced by an increase in total responses over time (Fig. 8a; $p < 0.001$; Table 2.). However, the primary measure of learning, reward preference, did not differ significantly between the groups (Fig. 8b; $p = 0.882$; Table 2.). While both groups showed some learning, neither consistently achieved high levels of accuracy (e.g., remaining below 70% preference) during the 14-day period, and performance did not consistently exceed chance levels

(50%). Thus, nonspecific MRR stimulation did not significantly impact the acquisition of reward preference during this initial learning period.

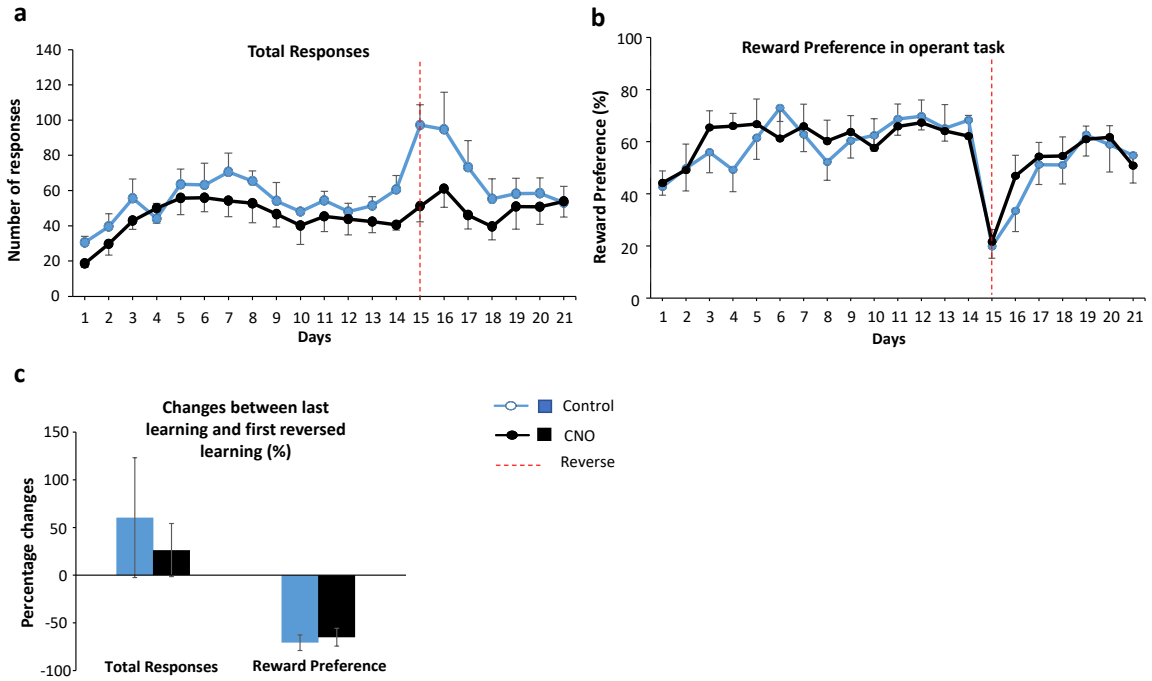

Figure 8 - Operant conditioning performance after nonspecific MRR stimulation. Graphs depict (a) total number of responses, (b) reward preference, and (c) change in performance from the last day of learning to the first day of reversal learning. Figure reproduced from Chaves et al., 2024.

Reversal Learning Phase (Days 15-21): Following the switch in the rewarded nose poke, total responses initially increased for both groups (Fig. 8a). During this phase, MRR-stimulated mice exhibited marginally lower total responses compared to controls ($p = 0.061$; Table 2.). However, no significant group differences were detected in reward preference during reversal learning (Fig. 8b; Table 2.). A direct comparison of performance change from the last day of learning to the first day of reversal also revealed no significant group differences in either reward preference ($p = 0.526$) or total responses ($p = 0.244$; Fig. 8c). Overall, despite marginal differences, nonspecific MRR stimulation did not clearly impair the ability to learn the reversed rule.

Table 2. - Statistical details for the whole MRR stimulation analyzed by repeated measures ANOVA

Experiment		Parameters	Effect	Degree of freedom	F	p
	Learning	Total Responses	Treatment	1,13	1.620	0.225

Operant Conditioning			Time	13,169	4.657	0.000
			Time x Treatment	13,169	0.399	0.968
		Reward Preference	Treatment	1,13	0.022	0.882
			Time	13,169	2.591	0.002
			Time x Treatment	13,169	0.666	0.793
	Reversal learning	Total Responses	Treatment	1,12	2.614	0.131
			Time	6,72	3.300	0.006
			Time x Treatment	6,72	2.117	0.061
		Reward Preference	Treatment	1,12	0.144	0.710
			Time	6,72	11.431	0.000
			Time x Treatment	6,72	0.418	0.864
	Learning +reversal learning	Total Responses	Treatment	1,12	3.521	0.085
			Time	20,240	4.080	0.000
			Time x Treatment	20,240	0.960	0.511
		Reward Preference	Treatment	1,12	0.133	0.722
			Time	20,240	4.503	0.000
			Time x Treatment	20,240	0.494	0.967
Active avoidance	Learning	N# of EDST	Treatment	1,7	0.007	0.933
			Time	4,28	16.205	0.000
			Time x Treatment	4,28	1.954	0.115
		N# of EDFS	Treatment	1,7	0.250	0.625
			Time	4,28	8.000	0.000
			Time x Treatment	4,28	0.388	0.815
		N# of ESFL	Treatment	1,7	0.386	0.544
			Time	4,28	0.810	0.524
			Time x Treatment	4,28	0.759	0.556
		Average latency to escape	Treatment	1,12	0.023	0.883
			Time	4,28	13.190	0.000

			Time x Treatment	4,28	0.634	0.641
	Reversal learning	N# of EDST	Treatment	1,7	1.053	0.323
			Time	4,28	16.419	0.000
			Time x Treatment	4,28	0.709	0.589
		N# of EDFS	Treatment	1,7	1.862	0.195
			Time	4,28	0.923	0.457
			Time x Treatment	4,28	1.478	0.222
		N# of ESFL	Treatment	1,7	1.372	0.262
			Time	4,28	7.288	0.000
			Time x Treatment	4,28	2.270	0.074
	Learning +Reversal learning	N# of EDST	Treatment	1,13	0.000	0.982
			Time	9,117	22.157	0.000
			Time x Treatment	9,117	0.838	0.582
		N# of EDFS	Treatment	1,13	1.474	0.246
			Time	9,117	32.055	0.000
			Time x Treatment	9,117	0.335	0.962
		N# of ESFL	Treatment	1,13	1.478	0.246
			Time	9,117	111.291	0.000
			Time x Treatment	9,117	0.933	0.499

Significant results in red; Marginally significant results in blue.

4.1.1.2 Active avoidance

Performance was evaluated across a learning phase (Days 1-5) and a subsequent reversal learning phase (Days 6-10), where the shocked compartment was switched (see Fig.9 for schematic timeline).

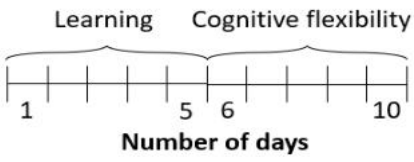

Figure 9 - Schematic timeline of the active avoidance test. The test consisted of 5 days of learning and 5 days of reversal learning phase. Each day comprised 40 trials of 30 seconds each, with 1-minute habituation before the start and 5-second intertrial

intervals. Learning was facilitated by sound and light cues. Figure reproduced from Chaves et al., 2024.

Learning Phase (Days 1-5): Both control and MRR-stimulated mice showed an increase in successful EDST across trials, suggesting learning of the avoidance response (Fig. 10a-b; Table 2.). This was accompanied by a gradual decrease in EDFS. Similarly, ESFL remained relatively low and did not change significantly during the learning phase (Fig. 10b). No significant differences were observed between the groups for EDST, EDFS, ESFL or average escape latency, a potential measure of impulsivity (Fig. 10a-c). These results suggest that nonspecific MRR stimulation does not significantly alter the acquisition of an active avoidance response, nor affect a gross measure of impulsivity.

Reversal Learning Phase (Days 6-10): Both groups exhibited a rapid and significant decrease in EDST (Fig. 10a), indicating successful adaptation to the reversed contingencies. ESFL (i.e., correct responses during reversal) increased in both groups across trials. While there was a marginal interaction between group and time for ESFL ($p = 0.07$; Table 2.; Fig 10b), suggesting that MRR stimulation may have subtly influenced the adaptation to the reversal, this trend did not reach the level of significance. Analysis of the change in performance between the last day of learning and the first day of reversal learning revealed no significant group differences for EDST, EDFS (Fig. 10d), or ESFL (Fig. 10e). These results indicate that, while both groups were able to adapt to the reversed contingencies, nonspecific MRR stimulation produced a marginally significant effect on the time course of adapting to the correct response, without significantly altering the overall rate of reversal learning.

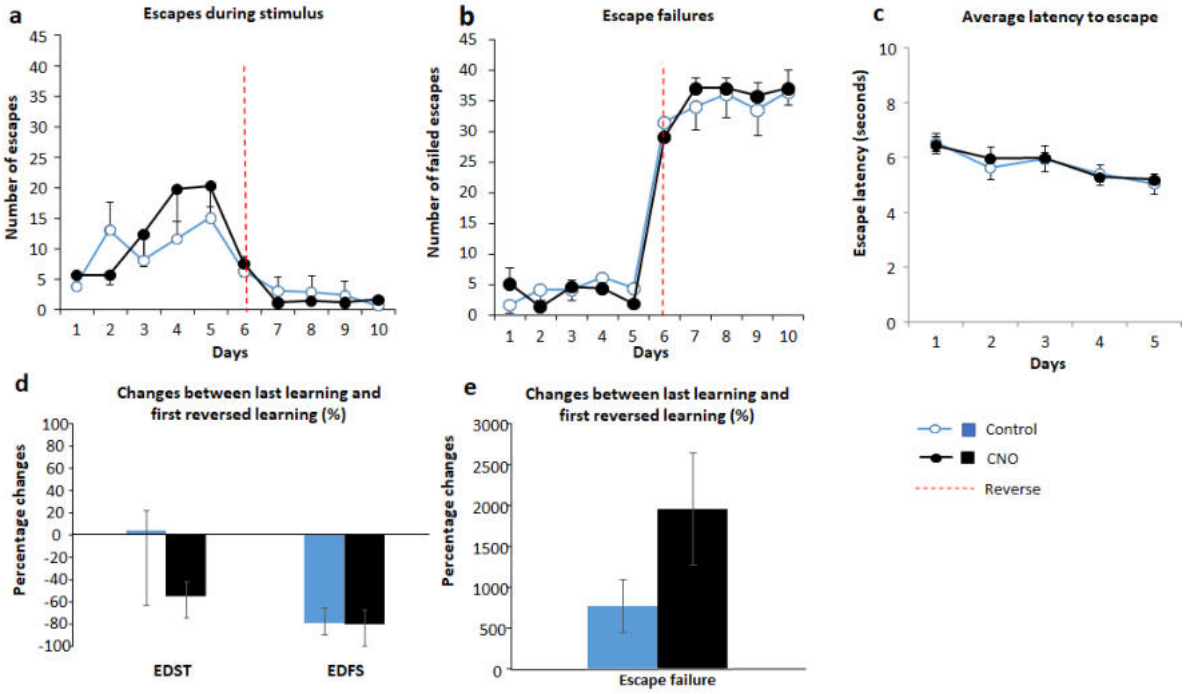

Figure 10 - Active avoidance after nonspecific MRR stimulation. Graphs show (a) EDST during learning and reversal phases, (b) ESFL, (c) average escape latency, (d) percentage change in EDST and EDFS, and (e) percentage change in ESFL between last learning day and first reversal day. Figure reproduced from Chaves et al., 2024.

4.1.2 Chemogenetic Manipulation of VGAT-MRR Neurons

IHC analysis confirmed successful transduction of GABAergic neurons in the MRR with the DREADD-containing AAV vectors, indicated by the presence of RFP (Fig. 11).

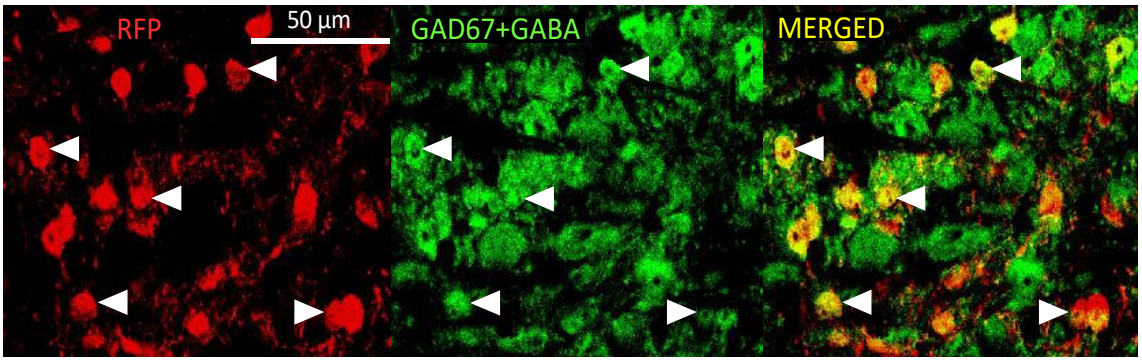

Figure 11 - Confirmation of the VGAT-Cre strain by IHC. The RFP was expressed in GABAergic neuron of the MRR of the VGAT-Cre mouse. RFP (the fluorophore of DREADD, red) as well as GABA (with a mixture of GABA and GAD67 antibodies, green) were labelled with double immunofluorescent staining and the last panel shows their overlap (yellow) indicated by arrows. Scale bar: 50 µm. Figure reproduced from Chaves et al., 2024.

However, the data do not allow to conclude whether all the GABAergic cells expressed RFP, and we cannot exclude the transfection of non-GABAergic cells, either.

4.1.2.1 Operant Conditioning

Learning Phase (Days 1-10; Fig. 12): Mice in all three groups demonstrated engagement with the operant conditioning task, as shown by a gradual increase in total responses over time (Fig. 13a; $p < 0.001$; Table 3.), reflecting motivation to perform the task. Learning, indexed by reward preference, also increased over the learning phase (Fig. 13b; $p < 0.001$; Table 3.). The overall repeated-measures ANOVA comparing the groups across the entire learning phase revealed no significant main effect of treatment or treatment × time interaction for reward preference (Table 3.). This indicates that manipulating VGAT-MRR neurons did not significantly alter the overall acquisition of reward preference.

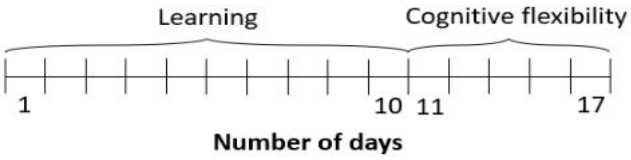

Figure 12 - Schematic timeline of the operant conditioning test in VGAT-Cre mice. The learning phase lasted for 10 days, while the reversal learning phase lasted seven days. Figure reproduced from Chaves et al., 2024.

Reversal Learning Phase (Days 11-17): While control and inhibitory DREADD groups showed the expected decrease in total responses after the rewarded nose poke change, the stimulatory DREADD group maintained a high level of responding (Fig. 13a), resulting in a significant main effect of treatment on total responses ($p = 0.027$; Table 3.). Furthermore, the stimulatory DREADD group displayed a higher reward preference during reversal learning compared to the other groups ($p = 0.035$; Table 3.). However, the initial adaptation (change from Day 10 to Day 11) did not differ significantly between groups (Fig. 13c).

Analysis of timeout responses, a measure of impulsivity, revealed a significant treatment effect specifically during the reversal learning phase ($p = 0.031$; Fig. 13d; Table 3.). Post hoc tests confirmed that the stimulatory DREADD group exhibited significantly more timeout responses than both the control and inhibitory DREADD groups ($p < 0.05$ for both).

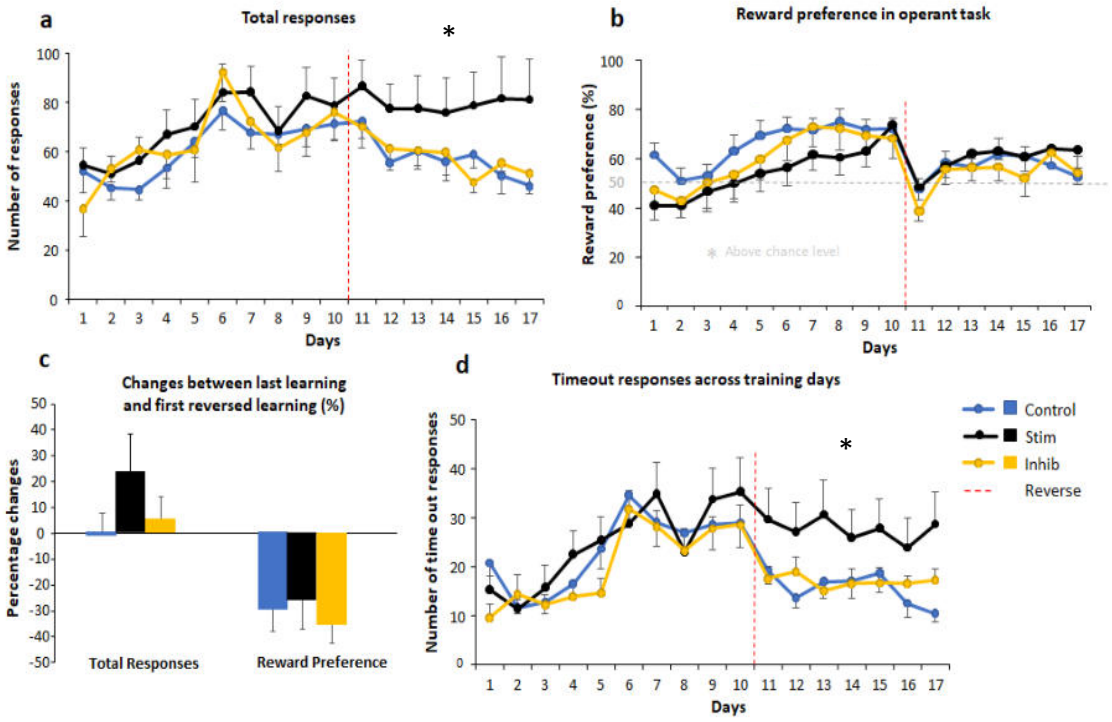

Figure 13 - Operant conditioning performance following manipulation of VGAT-MRR neurons. Graphs depict total number of responses (a), reward preference (b), change in performance from learning to reversal (c), and timeout responses (d) for control, stimulatory, and inhibitory groups. *$p < 0.05$. Figure reproduced from Chaves et al., 2024.

Taken together, the sustained high total response rate, coupled with the significantly increased timeout responses during the reversal phase, strongly suggests that stimulating VGAT-MRR neurons impairs behavioral flexibility and promotes perseverative or impulsive responding. These mice appeared less able to suppress the previously learned response pattern or inhibit responses during the timeout period when faced with changed task rules, highlighting a key role for VGAT-MRR neurons in adapting behavior under shifting reward conditions.

4.1.2.2 Active avoidance

During the learning phase (Days 1-7, Fig. 14): All groups showed an increase in EDST (Fig. 15a; Table 3.). The stimulatory DREADD group exhibited a significantly higher number of EDST compared to the control and inhibitory DREADD groups ($p < 0.05$; Fig 15a). EDFS and ESFL (Fig. 15b) gradually decreased in all groups, although these changes were not significant.

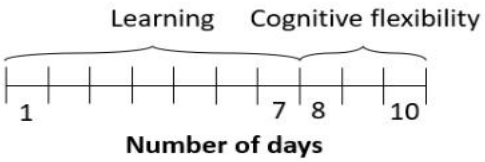

Figure 14 - Schematic timeline of the active avoidance test in VGAT-Cre mice. The learning phase lasted for seven days, while the reversal learning phase for three days. Figure reproduced from Chaves et al., 2024.

During the reversal learning phase (Days 8-10): The number of EDST decreased across trials in all groups (Fig. 15a). Similar to the nonspecific MRR stimulation, ESFL increased during reversal learning (Fig. 15b); however, there were no significant differences between groups. Considering the entire observation period, the difference in EDST between the stimulatory DREADD group and the other two groups was more pronounced and highly significant ($p < 0.01$; Fig. 15a; Table 3.). No significant group differences were observed in the change in performance between the last day of learning and the first day of reversal learning (Fig. 15c). Average escape latency during learning, a measure of impulsivity, did not differ significantly between groups (Fig. 15d).

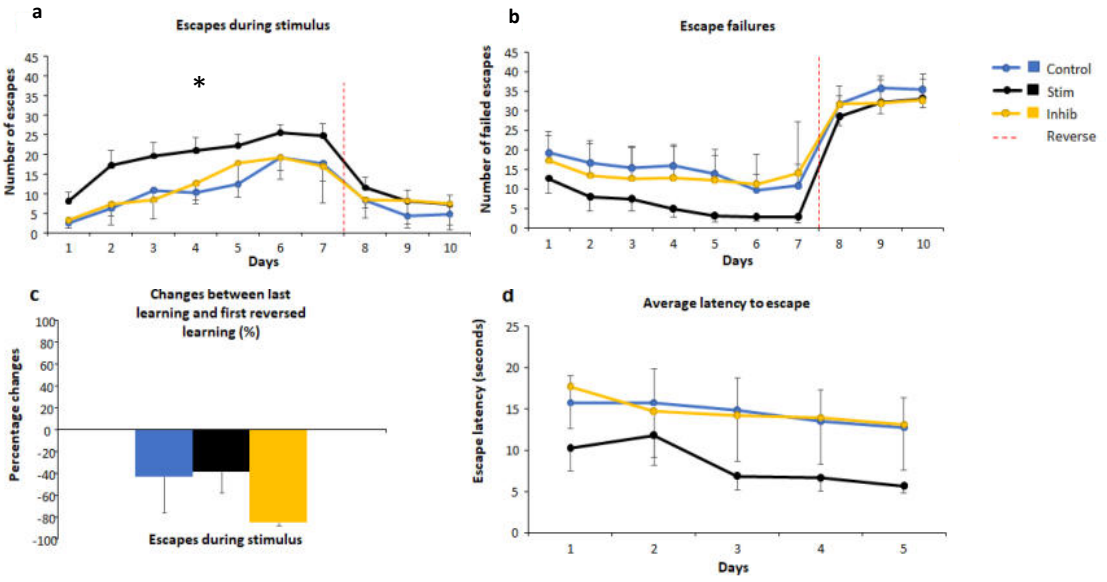

Figure 15 - Active avoidance after manipulation of VGAT-MRR cells. (a) EDST across learning and reversal phases. (b) ESFL (c) Percentage change in EDST between last learning day and first reversal day. (d) Average escape latency. *p < 0.05. Figure reproduced from Chaves et al., 2024.

Table 3. - Statistical details for VGAT-MRR manipulation analyzed by repeated measures ANOVA.

Experiment		Parameters	Effect	Degree of freedom	F	p
Operant Conditioning	Learning	Total Responses	Treatment	2,35	1.410	0.257
			Time	9,315	13.772	0.000
			Time x Treatment	18,315	1.094	0.356
		Reward Preference	Treatment	2,35	1.163	0.324
			Time	9,315	16.807	0.000
			Time x Treatment	18,315	0.909	0.567
		Timeout response	Treatment	2,35	0.539	0.588
			Time	9,315	16.883	0.000
			Time x Treatment	18,315	1.146	0.307
	Reversal learning	Total Responses	Treatment	2,35	4.031	0.027
			Time	6,210	2.941	0.009
			Time x Treatment	12,210	0.567	0.866
		Reward Preference	Treatment	2,35	3.721	0.035
			Time	6,210	7.652	0.000
			Time x Treatment	12,210	0.932	0.515
		Timeout response	Treatment	2,35	3.822	0.031
			Time	6,210	0.461	0.837
			Time x Treatment	12,210	0.512	0.906
	Learning + Reversal learning	Total Responses	Treatment	2,32	2.566	0.092
			Time	16,512	9.561	0.000
			Time x Treatment	32,512	0.974	0.511
		Reward Preference	Treatment	2,35	1.153	0.328
			Time	16,560	9.748	0.000
			Time x Treatment	32,560	1.584	0.024
		Timeout response	Treatment	2,35	1.753	0.188
			Time	16,560	9.174	0.000
			Time x Treatment	32,560	1.417	0.066
Active avoidance	Learning	N# of EDST	Treatment	2,27	4.570	0.019
			Time	6,162	24.146	0.000

			Time x Treatment	12,162	1.099	0.363
		N# of EDFS	Treatment	2,27	1.070	0.356
			Time	6,162	7.706	0.000
			Time x Treatment	12,162	1.255	0.250
		N# of ESFL	Treatment	2,27	2.325	0.116
			Time	6,162	3.054	0.007
			Time x Treatment	12,162	0.879	0.568
		Average latency to escape	Treatment	2,36	2.545	0.092
			Time	4,144	3.009	0.020
			Time x Treatment	8,144	0.406	0.916
	Reversal learning	N# of EDST	Treatment	2,36	0.330	0.720
			Time	2,72	10.168	0.000
			Time x Treatment	4,72	0.713	0.585
		N# of ESFL	Treatment	2,36	0.320	0.727
			Time	2,72	10.593	0.000
			Time x Treatment	4,72	0.741	0.566
	Learning + Reversal learning	N# of EDST	Treatment	2,27	7.555	0.002
			Time	9,243	16.859	0.000
			Time x Treatment	18,243	0.818	0.678
		N# of ESFL	Treatment	2,27	3.124	0.060
			Time	9,243	49.196	0.000
			Time x Treatment	18,243	1.066	0.388

Significant results in red; Marginally significant results in blue.

4.2 Project II. - VGAT-MRR neurons contribute to social interest in mice

4.2.1 Chemogenetic efficacy and neuronal activation

To validate the efficacy and specificity of our Cre-dependent DREADD-mediated chemogenetic approach within the MRR, we first examined neuronal activation using c-Fos IHC, similarly as we did for non-Cre-dependent viruses in Project I. (see Fig.6). As expected, CNO injection significantly increased the overall number of c-Fos-positive neurons throughout the MRR in the stimulatory group compared to the control group ($F(1,6) = 22.370$, $p = 0.003$; Fig. 16b-c), confirming successful DREADD-mediated neuronal activation. While the total count of neurons co-expressing c-Fos and RFP showed only a marginal increase ($F(1,6) = 3.927$, $p = 0.095$; Fig. 16d). Notably, the overall increase in c-Fos positive cells in the MRR (Fig. 16c) was substantially greater than the increase within the RFP-positive population alone (Fig. 16d), indicating a

significant indirect activation of the surrounding, non-transduced neuronal network Critically, the proportion of RFP-positive GABAergic neurons that also expressed c-Fos was significantly higher in the stimulatory compared to control group ($F(1,5) = 13.583$, $p = 0.014$; Fig. 16e). These results confirm that our chemogenetic strategy successfully targets VGAT-MRR neurons and that CNO effectively engages the stimulatory DREADD to increase neuronal activity within this specific population.

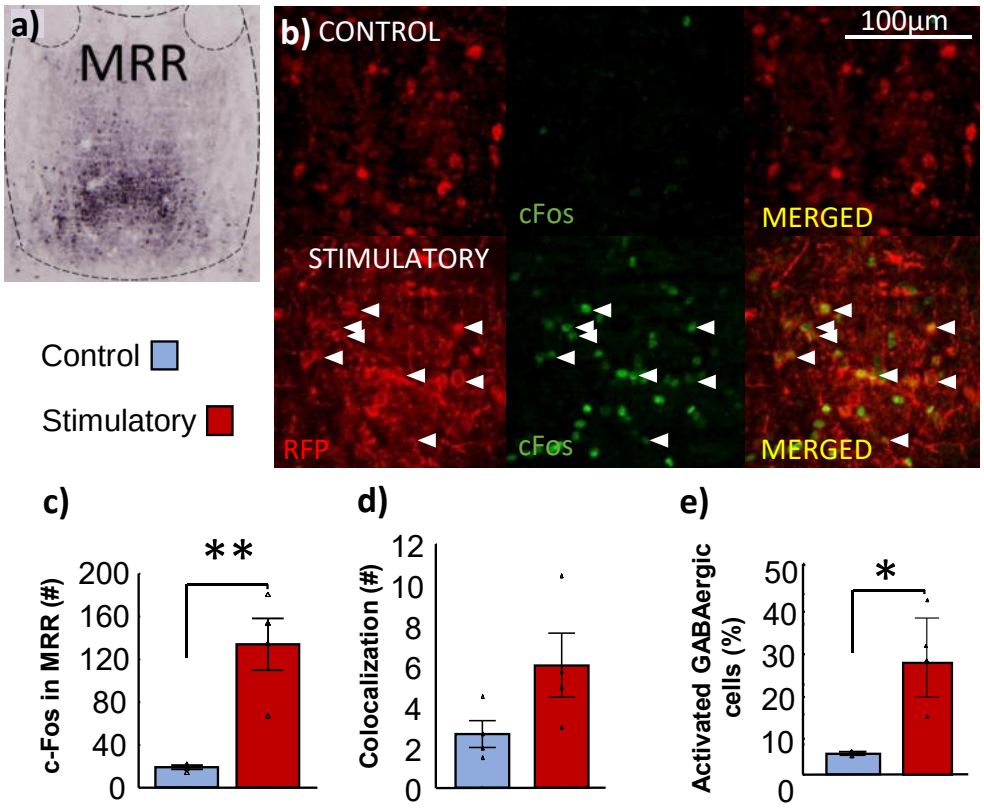

Figure 16 - Confirmation of the chemogenetic technique by IHC. a) A representative image showing successful viral spread and targeting within the MRR in VGAT-Cre mouse. Scale bar: 250 µm b) Representative image of immunofluorescence labeling of RFP (red) and c-Fos (green) as well as their colocalization (yellow) 90 min after CNO injection in the MRR of VGAT-Cre mice. Representative cells are indicated by arrows. Scale bar: 100 µm c) Number of c-Fos expressing cells in the MRR. d) Number of colocalizations between c-Fos and RFP positive cells in control and stimulatory DREADD containing virus injected VGAT-Cre mice. e) Percentage of GABAergic neurons activated after CNO injection in the MRR. *$p < 0.05$, **$p < 0.01$. Figure extracted and adapted from Chaves et al., 2022.

4.2.2 Behavioral testing

Next we investigated the behavioral consequences of bidirectionally manipulating this VGAT-MRR population (see Fig.17 for detailed timeline).

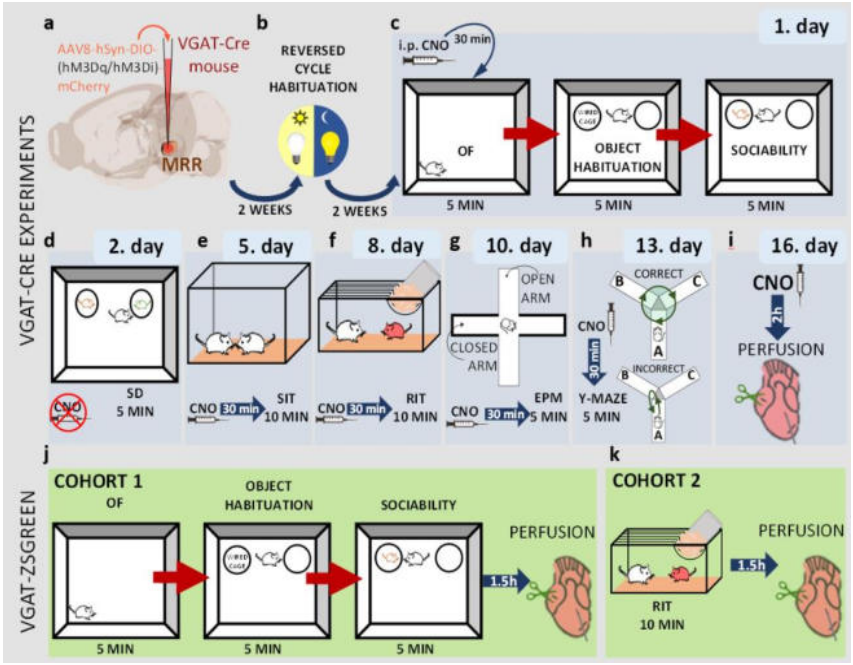

Figure 17 - Experimental outline of Project II. (a) Schematic of AAV injections into the MRR. (b) Timeline of postsurgical recovery and acclimation. (c-i) Behavioral tests conducted in VGAT-Cre mice, with CNO administration 30 minutes prior to each test (except SDT). (j-k) Behavioral tests and perfusion timeline for VGAT-Cre x ZsGreen mice. Figure reproduced from Chaves et al., 2022.

4.2.2.1 Locomotion

Assessing locomotion was critical as its alterations could confound interpretation of behavior tests, rely heavily on the ability of the animal to move and explore.

Table 4. - Locomotion in VGAT-Cre mice injected with control, excitatory or inhibitory DREADD virus into the MRR 30 min after an i.p. injection of 1mg/kg CNO.

	DREADD type	Control (N=12)	Excitatory (N=9)	Inhibitory (N=10)	F-value	p-value
Locomotion	**Open Field - Distance** (cm)	1979±228	2105±132	2317±268	0.556	0.580
	Y-Maze – Number of all arm entries (count)	27.9±2	27.8±5	22±2.1	1.188	0.321
	EPM – Number of Closed Arm entries (count)	13.7±1.1	17.2±2	15.5±0.8	2.649	0.091

During the OF the distance travelled was analyzed by Ethovision in centimeters (cm), during the EPM test the number of closed arm entries served as a measure of locomotion, while in the y-maze test the number of all arm entries reflected the locomotion. No significant difference was found between the groups.

Chemogenetic manipulation of VGAT-MRR neurons did not affect locomotor activity in any of the tests employed (OF, EPM, Y-maze; Table 4.). Specifically, there were no significant group differences in distance traveled in the OF, number of closed arm entries in the EPM, or total arm entries in the Y-maze. Thus, this ensured that any observed social effects were specific to social processing rather than general behavioral disruption.

4.2.2.2 Social Behavior

Sociability

Introduction of a new juvenile mouse under one of the wire cages significantly increased its investigation (sniffing frequency: $F(1,27) = 45.574$, $p < 0.001$; Fig.18a). There was a significant main effect of treatment group ($F(2,27) = 3.564$, $p = 0.042$) and a significant interaction between treatment and cage preference ($F(2,27) = 6.905$, $p = 0.004$) on sniffing frequency (Fig. 18b). Post hoc analysis revealed that stimulation of VGAT-MRR neurons significantly increased the frequency of investigating the mouse-containing cage compared to both the control ($p = 0.001$) and inhibitory ($p < 0.001$) groups. Although all groups displayed an SI above chance level (50%), indicating intact social preference (Control: $t(11) = 7.626$, $p < 0.001$; Stimulatory: $t(9) = 18.514$, $p < 0.001$; Inhibitory: $t(9) = 11.400$, $p < 0.001$; Fig. 18c), there were no significant differences between groups.

Analysis of the duration of investigation revealed a significant preference for the mouse-containing cage ($F(1,27) = 82.808$, $p < 0.001$; Fig. 18d). Treatment marginally influenced this preference ($F(2,27) = 2.808$, $p = 0.078$). Post hoc analysis showed that the stimulatory group spent significantly more time investigating the mouse-containing cage compared to the control group ($p = 0.007$), with a marginal difference from the inhibitory group ($p = 0.076$). While the Social Preference Index (Fig. 18c) did not differ significantly between groups, the significant increase in absolute time spent investigating the conspecific (Fig. 18d), with no corresponding increase in time spent with the empty cage,

suggests the stimulation specifically enhanced social motivation rather than general exploration.

In VGAT-Cre x ZsGreen mice, the sociability test significantly increased c-Fos expression in VGAT-MRR neurons (Fig.18e-f). This was evidenced by both a significant increase in the number of c-Fos and ZsGreen colocalized cells ($F(1,14) = 7.234$, $p = 0.017$; Fig. 18g) and a significant increase in the percentage of c-Fos-positive cells that were also ZsGreen-positive ($F(1,14) = 8.170$, $p = 0.012$; Fig. 18h). Representative images of c-Fos and ZsGreen staining in control and sociability-tested mice are shown in Fig. 18e-f.

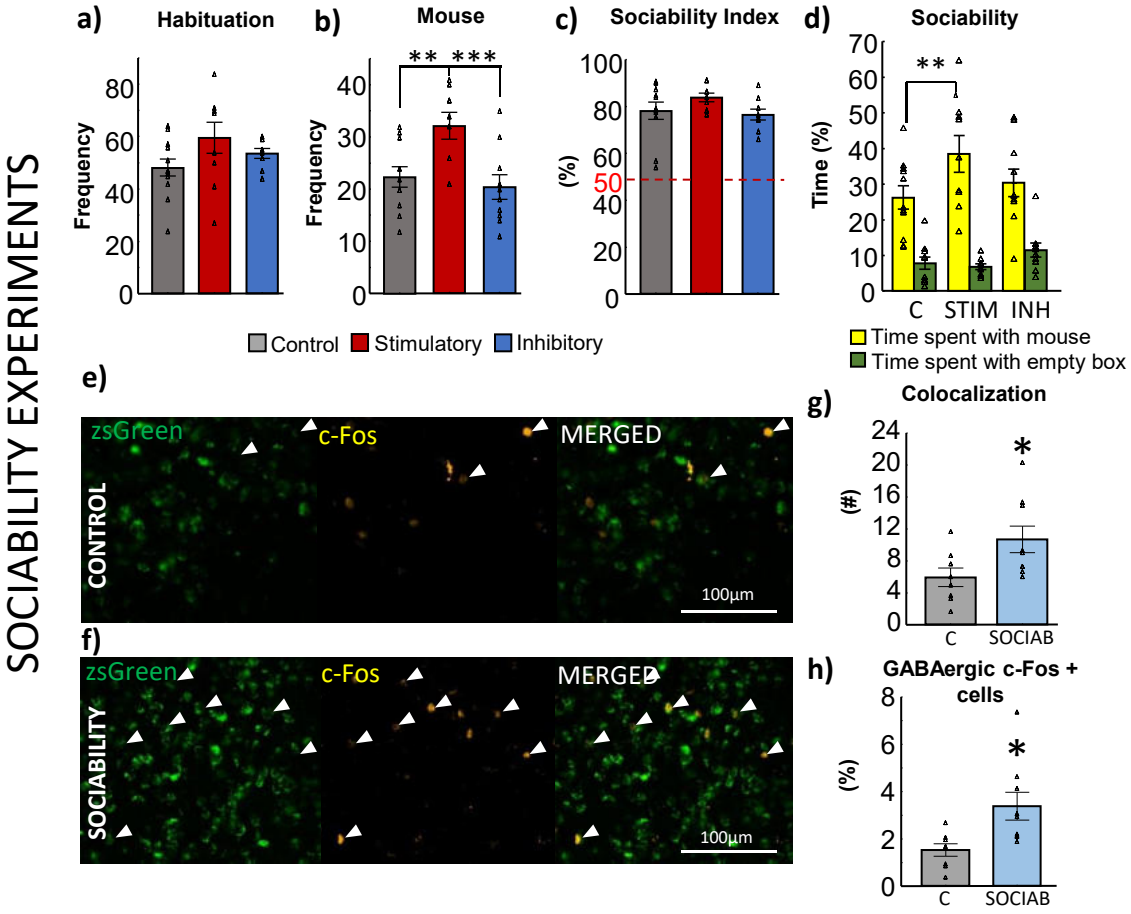

Figure 18 - Sociability test. A–D: Sociability results in VGAT-Cre mice. E–H: ZsGreen (GABA) c-Fos colocalization in the MRR after sociability (E–H) a) The frequency of the object visits (left and right together) for each group during habituation phase. b) The frequency of the visits of the stimulus mouse (J1) for each group during sociability phase. c) Sociability index during the third phase of the sociability test. All animals performed above threshold (50%), displaying intact social preference. d) Each group spent more time with the stimulus mouse than the empty box during sociability phase, however, this was significantly higher in MRR-GABA stimulated than control VGAT-Cre mice. e) Merged photos of c-Fos and ZsGreen (GABA) in the MRR in control, home cage animals. Scale bar: 100 µm f) Merged photos of

c-Fos and ZsGreen (GABA) in the MRR after the sociability test. Scale bar: 100 μm g) Number of colocalized of c-Fos and ZsGreen positive cells in the MRR. h) Percentage of GABAergic neurons among c-Fos positive MRR cells after sociability test. *p < 0.05, **p < 0.01,***p < 0.001. Figure extracted and adapted from Chaves et al., 2022.

Taken together, these results indicate that stimulation of VGAT-MRR neurons increases overall investigation frequency and duration towards a social stimulus. While the preference index itself did not differ significantly between groups, the heightened interaction in the stimulatory group may reflect an increase in general exploratory drive or motivation directed towards salient stimuli, rather than a specific enhancement of social preference. This aligns with recent findings by Ahmadlou et al. (2025) showing that MRN-GABAergic neurons critically regulate the balance between perseverative and exploratory behavioral states across multiple contexts.

Social Interaction Test

To complement the sociability findings and provide a more comprehensive assessment of reciprocal social behavior, we conducted SIT. During the 10-minute test conducted under bright light, mice across all groups displayed significantly more prosocial than aggressive interactions (frequency: $F(1,26) = 90.310$, $p < 0.001$; Fig. 19a).

Analysis of the total frequency of all social behaviors (prosocial + aggressive + defensive) revealed a significant difference between groups ($F(2,26) = 7.443$ $p = 0.003$; Fig. 19b). Post hoc analysis showed that the stimulatory group interacted with the conspecific significantly more frequently overall than both the control ($p = 0.004$) and inhibitory ($p = 0.001$) groups. However, there were no significant group differences in the total duration of time spent engaged in either prosocial (Fig. 19c) or aggressive (Fig. 19d) interactions ($p > 0.05$ for both comparisons).

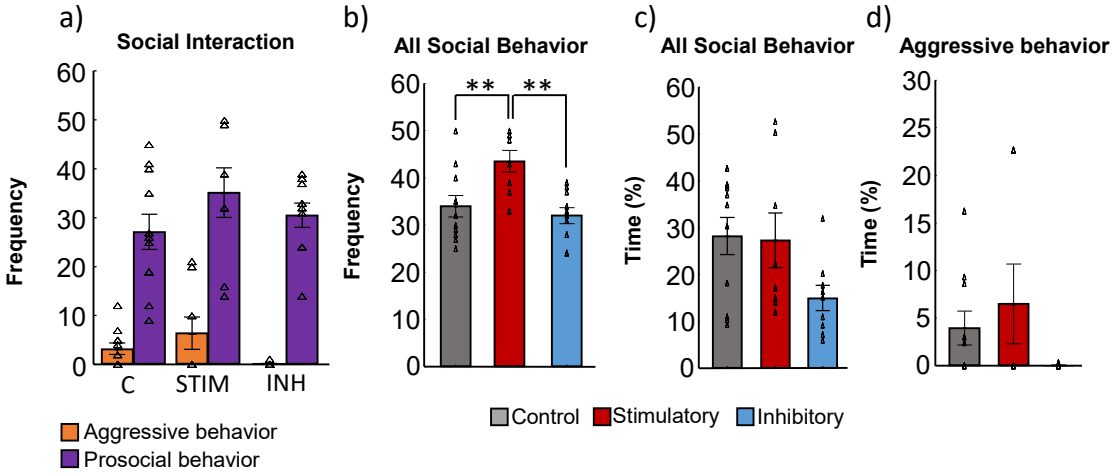

Figure 19 - Effects of VGAT-MRR neuron manipulation on SIT. a–d: SIT reflects both social investigation as well as anxiety. a) All groups showed more social than aggressive behavior frequency. b) In case of all number of social interaction (Prosocial + Aggressive + Defensive) the stimulated group showed the highest level. c) In case of the time engaged in social behavior there were no differences between groups. d) No difference was observed between the groups in the time spent with aggressive interaction as well. **p < 0.01. Figure reproduced from Chaves et al., 2022.

These results suggest that while VGAT-MRR neuron stimulation increases the overall frequency of social engagement in this context, it does not specifically alter the relative time spent in prosocial versus aggressive interactions.

Resident Intruder Test

As expected, mice exhibited more frequent aggressive behavior and spent a greater proportion of time engaged in aggression during the RIT compared to the SIT (control group: mean aggression frequency = 3.18 ± 1.17 for SIT vs. 11.20 ± 1.74 for RIT; mean percentage of time spent in aggression = 6.54 ± 3.03 for SIT vs. 13.20 ± 4.67 for RIT). However, a direct statistical comparison between the SIT and RIT could not be performed due to the tests being conducted on different days. No significant differences were observed between the treatment groups (control, stimulatory, inhibitory) in any of the measured parameters during the RIT (Fig. 20a-d; Table 5.).

Consistent with the behavioral findings, there was no significant change in the number of activated (c-Fos-positive) VGAT-MRR neurons after the RIT compared to cage controls ($F(1,10) = 0.186$, $p = 0.648$; Fig. 20e-h). These results suggest that while VGAT-MRR neurons play a role in regulating general social interest and interaction, they do not significantly modulate territorial aggression.

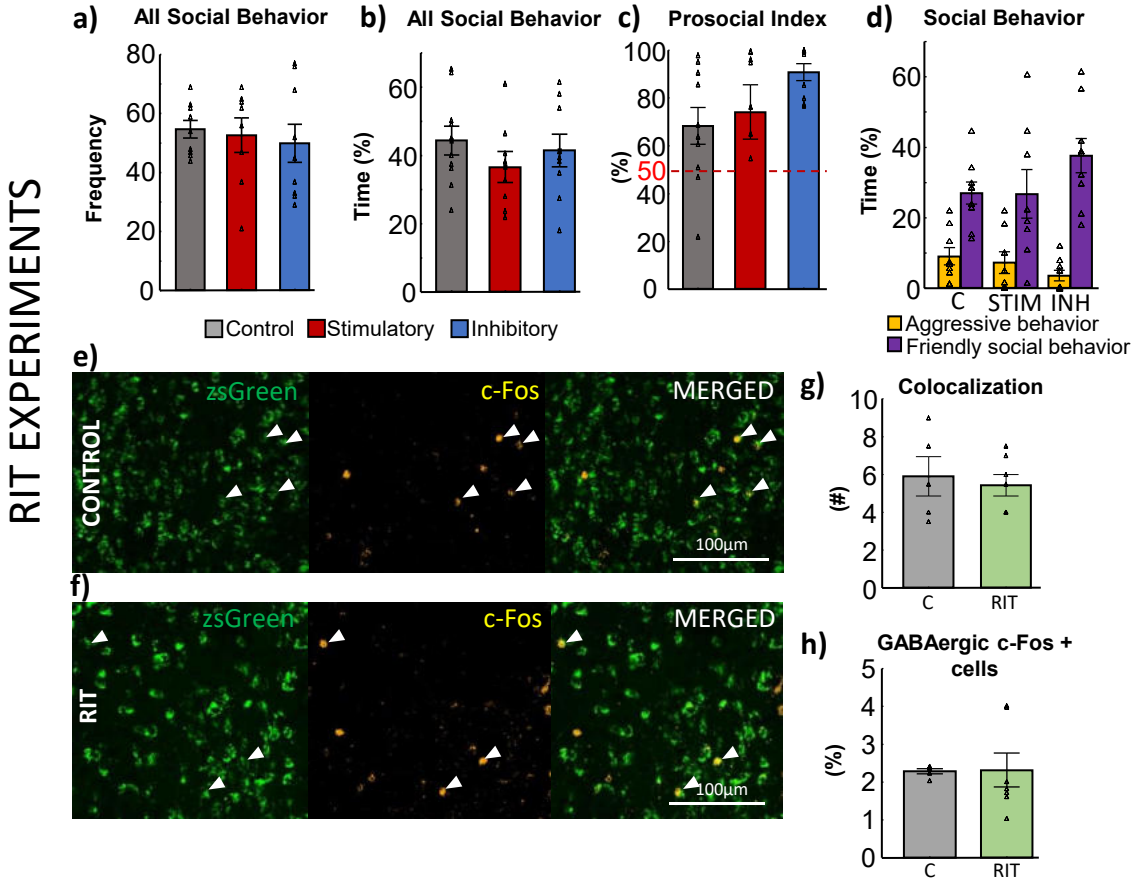

Figure 20 - RIT in VGAT-Cre mice after MRR manipulations. (a) Frequency and (b) percentage time of total social behavior. (c) Prosocial behavior index (chance=50%). (d) Time in prosocial vs. aggressive interaction during the 10 min test. (E-H) c-Fos expression in MRR ZsGreen+ (GABAergic) neurons after RIT: (e) Representative control and (f) post-RIT images (Scale bars: 100 µm). (g) Number of double-labeled (c-Fos+/ZsGreen+) cells. (h) Percentage of c-Fos+ cells expressing ZsGreen. Figure extracted and adapted from Chaves et al., 2022.

Table 5. - RIT after manipulating GABAergic cells in the MRR.

DREADD type		**Control (N=10)**	**Excitatory (N=8)**	**Inhibitory (N=9)**	**F-value**	**p-value**
Frequency (#)	Aggressive Behavior	11.2±1.7	8.8±2.3	5.5±2.2	1.897	0.171
	Social Behavior	45.5±4.4	41.5±7.3	44.1±5.0	0.130	0.878
	Social Sum	57.4±3.8	52.6±5.8	49.8±6.4	0.531	0.594

Time (%)	Aggressive Behavior	13.2±4.6	7.3±3.0	3.6±1.4	2.012	0.155
	Social Behavior	30.7±4.6	26.7±6.8	37.6±4.8	0.988	0.386
	Social Sum	44.4±4.2	36.6±4.5	41.4±4.7	0.729	0.492
Prosocial Index		71.5±7.4	74.1±11.3	90.8±3.5	1.835	0.181

Degree of freedom (df) for the one-way ANOVA for the frequency and time (%) was (2,24).

4.2.2.3 Anxiety

In the OF test (representing the first 5 minutes of the subsequent sociability test), no significant group differences were observed in the time spent exploring the center zone (Fig. 21a), a common index of anxiety-like behavior in this paradigm.

In the EPM, analysis of traditional anxiety metrics revealed no significant group differences in the time spent in the open arms (Fig. 21b) or the ratio of open arm entries to total arm entries (Fig. 21c). Interestingly, there was a marginal effect of treatment on the latency to first enter the closed arms ($F(2,24) = 2.868$, $p = 0.070$; Fig. 21d), with slightly lower levels in the inhibitory group. Additionally, chemogenetic manipulation of VGAT-MRR neurons significantly affected the latency to first enter the open arms ($F(2,22) = 4.096$, $p = 0.030$; Fig. 21e), with higher levels in the inhibitory compared to both the control ($p = 0.030$) and stimulatory ($p = 0.010$) groups. No significant group differences were observed in the frequency of risk assessment behaviors (head dipping, stretched attend posture, rearing) or grooming. Overall, these results suggest a mild anxiogenic effect of VGAT-MRR inhibition.

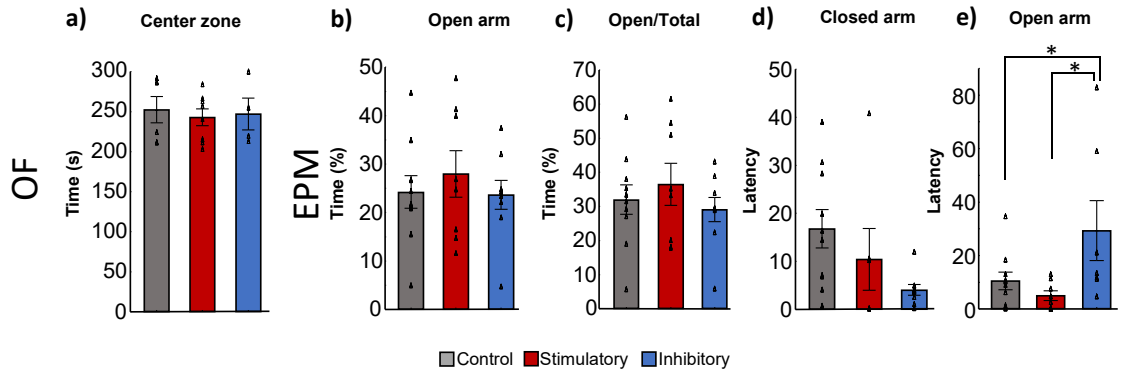

Figure 21 - Effects of VGAT-MRR neuron manipulation on anxiety. (a) OF test: Center time. (b-e) EPM test: (b) Open arm time, (c) Open arm entry ratio, (d) Closed arm latency, (e) Open arm latency. No group differences in (a, b, c) and significantly increased latency in (e, $p<0.05$). *$p < 0.05$. Figure reproduced from Chaves et al., 2022.

4.2.2.4 Memory

In the SDT, conducted 24 hours after CNO injection, all animals spent a similar amount of time investigating the stimulus mice (Fig. 22a; Table 6.). One-sample t-tests on DI comparing group means to the 50% chance level revealed that none of the groups exhibited a significant preference for the novel mouse (Control: $p = 0.825$; Stimulatory: $p = 0.841$; Inhibitory: $p = 0.795$, Fig. 21b). Time spent investigating the familiar ("old") mouse versus the novel ("new") mouse revealed no significant main effect of treatment ($F(2,26) = 0.724$, $p = 0.494$) or choice ($F(1,26) = 1.853$, $p = 0.185$), or treatment × choice interaction ($F(2,26) = 0.517$, $p = 0.602$), either. Additionally, non-social behaviors (grooming, rearing, and cage exploration) was also not different between groups ($F(2,26) = 1.217$, $p = 0.313$). Thus, social recognition memory was not evident in any group, and manipulation of VGAT-MRR neurons did not significantly affect the performance. While these neurons modulate social approach and interaction, they do not appear to play a significant role in the formation or retrieval of social recognition memory.

In the Y-maze, all groups made a substantial number of arm entries (Fig. 22c), indicating adequate exploration for assessing spontaneous alternation. The mean alternation percentages were above 50% for all groups (Control: 63.0 ± 3.3%; Stimulatory: 62.9 ± 6.2%; Inhibitory: 62.0 ± 2.6%; Fig. 22d). However, due to variability, these values were not significantly different from the chance level of 50% based on one-sample t-tests (Control: $p = 0.808$; Stimulatory: $p = 0.821$; Inhibitory: $p = 0.767$). Crucially, comparison between the treatment groups revealed no significant differences in spontaneous alternation ($p = 0.980$; Table 6.). This indicates that manipulation of VGAT-MRR neurons did not affect spatial working memory performance in this task.

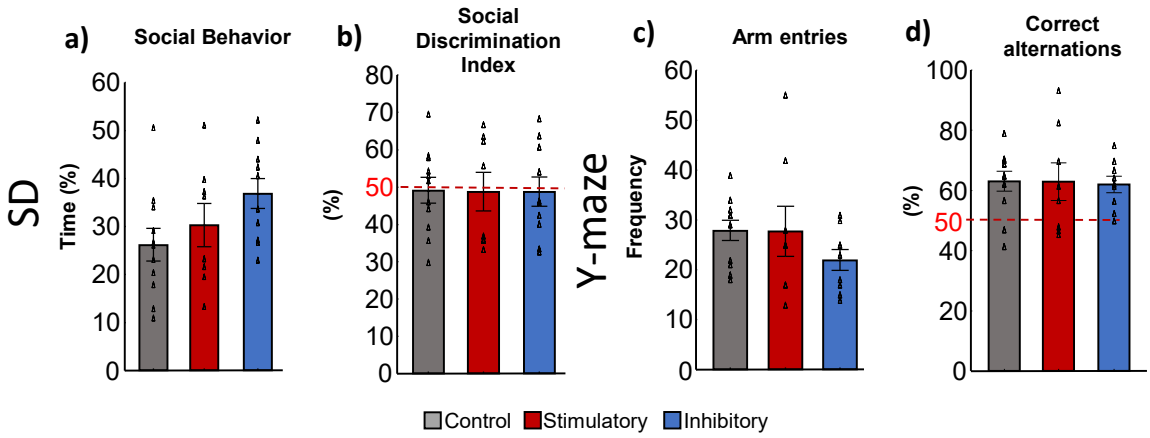

Figure 22 - Short term memory after manipulating the VGAT-MRR cells in VGAT-Cre mice. a–b: Social discrimination. c–d: Y-maze. a) Percentage of time each group spent with stimulus mice. b) Social discrimination index. All the animals performed below threshold (50%), displaying no preference for a new mouse without group differences. c) Total number of alternations on Y-maze reflecting locomotion. d) Total number of "good" alternations on Y-maze. All groups had intact short-term memory in this test. Figure reproduced from Chaves et al., 2022.

Table 6. - Memory parameters after manipulating VGAT-MRR cells.

DREADD type		**Control (N=12)**	**Excitatory (N=9)**	**Inhibitory (N=10)**	**F-value**	**p-value**
Frequency	**'Old' mouse**	24.5±2.4	26.5±2.6	23.6±1.7	Treatment: 1.396	0.265
	'New' mouse	23.1±1.4	25.7±2.4	21.2±0.9	Choice: 1.065 Treatment×Choice: 0.1051	0.311 0.900
	'Other' behavior	47.9±2.8	51.1±3.4	43.9±2.5	1.411	0.261
Time (%)	**'Old' mouse**	14±2.4	15.5±2.7	19.4±2.7	Treatment: 2.376	0.1127
	'New' mouse	12.1±1.2	14.7±2.6	17.4±1.5	Choice: 1.045	0.3160 0.9464

					Treatment×Choice : 0.055	
	'Other' behavior	73.8±3.4	69.6±4.5	63.1±3.1	2.376	0.112
Discrimination index		49.1±3.4	48.7±5.1	48.8±3.9	0.002	0.997
Y Maze – Spontaneous Alternation		63.0±3.3	62.9±6.2	62±2.6	0.020	0.9799

The last row contains the results of the y-maze test, while all other rows represent the values of the SDT. No significant differences were detected. Degree of freedom (df) for one-way ANOVA was (2,26). Degree of freedom for the repeated-measures ANOVA was (1,26) for the effect of choice, while (2,26) for the effect of treatment and treatment × choice interaction.

4.3 Project III. - The DAT-MRR Cells Regulate Social Behavior in Male Mice

4.3.1 Presence of Dopaminergic Cells in the MRR

Double immunofluorescence revealed TH-positive neurons in the MRR that colocalized with RFP, indicating successful viral transduction of TH-expressing cells (Fig. 23a-d). Importantly, these TH-positive/RFP-positive neurons lacked DBH, the enzyme that converts dopamine to norepinephrine, strongly suggesting a dopaminergic, rather than noradrenergic, phenotype (Fig. 23e-h; Fig 24a-e). Furthermore, we observed colocalization of RFP and DAT, confirming that the virally transduced neurons express them (Fig. 24f-i).

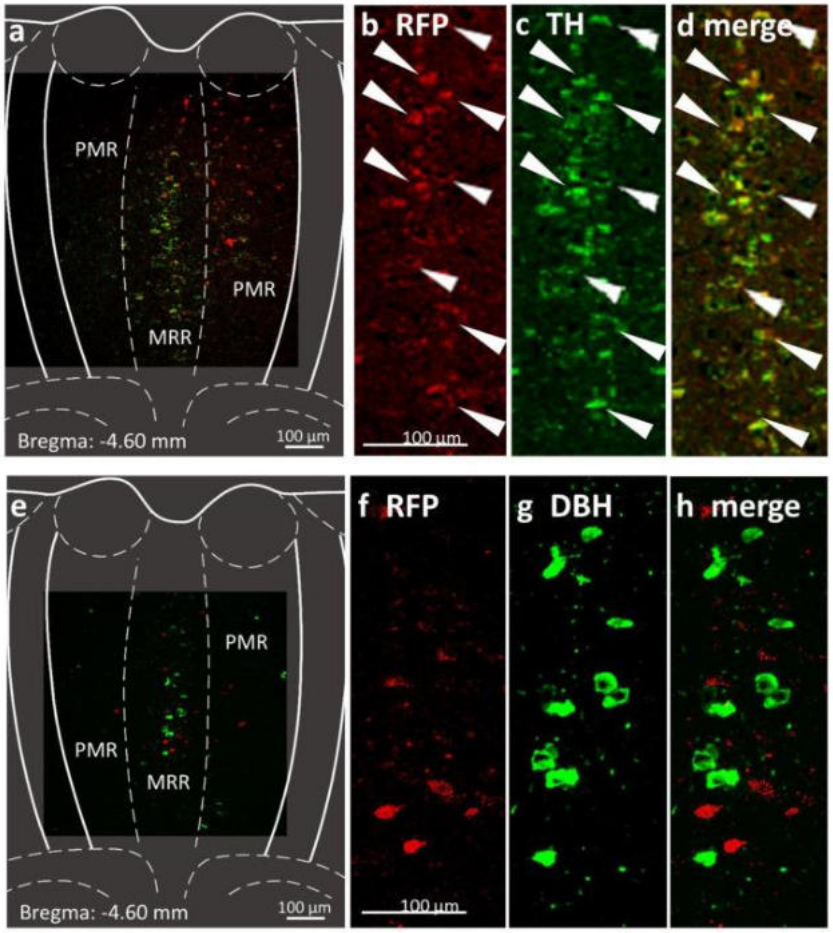

Figure 23 - Confirmation of dopaminergic neurons and viral targeting in the MRR of DAT-Cre mice. (a) Fluorescent micrographs showing representative MRR sections with RFP (red) and TH (green) labeling. (b-d) High-magnification confocal images showing colocalization of RFP and TH in representative MRR neurons (arrows). (e) Fluorescent micrographs showing representative MRR sections with RFP (red) and DBH (green) labeling. (f-h) High-magnification confocal images showing a lack of colocalization between RFP and DBH. Figure extracted and adapted from Chaves et al., 2024.

Although formal stereological quantification was not conducted, the consistent qualitative observations across multiple animals and sections provided sufficient evidence to validate the presence of the target dopaminergic population (TH+/RFP+/DBH-) and the specificity of viral transduction (RFP+/DAT+) for the subsequent functional experiments.

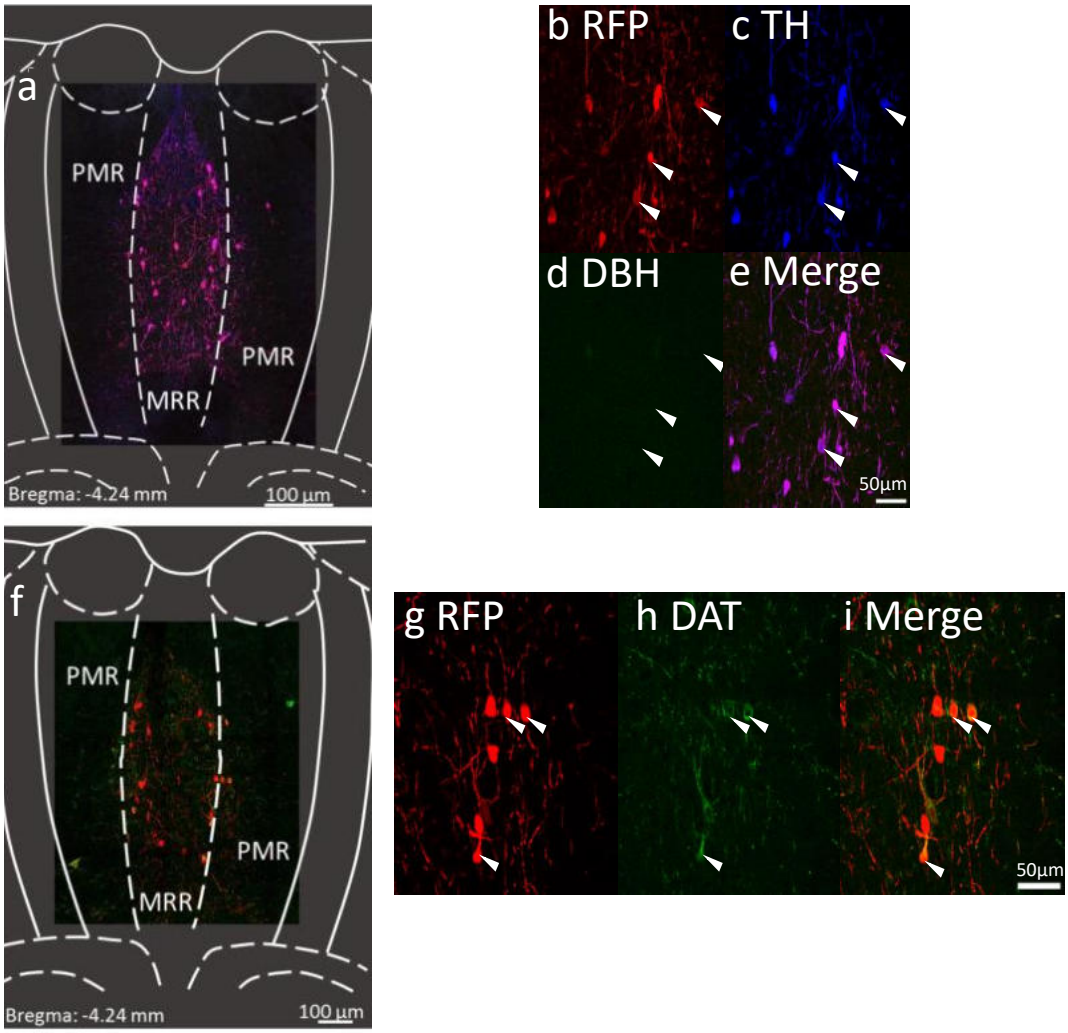

Figure 24 - Co-localization of DREADD Marker (RFP) with Dopaminergic Markers (TH and DAT) in the MRR. (a-e) Confocal laser scanning images of triple IHC staining of DREADD marker RPF-positive, TH-positive but DBH-negative neurons in the MRR, indicating dopaminergic phenotype. (f–i) Confocal laser scanning images show co-localization of RFP and DAT. Figure extracted and adapted from Chaves et al., 2024.

To increase translational relevance RT-PCR analysis confirmed the expression of Dat mRNA in both mouse and human MRR tissue samples (Fig. 25a,b). This highly sensitive and specific technique was employed to detect and quantify key neurotransmitter-related genes, providing crucial molecular evidence for the presence of dopaminergic and noradrenergic markers in specific brainstem regions. In mouse MRR and DRN Th and Dbh mRNA were also present (Fig. 25a), consistent with the presence of both dopaminergic (TH-positive, DBH-negative) and noradrenergic (TH-positive, DBH-positive) neurons. Importantly, we confirmed the presence of DAT mRNA in

human post-mortem brainstem samples containing the pontine raphe nucleus (considered the human equivalent of the mouse MRR; Fig. 25b). In contrast, DAT mRNA was not detected in human temporal or frontopolar cortex samples, demonstrating regional specificity (Fig.25c).

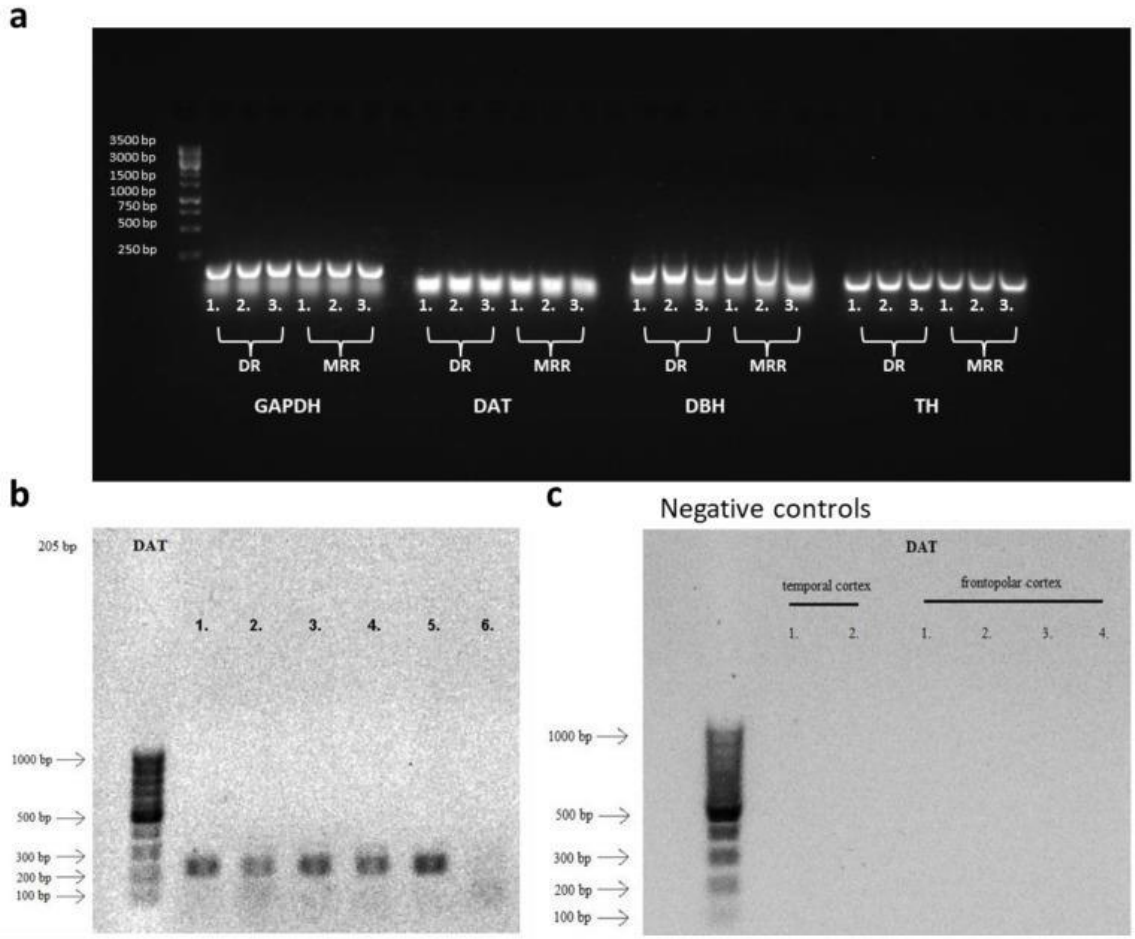

Figure 25 - RT-PCR amplification products. (a) Dat, Th, and Dbh mRNA expression in mouse DRN and MRR. (b) DAT mRNA detection in human pontine raphe nuclei. (c) Absence of DAT mRNA in human cortical samples. Figure reproduced from Chaves et al., 2024.

4.3.2 Behavioral Testing

We used a test battery similar to Project II. (Fig.26).

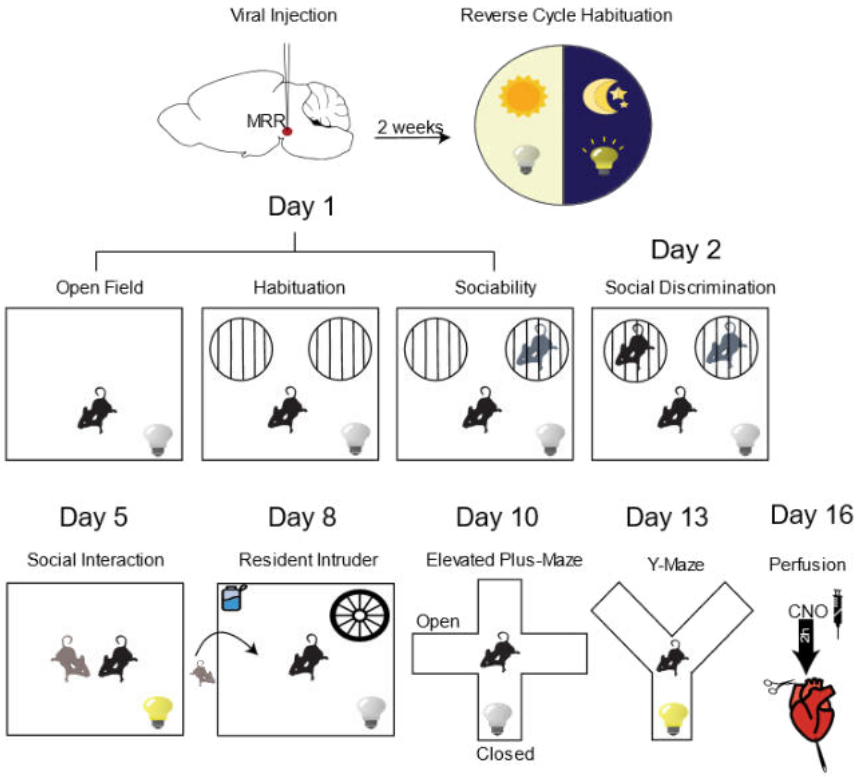

Figure 26 - Timeline of Behavioral Tests. (a) Schematic of AAV injections into the MRR. (b) Diagram of recovery and habituation periods. (c-i) Sequence of behavioral tests in DAT-Cre mice, with CNO injections 30 min prior to each test (except SD). Tests: (c) OF, habituation, and sociability; (d) SD (24h after CNO); (e) SIT; (f) RIT; (g) EPM; (H) Y-maze; (i) Final CNO injection and perfusion (2h post-injection). Figure reproduced from Chaves et al., 2024.

4.3.2.1 Locomotion

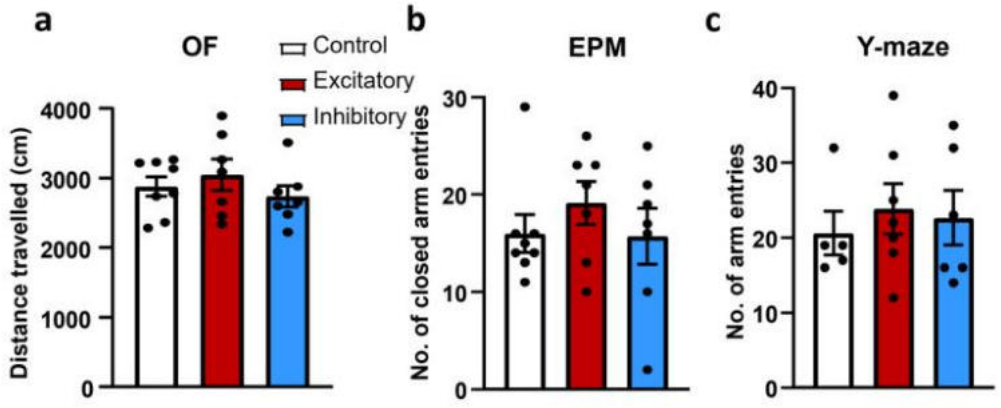

Figure 27 - Locomotion after chemogenetic manipulation of DAT-MRR in male DAT- Cre mice. No difference was observed between treatment groups. (a) Distance travelled in cm in the Open Field test. (b) Number of closed arm entries during the 5 min EPM test. (c) Number of entries in the arms of the Y-maze. Figure reproduced from Chaves et al., 2024.

To see if general motility is affected by DAT-MRR neurons, we investigated the locomotion during several tests, namely OF, EPM and the Y-maze. Manipulation of the DAT-MRR cells had no effect on locomotion in either studied parameters and tests:

distance travelled in the OF, closed arm entries in EPM, total arm entries in Y-maze (Fig. 27).

4.3.2.2 Social Behavior

During habituation a significant preference for investigating one cage location over the other was observed ($p = 0.030$), indicating a baseline side bias in the empty arena. However, there was no significant difference in the total time spent investigating the two empty cage locations between groups ($p = 0.300$). It is important to note that this side preference was identified during analysis, thus, could not be balanced during the test.

Following the introduction of the juvenile mouse during the subsequent **sociability** phase, all groups directed significantly more investigation towards the mouse-containing cage compared to the empty cage, both in terms of frequency ($p < 0.001$) and duration ($p < 0.001$) (Fig. 28a,b). There were no significant main effects of treatment. Furthermore, all groups exhibited a social preference represented in SI above chance (50%), indicating intact social preference (Control: $t(8) = 18.006$, $p < 0.001$; Stimulatory: $t(7) = 13.114$, $p < 0.001$; Inhibitory: $t(6) = 6.492$, $p < 0.001$; Fig. 28c).

In the **SDT**, conducted 24 hours after CNO injection, a significant effect of treatment was observed on the total time spent investigating both the familiar and novel mice ($F(2,16) = 8.460$, $p < 0.002$; Fig. 28d). Post hoc analysis revealed that the stimulatory DREADD group spent significantly less time investigating the mice than both the control ($p = 0.002$) and inhibitory ($p = 0.004$) groups. This reduction in overall social investigation likely reflects a lingering effect on social motivation or approach behavior resulting from the strong dopaminergic stimulation administered 24 hours prior.

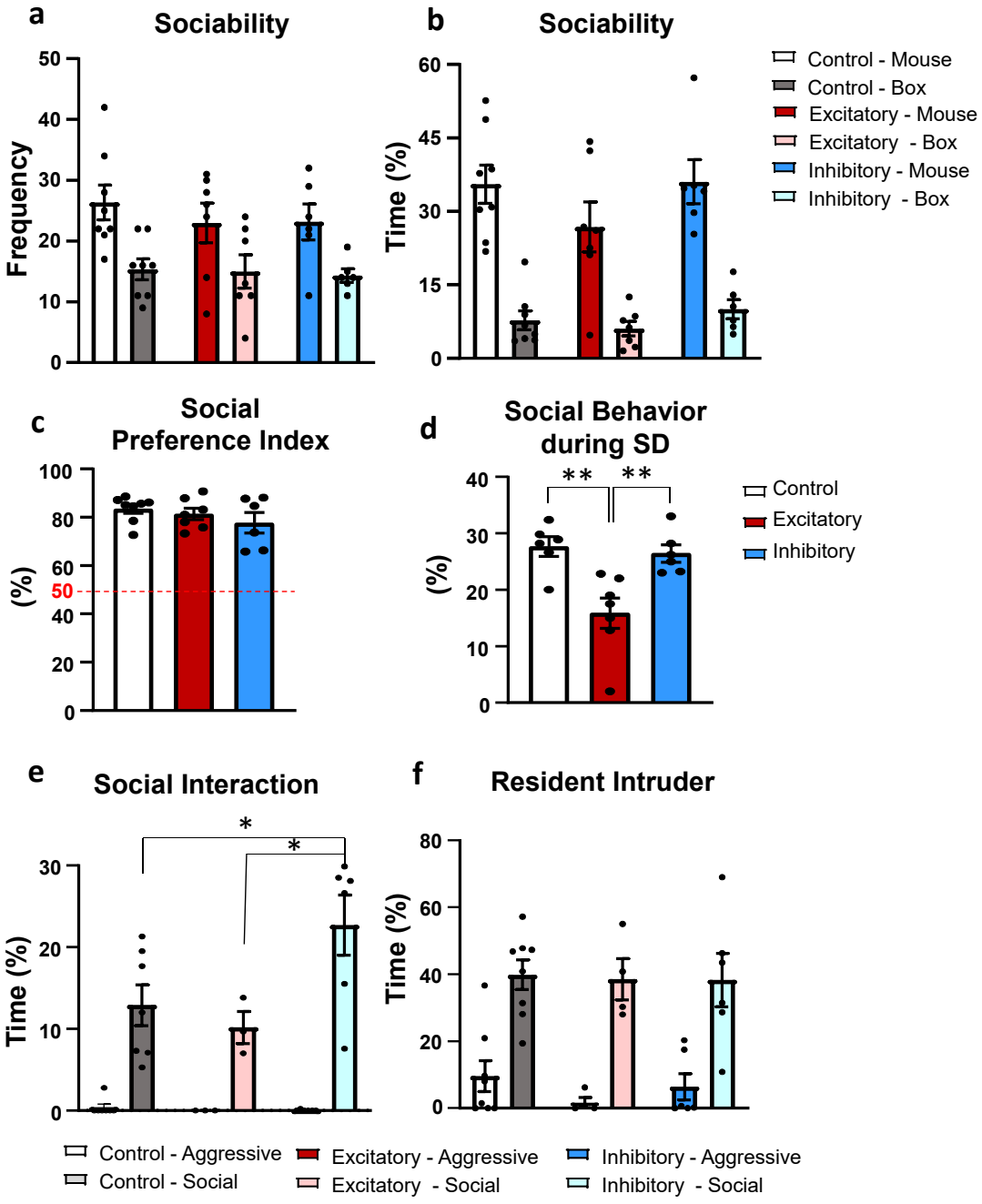

Figure 28 - Results of social behavior tests. (a) Frequency of the interaction (sniffing) between the test mice and the empty cage (box) or caged mice (mouse). (b) Time of this interaction. (c) Social Preference Index displayed the social preference toward the stimulus mice. All groups performed above the chance level 50 %. (d) Time spent interacting with mice (caged familiar and caged unfamiliar mice) during social discrimination. (e) Time spent interacting with conspecific animal during SIT. (f) Time spent interacting with conspecific animals during RIT. *p < 0.05, **p < 0.01. Figure reproduced from Chaves et al., 2024.

During the **SIT**, mice exhibited significantly more prosocial than aggressive interactions (frequency: $F(1,13) = 414.678$, $p < 0.001$), without influence of the treatment ($F(2,13) = 1.423$, $p = 0.276$). The main parameter, time spent interacting, showed not only significantly more time spent in prosocial than aggressive behavior ($F(1,13) = 61.476$, $p < 0.001$), but also a significant interaction between the treatment and social behaviors ($F(2,13) = 4.410$, $p = 0.034$; Fig. 28e). Post hoc analysis indicated that the inhibitory group spent significantly more time exhibiting prosocial social behavior compared to both control and excitatory groups ($p = 0.01$ for both), with no significant differences between the groups in aggressive behavior ($p>0.05$).

In the **RIT**, mice displayed significantly more prosocial contacts than aggressive interactions, both in terms of frequency ($F(1,15) = 190.106$, $p < 0.001$) and duration ($F(1,15) = 48.138$, $p < 0.001$; Fig. 28f). There were no significant effects of treatment on either parameter ($p>0.05$). Thus, chemogenetic manipulation of DAT-MRR neurons does not significantly modulate territorial aggression

4.3.2.3 Anxiety

In the EPM there were no significant differences between the treatment groups in either the time spent in the open arms ($F(2,19) = 0.654$, $p = 0.530$; Fig. 29a) or the open arm entry ratio (open arm entries / total arm entries; $F(2,19) = 1.371$, $p = 0.277$; Fig. 29b).

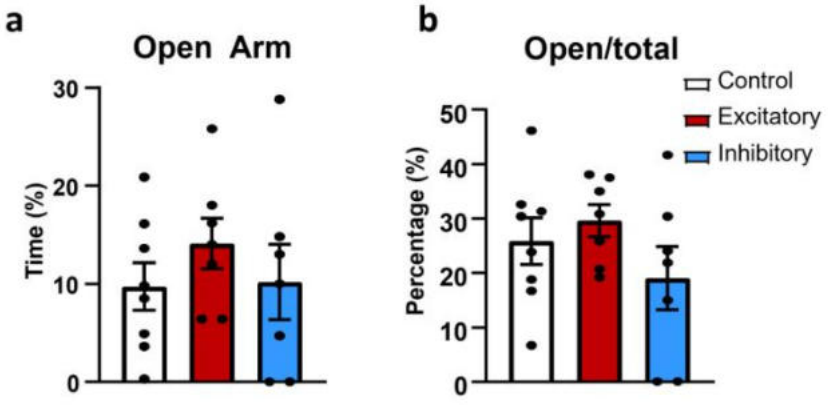

Figure 29 - Results of EPM. (a) The time spent in the open arm in the EPM during the 5 min observation was without group difference. (b) The open/total arm entries show the index of anxiety without group difference. Figure extracted and adapted from Chaves et al., 2024.

4.3.2.4 Memory

All treatment groups demonstrated intact spatial working memory in the Y-maze, performing significantly above chance (50%; Control: $t(5) = 9.313$, $p < 0.001$; Stimulatory: $t(7) = 5.161$, $p < 0.001$; Inhibitory: $t(6) = 5.208$, $p < 0.001$; Fig.30a). There were no significant differences in Y-maze performance between the treatment groups ($F(2,15) = 2.408$, $p = 0.123$).

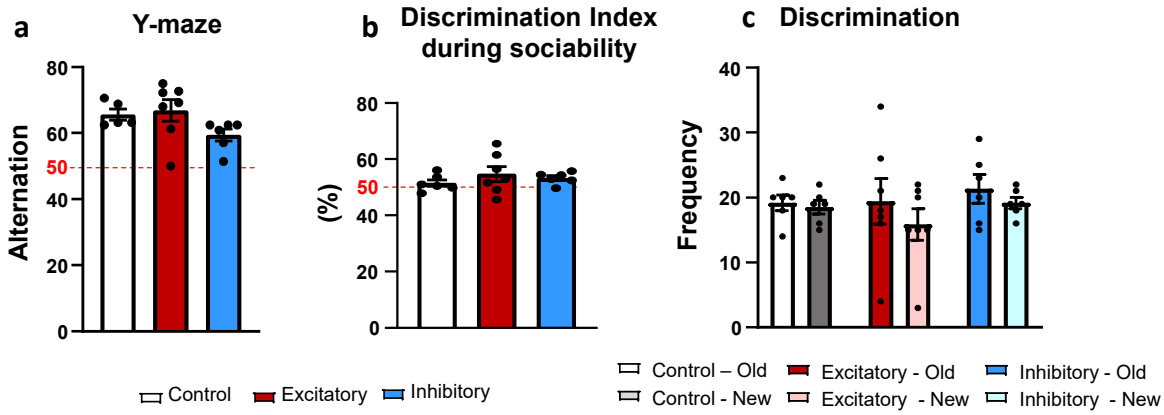

Figure 30 - Results of memory tests. (a) Percentage of "good" alternations in the Y-maze. All animals performed above the chance level (marked red, 50). (b) Discrimination index during the SDT. Animals were not able to distinguish between familiar and unfamiliar mice 24 h after "sampling" (no significant difference from the 50% chance level). (c) Frequency of sniffing conspecifics during the SDT revealed no difference between groups. Figure extracted and adapted from Chaves et al., 2024.

In the SDT, single-sample t-tests of DI comparing group means to the 50% chance level showed that none of the groups (Control: $p = 0.305$; Stimulatory: $p = 0.126$; Inhibitory: $p = 0.137$) exhibited a significant preference for the novel mouse (Fig. 30b). Additionally, DI ($F(2,16) = 0.756$, $p = 0.485$; Fig.30b) and sniffing frequency ($F(2,16) = 0.429$, $p = 0.658$; Fig. 30c) did not differ between treatment groups, either.

5 Discussion

Our results confirmed the potential of different cell-types (especially GABAergic and dopaminergic) of the MRR in shaping the behavior (Table 7.). VGAT-MRR neurons influenced reinforcement-based learning, social interaction, and anxiety-related responses, while DAT-MRR cells specifically modulated some aspects of social behavior. Although, in many cases the differences were subtle and affected only specific behavioral domains, but it is reasonable as i) the large number of GABAergic neurons are heterogenous and subpopulations might have opposing functions; ii) DA neurons are sparse. Nevertheless, our findings highlight the complexity of MRR circuitry and its involvement in a range of behaviors relevant to neuropsychiatric disorders.

Project I. focused on ***learning***. Interestingly, nonspecific stimulation of the entire MRR produced only marginal effects on behavior. While there was a slight decrease in total responses during the reversal learning phase of the *operant conditioning task* representing reward-based learning and a marginal increase in ESFL during reversal learning in the active avoidance task, these effects were not significant. This lack of strong effects following whole-MRR stimulation highlights the complex interplay of neuronal populations within this brain region, therefore we turned to cell-type specific manipulations.

Chemogenetic manipulation of **VGAT-MRR neurons** produced more pronounced and consistent behavioral changes. Stimulation of VGAT-MRR neurons resulted in increased total responses, particularly during the reversal learning phase, accompanied by a higher number of timeout responses. This pattern of behavior, characterized by increased responding during periods when responses were not rewarded (timeouts) and difficulty in altering response strategy during the reversal phase, suggests a role for VGAT-MRR neurons in response inhibition and behavioral flexibility. Specifically, the increased premature responding during the timeout period can be seen as a form of response disinhibition. Thus, VGAT-MRR cells might contribute to maladaptive, repetitive response patterns or a failure to disengage from ongoing actions. This presents an intriguing comparison with the recent 'subcortical switchboard' model by Ahmadlou et al. (2025), where suppression of VGAT-MRR neurons was shown to

promote perseverative behavior, such as prolonged interaction with a single object or continued selection of a previously rewarded option.

Table 7. - Summary of the results of all projects

Project		Tests/Parameters	Results(s)
Project 1	Nonspecific MRR manipulation	Operant Conditioning	Marginally decreased total responses during reversal learning.
		Active Avoidance	Marginally increased escapes failures during reversal learning.
	VGAT-MRR neuron	Operant Conditioning	Excitatory group presented increased reward preference and total responses during reversal learning
		Active Avoidance	Excitatory group presented increased EDST during the learning phase.
Project 2 VGAT-MRR in behavior		Locomotion (OF, EPM, Y-maze)	No difference between groups.
		Social Behavior (Sociability, SD, SIT, RIT)	Excitatory group presented increased sniffing frequency during sociability and increased frequency carrying out prosocial behavior during SIT.
		Anxiety (EPM)	No difference between groups.
		Memory (Y-Maze, SD)	No difference between groups.
Project 3 DAT-MRR in behavior		Locomotion (OF, EPM, Y-maze)	No difference between groups.
		Social Behavior (Sociability, SD, SIT, RIT)	Excitatory group demonstrated a decreased time spent sniffing both the familiar and unfamiliar mice. Inhibitory group demonstrated an increased time carrying out prosocial behavior.
		Anxiety (EPM)	No difference between groups.
		Memory (Y-Maze, SD)	No difference between groups.

While both manipulations appear to affect behavioral persistence, their manifestations differ. Ahmadlou et al. (2025) found that reducing MRN-GABAergic activity promotes choice-specific perseveration, whereas our stimulation led to a more generalized increase in responding and impaired strategy shifting during reversal. This discrepancy suggests that optimal behavioral flexibility might require a finely tuned level of VGAT-MRR tone, with both hypo- and hyperactivity leading to distinct forms of inflexible behavior, possibly due to differing impacts on downstream circuits or the specific type of perseveration assessed.

Furthermore, while no significant effect on memory formation was observed during operant conditioning, this paradigm also assesses reward processing, which is closely associated with the mesolimbic dopaminergic system (Baik, 2020). The VTA, a key component of this system, contains both dopaminergic and GABAergic neurons (Creed, Ntamati, & Tan, 2014). While direct, extensive GABAergic projections from the MRR to the VTA are not as clearly established as other MRR outputs, the MRR is known to be part of broader circuits influencing midbrain dopamine systems. It is plausible that VGAT-MRR neurons could indirectly influence dopaminergic activity in the VTA, perhaps via polysynaptic pathways or by modulating other inputs to the VTA. Such indirect influence could still impact reward processing and potentially contribute to the observed changes in response patterns (Hynes et al., 2021). Additionally, the MRR sends glutamatergic projections (e.g., VGluT2+ and VGluT3+) to various forebrain and midbrain regions, some of which could ultimately interface with VTA circuitry (Sos et al., 2017; Xu et al., 2021). This suggests that the MRR may influence reward-related behaviors and decision-making through complex, possibly multi-synaptic interactions with the VTA and associated structures.

In the *active avoidance paradigm*, targeted stimulation of VGAT-MRR neurons significantly increased EDST in the learning phase compared to controls. This suggests heightened VGAT-MRR activity promotes more proactive avoidance behavior in response to threat cues, potentially by enhancing sensitivity or facilitating active coping, without altering latency. This effect was not observed during reversal learning, potentially due to the strong aversive stimulus or the shift to response inhibition.

Shifting our focus from reinforcement-based learning to ***social behaviors***, **Project II** investigated the role of VGAT-MRR neurons in social behavior and anxiety. Our findings demonstrated that stimulating these neurons enhances *social investigation*, as evidenced by increased interaction with the juvenile mouse during the sociability test and increased social interaction frequency during the SIT. Interestingly, inhibiting VGAT-MRR neurons did not produce a corresponding decrease in social investigation, suggesting an asymmetry in the behavioral consequences of stimulating versus inhibiting these neurons. This asymmetry might stem from the different intracellular signaling pathways engaged by stimulatory (Gq) versus inhibitory (Gi) DREADDs, which could lead to divergent downstream cellular effects (Sharma & Pienaar, 2018). While the neurochemical complexity of the MRR, including transmitter co-expression, could theoretically contribute to such asymmetries, the specific possibility involving GABA/VGluT3 co-release appears unlikely. Evidence indicates that co-expression of VGluT3 within VGAT-MRR neurons is exceedingly rare, estimated at less than 1% (Sos et al., 2017). This minimal overlap suggests that significant co-release of GABA and glutamate specifically from this GABAergic subpopulation is unlikely to be a major functional factor. Therefore, while chemogenetic stimulation of GABAergic neurons would predominantly enhance inhibition, any contribution from VGluT3 in these few co-expressing cells would likely be negligible. Similarly, inhibiting GABAergic neurons would primarily reduce GABA release, and it is improbable that 'unmasking' glutamate release solely from this <1% population would be sufficient to functionally counteract the loss of inhibition or maintain social investigation levels. Although manipulating the broader population of MRR VGluT3+ neurons demonstrably impacts social behaviors (Fazekas et al., 2024), attributing the lack of decreased social investigation during GABAergic inhibition specifically to residual glutamate from this tiny co-expressing subgroup is difficult to justify based on current co-localization data.

Our finding that the sociability test itself activated VGAT-MRR neurons, as indicated by increased c-Fos expression in VGAT-Cre x ZsGreen mice, strongly supports their engagement during social encounters. The observation that stimulation of these neurons promoted active and sustained investigation towards a social stimulus suggests an enhanced motivational drive or a reduced threshold for initiating and maintaining social interaction. This propensity for heightened and sustained social engagement

following VGAT-MRR stimulation is consistent with the behavioral inflexibility and perseverative-like responding observed in our operant conditioning task (Project I.) under similar neuronal manipulation.

Collectively, these findings from distinct behavioral domains indicate that increased VGAT-MRR activity may generally foster a state of behavioral persistence, making it more difficult for animals to disengage from a current focus, whether that focus is a social partner or a learned response strategy. Such a role in modulating the intensity or duration of engagement aligns with the broader understanding of the MRR as a regulatory hub influencing behavioral states. While direct GABAergic projections from the MRR to key social processing areas like the mPFC appear limited (Xu et al., 2021), the observed effects on social behavior could be mediated indirectly through polysynaptic pathways or by modulating other MRR neuronal populations, such as its glutamatergic (VGluT3-positive) and serotonergic neurons known to project robustly to the forebrain (Azmitia & Segal, 1978; Szonyi et al., 2016; Vertes & Martin, 1988). The precise circuit mechanisms by which VGAT-MRR neurons contribute to social behavior require further detailed investigation.

In contrast to the enhancement of social investigation observed upon stimulation, manipulation of VGAT-MRR neurons did not significantly impact *aggressive behavior* in either the SIT or the RIT. This contrasts with some findings in the literature suggesting a link between GABA and aggression, though, this relationship is complex and context-dependent (Narvaes & Martins de Almeida, 2014). For instance, while the classic hypothesis proposes a negative correlation between GABAergic activity and aggression, studies have also shown that positive allosteric modulators of GABA receptors, such as alcohol, benzodiazepines, and the neurosteroid allopregnanolone, can increase aggressive behavior (Miczek, Fish, & De Bold, 2003). These seemingly contradictory effects might be related to the role of GABA in regulating serotonin levels in the DRN (Takahashi, Kwa, et al., 2010; Takahashi, Shimamoto, et al., 2010). However, consistent with our findings, previous studies have shown that manipulating GABA receptors in the MRR, unlike the DRN, does not escalate aggressive behavior (Narvaes & Martins de Almeida, 2014). This difference might be attributed to the distinct projection patterns of the MRR and DRN (Vertes & Linley, 2007). It is also important to distinguish between manipulations of GABA receptors, which have broad effects due to their expression on

multiple neuronal subtypes, and manipulations of GABAergic neurons themselves, as in our study. Our findings suggest that specifically targeting GABA neurons in the MRR does not strongly influence aggressive behavior in the paradigms we employed. Notably, the MRR projects to key aggression-related areas, including the amygdala and hypothalamus (Azmitia & Segal, 1978; Bobillier et al., 1975; Bobillier et al., 1976; Vertes, Fortin, & Crane, 1999). While serotonergic projections from the raphe nuclei are broadly implicated in aggression modulation (Pucilowski & Kostowski, 1983), functional studies reveal a critical dissociation: decrease in serotonergic neurotransmission originating from the DRN—but not MRR—reliably enhance aggressive behavior (Pucilowski & Kostowski, 1983). Although these serotonergic distinctions provide valuable insight, the role of non-serotonergic systems originating from the MRN is less clear.

To assess the impact of VGAT-MRR neuron manipulation on ***locomotion***, we analyzed several parameters across multiple tests. No significant effects of the chemogenetic manipulation were observed on locomotion in any of the measures examined: distance traveled in the OF, closed arm entries in the EPM, and total arm entries in the Y-maze. These metrics provide a measure of overall activity and exploration, though they do not capture finer details of movement dynamics. While subtle alterations in movement patterns cannot be excluded based solely on these analyses, the lack of significant changes in gross locomotor activity suggests that a fundamental motor impairment is unlikely to be confounding the interpretation of the social behavior results. Although previous studies have shown that manipulating GABA levels or receptor activity can affect locomotion (Asin & Fibiger, 1983; Grimm et al., 1975; Jones, Mogenson, & Wu, 1981; Wirtshafter & Asin, 1982; Wirtshafter, Stratford, & Pitzer, 1993; Wirtshafter, Trifunovic, & Krebs, 1989), these studies often involved broader manipulations of GABAergic signaling (e.g., systemic drug administration, receptor agonists/antagonists) or lesions, as opposed to our targeted manipulation of VGAT-MRR cells. However, microinjection of the $GABA_B$ receptor agonist baclofen into the MRR induced hyperactivity, an effect that could be reversed by the antagonist 2-hydroxysaclofen (Wirtshafter, Stratford, & Pitzer, 1993). The specificity of this effect likely stems from the high colocalization of $GABA_B$ and 5-HT1A receptors on serotonergic neurons in the MRR (Wirtshafter & Sheppard, 2001). Therefore, the

observed hyperactivity following baclofen administration could result from indirect effects on serotonergic pathways via modulation of local MRR circuitry, rather than reflecting a general outcome of altering GABAergic output from the MRR to its projection targets. This contrasts with our DREADD-based approach, which modulates the entire GABAergic neuron (soma, dendrites, and axons), thereby influencing both local MRR circuits and downstream targets via long-range projections. The lack of locomotor effect with our whole-neuron manipulation suggests that the primary influence of these VGAT-MRR neurons on locomotion, if any, might be more nuanced than that revealed by local receptor agonism, or that their projections to motor-related areas do not strongly drive gross locomotor changes. These broader manipulations, which affect GABAergic signaling across multiple brain regions and neuronal subtypes, may explain discrepancies between our findings and earlier studies.

Our investigation of ***anxiety-related behavior*** revealed a mild anxiogenic effect of inhibiting VGAT-MRR neurons, evidenced by increased latency to enter the open arms of the EPM. This finding adds nuance to the traditional view of GABA as primarily anxiolytic (Nuss, 2015) and suggests that VGAT-MRR neurons might contribute to anxiety regulation in specific contexts or through specific pathways.

Finally, our findings indicate that manipulating VGAT-MRR neurons did not affect ***short-term*** social ***memory*** or working memory, as assessed by SDT and Y-maze. The MRR, through its projections to the HC, has been implicated in memory acquisition and consolidation, especially for fear-related memories (Balazsfi et al., 2017; Wang et al., 2015). However, previous studies identifying specific MRR neuronal populations mediating these memory functions have primarily pointed to non-GABAergic cells within the MRR. Our finding that manipulating VGAT-MRR neurons did not affect social and spatial working memory is therefore consistent with the idea that other MRR cell types may be more critically involved in these specific memory-related functions. Several factors could contribute to the lack of effect observed in our study. It might reflect the specific type of memory tested; for instance, the role of MRR might be more prominent in aversive memory consolidation than in the social recognition or working memory tasks employed here. Alternatively, parameters such as the relatively short "sampling" time (5 min) during the sociability test (for the SDT) or the 24-hour retention interval could have influenced the outcome. It is also notable that in the SDT, none of the groups, including

controls, showed robust social memory, as evidenced by their performance not differing significantly from the 50% chance level. This suggests that factors inherent to the paradigm or other variables, independent of VGAT-MRR manipulation, might have contributed to this general lack of social memory under our specific conditions. Nonetheless, based on our results, VGAT-MRR neurons do not appear to play a major direct role in the specific forms of short-term social or spatial working memory assessed in this dissertation. Importantly, this further strengthens the interpretation that the observed changes in social approach and interaction behaviors are primary effects of the manipulation, rather than being secondary to impairments in memory.

Project III. shifted focus to the less-studied **DAT-MRR neurons**. We first confirmed the presence of these neurons in both mice and humans using IHC and RT-PCR. This finding has important translational implications, as it suggests that the role of DAT-MRR neurons in behavior can be generalized across species. The presence of DAT in the human pontine raphe nucleus, which is considered the human equivalent of the mouse MRR, further strengthens the translational relevance of our findings. While most human samples showed clear DAT mRNA expression, one sample exhibited only faint expression. This individual experienced a prolonged period of agony before death and had a history of pneumonia, which could have compromised RNA stability (Tiana et al., 2020) and thus led to lower detectable DAT mRNA levels. The absence of DAT mRNA in cortical samples is consistent with previous findings in rats (Shimada et al., 1992) and supports the idea that DAT expression is primarily localized to neuronal cell bodies rather than axon terminals.

Our chemogenetic experiments revealed a specific role for DAT-MRR neurons in modulating ***social behavior***. Stimulating these neurons decreased social investigation during the SDT, while inhibiting them increased prosocial behavior during the SIT.

Before discussing further these specific behavioral outcomes, it is pertinent to note some observations from the initial habituation phase of the sociability test. A baseline side preference for investigation frequency (but not duration) was observed during the habituation phase. Although stimulus placement was systematically varied, this pre-existing frequency bias, identified retrospectively, was not used for individual counterbalancing. Since the bias was frequency-specific and did not affect investigation

duration, a significant confounding effect on our overall social preference assessment (considering both time and frequency) is unlikely, though subtle influences on initial approach frequencies cannot be entirely dismissed. Additionally, there were no indications of object fear or aversion in any of the groups, suggesting that the subsequent social interaction results were not confounded by anxiety-related responses to the novel objects (i.e., wired cages).

In the *sociability test* itself, all animals displayed a clear preference for the conspecific over the empty cage, consistent with intact social motivation. While we did not observe any significant differences between groups during the initial sociability phase, the SDT, conducted 24 hours after CNO injection, revealed a significant reduction in social investigation in the stimulatory DREADD group. This finding is in line with studies showing that increased dopaminergic tone can lead to reduced social interest (Liu et al., 2017). However, it contrasts with other studies, such as Bariselli et al. (2018), who reported that inhibiting VTA dopamine neurons decreased sociability. This discrepancy highlights the distinct roles that dopamine plays in different brain regions. Moreover, the fact that inhibiting DAT-MRR neurons increased prosocial behavior during the *SIT* further emphasizes the complexity of dopaminergic modulation of social interaction and its dependence on specific brain circuits and behavioral contexts. It also suggests that there may be a delicate balance in activity among DAT-MRR cells that allows normal social behavior to take place. In the *RIT*, there were no significant differences observed between groups. This might be due to differences in the motivational and contextual factors driving behavior in the RIT compared to the SIT, with the RIT likely being less anxiogenic due to its dark testing conditions. As shown by Haller et al. (2004), the anxiogenic nature of the testing environment, such as light vs. dark and familiar vs. unfamiliar surroundings, can influence aggressive behavior.

These findings suggest that DAT-MRR neurons in modulating social behavior might be context-dependent, influencing social investigation and interaction under anxiogenic conditions but with no major influence on territorial aggression. Overall, these results strongly implicate DAT-MRR neurons in the fine-tuning of social behavior, although further research is needed to delineate the specific contexts and neural circuits through which they exert their influence.

Interestingly, we did not observe any effects of DAT-MRR manipulation on locomotion, anxiety, or short-term memory. This was somewhat unexpected, given the established roles of dopamine in these functions (Beninger, 1983; Grogan et al., 2015; Kalisch, Gerlicher, & Duvarci, 2019).

Regarding ***locomotion***, our findings contrast with previous studies demonstrating that manipulations of the MRR, including injections of GABA agonists or opioid agonists, can induce hyperlocomotion (Shim, Stratford, & Wirtshafter, 2014). However, those studies targeted GABA or opioid receptors, which are expressed on various neuronal populations within the MRR, and not dopamine neurons specifically. Moreover, not all of the observed hyperlocomotion effects could be blocked by the D2 antagonist haloperidol, suggesting both dopamine-dependent and -independent mechanisms (Shim, Stratford, & Wirtshafter, 2014; Wirtshafter, Klitenick, & Asin, 1988). Our findings suggest that DAT-MRR neurons, despite their presence in a region associated with locomotion, might not be directly involved in controlling this behavior, given their limited influence when specifically targeted with chemogenetic manipulations.

Regarding ***anxiety***, the lack of an effect of DAT-MRR manipulation on anxiety-like behavior in the *EPM* contrasts with findings by (Bahi & Dreyer, 2019), who observed decreased anxiety following DAT silencing in the NAcc. This discrepancy likely reflects the different brain regions targeted.

Finally, the lack of effect of DAT-MRR manipulation on ***memory***, as assessed by the *Y-maze* and *SDT*, may be due to the specific types of memory tested, the timing of the DREADD manipulation relative to the tests, or the specific targets of DAT-MRR neurons. Furthermore, it is important to consider that DAT-expressing neurons constitute a very small population within the MRR (Jahanshahi, Steinbusch, & Temel, 2013), and our viral transduction, while targeted, would have affected only a portion of these cells. Consequently, any modulatory influence this subpopulation exerts on these specific memory tasks might be subtle, and our manipulation may not have reached the threshold necessary to produce a detectable behavioral effect. Other studies suggest potential roles for dopamine in various memory processes (De Marco & Venneri, 2018; Grogan et al., 2015; Guzman-Ramos et al., 2012). For example, injection of a D1/D5 antagonist into the hippocampal CA1 region impaired social discrimination abilities (Garrido Zinn et al.,

2016). Given that VGluT3-expressing neurons from the MRR project to the HC (Szonyi et al., 2016), it is plausible that these neurons contribute to memory processes. Further research is needed to elucidate if there is any relationship between VGluT3 and dopamine in the MRR, as well as the involvement of DAT-MRR neurons in various memory processes, including spatial memory. The apparent lack of social memory in the SDT in all groups corroborates the transient nature of social memory observed in laboratory settings (Bluthe, Gheusi, & Dantzer, 1993; Thor & Holloway, 1982), which can, however, be modulated by factors like vasopressin release and group housing (Bluthe, Gheusi, & Dantzer, 1993; Kogan, Frankland, & Silva, 2000). Regarding social recognition memory, the social discrimination test proved inconclusive in our study, as even control animals failed to show a preference for the novel mouse. Therefore, while our data show no effect of DAT-MRR neuron manipulation, this result must be interpreted with caution; the experiment could not definitively assess the role of these neurons in social memory due to the lack of a measurable behavioral baseline. These neurons could still participate in other memory processes not assessed in this study.

While this study focused on DAT-expressing neurons within the MRR, it is noteworthy that the adjacent DRN contains a distinct population of dopaminergic neurons (Cho et al., 2017; Stratford & Wirtshafter, 1990) that modulate arousal and responsiveness to salient stimuli. Although our viral injections were anatomically targeted to minimize DRN transduction, and retrograde spread was mitigated through careful vector selection, future work should explicitly examine potential functional interplay between MRR and DRN DA systems. The DRN DA population—which projects to motivation-related regions like the NAcc and PFC—may operate in parallel with MRR DAT+ neurons to fine-tune social behavior, particularly under anxiogenic conditions where detecting environmental salience is crucial (Cho et al., 2017).

Furthermore, while both dopaminergic (DAT-expressing) and GABAergic neurons are present in the MRR, direct evidence for significant colocalization within the same MRR neuron is currently lacking in the literature, suggesting these populations may operate largely independently. Additionally, while recent work suggests that MRR VGluT2 neurons regulate the acquisition of negative experiences (Szonyi et al., 2019), it is still unknown whether there are interactions between dopamine and VGluT2 neurons within the MRR.

5.1 Integrating Findings

This dissertation highlights the distinct roles of GABAergic and dopaminergic neurons within the MRR in modulating behavior. Our findings reveal a complex interplay between these neuronal populations and their contributions to reinforcement-based learning, social interaction, and anxiety. The lack of robust effects following whole-MRR stimulation in Project I. underscores the importance of cell-type-specific manipulations, such as those employed in Projects II. and III., which revealed the unique contributions of GABAergic and dopaminergic neurons. Specifically, stimulating VGAT-MRR neurons enhanced both social investigation (Project II.) and aversive learning (Project I), suggesting a potential functional link between these seemingly disparate behaviors. However, stimulating DAT-MRR neurons decreased social investigation (Project III.), demonstrating opposing roles for these two neuronal subtypes within the MRR in modulating social behavior. This raises the question of whether there are direct or indirect interactions between GABAergic and dopaminergic neurons in the MRR, and how these interactions might shape social behavior under different contexts. The context-dependent nature of the social behavioral effects observed in Project III. further emphasizes the need for future studies to investigate the influence of DAT-MRR neurons under a wider range of social and environmental conditions.

The ineffectiveness of DAT-MRR manipulation on locomotion, anxiety, and memory, despite established role of DA in these functions, suggests that these neurons may contribute to these processes through distinct pathways or in interaction with other MRR neuronal populations. Our results suggest DAT-MRR neurons might not be directly involved in locomotor control, but do not exclude the possibility of more subtle or indirect influences. It is possible that DAT-MRR neurons primarily modulate the activity of other MRR neurons (e.g., GABAergic or glutamatergic) to indirectly shape various behavioral outputs. Moreover, the lack of observed social memory in any of the experimental groups of Project II. underscores that while VGAT-MRR cells do not seem to play a major role in social recognition memory, other factors or brain regions are likely more central to this process. The absence of robust social memory in our study might be attributed to the specific parameters used (5-minute sampling time, 24-hour retention interval) or to strain differences, as other studies have reported memory effects under different conditions (Camats Perna & Engelmann, 2017).

5.2 Methodological Considerations and Limitations

Despite these valuable insights, it is crucial to acknowledge certain methodological limitations. A primary limitation stems from the inherent constraints of chemogenetics. While DREADDs allow for cell-type-specific manipulations, they lack the temporal precision of techniques like optogenetics. The relatively slow onset and offset of DREADD effects make it challenging to pinpoint the precise timing of neuronal activity changes in relation to specific behavioral events. This limitation is particularly relevant in dynamic behavioral paradigms like the operant conditioning and active avoidance tasks used in Project I., where rapid shifts in behavior and reward contingencies occur. Furthermore, the use of CNO raises concerns about potential off-target effects, including its back-metabolism to clozapine (Fazekas et al., 2021). Although we mitigated this by including CNO control groups, future studies would benefit from employing more selective DREADD ligands or alternative chemogenetic approaches to minimize potential confounds. Moreover, a single CNO dose and a fixed time point for behavioral testing might not capture the full spectrum of DREADD effects, which are influenced by CNO pharmacokinetics and the temporal dynamics of intracellular signaling pathways downstream of DREADD activation/inhibition.

The extensive battery of behavioral tests employed in Projects II. and III., while providing a comprehensive assessment of social behavior, anxiety, locomotion, and memory, also introduces potential confounds related to repeated testing and carryover effects. The repeated handling and exposure to different testing environments could induce stress or alter the animals' behavioral responses over time, potentially interacting with the effects of the chemogenetic manipulations. Furthermore, some of the behavioral paradigms (SIT and RIT) had overlapping components (e.g., types of social interactions measured), but were performed under varying anxiogenic conditions (bright vs. dim/dark). While we observed some marginally significant effects that might be attributable to the limitations of our current experimental setup (e.g., marginal significance of total responses during reversal learning phase of the operant conditioning task in Project I., Experiment 1., or even marginal effect of treatment on closed arm latency in Project II.), it is difficult to draw definite conclusions about their biological significance.

Furthermore, the works here presented exclusively utilized male mice for all behavioral experiments. While this controls for hormonal cycle variability inherent in female rodents, it means that the findings may not directly generalize to females, who can exhibit sex-specific differences in many of the behaviors assessed, including social interaction, anxiety, and responses to stress or reward (Becker et al., 2005; Beery & Zucker, 2011). Future research incorporating female subjects is therefore essential.

Finally, another limitation to address is the exclusion of operant conditioning data from Project III. While we initially intended to include operant conditioning to assess the role of DAT-MRR neurons in reward-based learning (given the known association between dopamine and reward), analysis of viral injections revealed substantial off-target staining in most animals. To maintain the rigor and validity of our findings, we decided to exclude these data. This highlights the challenges of achieving precise and consistent viral targeting in deep brain structures like the MRR and underscores the importance of thorough post-hoc verification of injection sites. Moreover, despite our efforts to minimize variability in viral targeting and transduction efficiency by carefully verifying injection sites, variability in the distribution and number of transduced neurons could have contributed to the marginal effects or the lack of significant changes observed in some experiments.

Beyond the technical challenges of viral targeting and DREADD pharmacology, a significant conceptual limitation arises from the potential functional heterogeneity within the targeted neuronal populations of the MRR. While this dissertation focused on GABAergic and dopaminergic neurons within the MRR, the role of other neurotransmitter systems, particularly glutamatergic neurons, should not be overlooked. Notably a large group of VGluT3-expressing glutamatergic neurons projecting to areas like the HC (Szonyi et al., 2016; Varga et al., 2009). Critically, even within a genetically or neurochemically defined cell type, individual neurons may exhibit diverse firing patterns and respond differently to behavioral events or stimuli (Paquelet et al., 2022). Illustrating this point with data from our current lab, recent in vivo electrophysiological recordings combined with optogenetic identification of these MRR VGluT3+ neurons provide a compelling example: distinct subsets of these neurons show activation, while others show inhibition in response to salient stimuli such as an air puff versus a reward (Fig. 31). This observed functional heterogeneity implies that a bulk manipulation

technique, whether chemogenetic as used in this dissertation or optogenetic, likely affects neurons that are performing different computations or encoding opposing information at any given moment. Consequently, the overall behavioral outcome reflects an average effect across a potentially functionally diverse population, complicating the interpretation of how the manipulation relates to specific aspects of behavior and underscoring the need for complementary, higher-resolution techniques like single-unit recording to fully dissect circuit function.

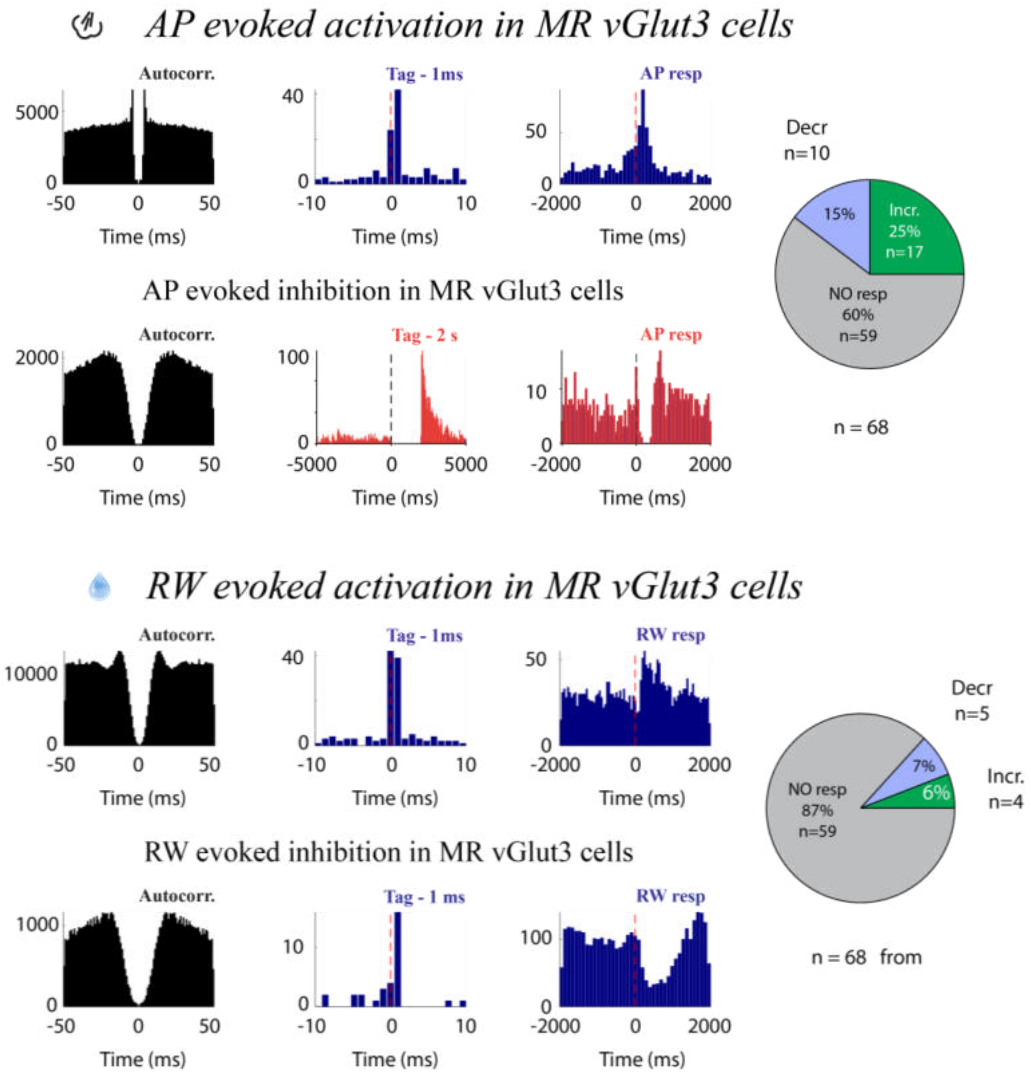

Figure 31 - Examples of air puff (AP, upper block) and reward (RW, lower block) evoked activation and inhibition of VGluT3+ MR cells. Left panel shows autocorrelations of VGluT3+ neurons. Middle panels display the laser stimulus evoked activation response and the PSTH panels at the right show the salient stimuli evoked changes in the firing frequency. Figure from unpublished data.

5.3 Future Directions

Several promising directions for future research emerge from these findings. Electrophysiological recordings (patch-clamp or in vivo silicon probe) will provide valuable insights into the real-time activity dynamics of VGAT-MRR and DAT-MRR neurons during behavior. Furthermore, utilizing optogenetics, with its superior temporal precision, could allow for more nuanced investigations of the causal role of these neurons in specific behavioral events. Additionally, detailed anatomical studies using advanced tracing methods are crucial for mapping the efferent and afferent projections of DAT-MRR neurons. Combining chemogenetic or optogenetic manipulations of multiple neuronal subtypes, including VGluT2-expressing neurons, would enable dissection of their complex interactions and combined influence on behavior. This approach could also help to elucidate the role of the unlabeled neurons observed in Project I. By including additional neuronal markers (e.g., cholinergic markers) or performing single-cell RNA sequencing on MRR tissue, we could gain a more comprehensive understanding of the cellular diversity within this region and the potential contributions of other neuronal subtypes to the observed behaviors. Addressing these unanswered questions will provide a more complete picture of MRR function and its involvement in the neural circuitry underlying complex behaviors relevant to neuropsychiatric disorders. Future research could incorporate additional tests that specifically assess anxiety-state, such as the light-dark box or the elevated zero maze, to provide a more comprehensive evaluation of anxiety-related phenotypes.

A crucial next step will be to extend these investigations to female mice. This is essential as recent evidence indicates significant sexual dimorphism in the MRR, with sex-specific differences reported in the function of its serotonergic and glutamatergic systems, as well as in its anatomical structure (Collins et al., 2023; Cordero et al., 2000; van der Veldt et al., 2025). This underscores that the findings from the present all-male study cannot be assumed to generalize across sexes.

Moreover, further characterization of the neurochemical and electrophysiological properties of different GABAergic neuron subtypes in the MRR (Mihaljevic et al., 2019; Olsen & Sieghart, 2009) would help to refine our understanding of their specific functions. Similarly, further exploring the potential interactions between GABAergic, glutamatergic, and dopaminergic neurons within the MRR is critical.

6 Conclusion

This dissertation investigated the distinct roles of GABAergic and dopaminergic neurons within the MRR in modulating complex behaviors relevant to neuropsychiatric disorders. Project I. demonstrated that chemogenetic manipulation of VGAT-MRR neurons altered reinforcement-based learning, with stimulation increasing response disinhibition and aversive learning. Project II. highlighted these neurons' importance in social behavior: stimulation enhanced social investigation, while inhibition did not produce a clear opposing effect, suggesting an asymmetrical modulation within this circuitry. Inhibition of VGAT-MRR neurons also revealed a mild anxiogenic effect, challenging the traditional view of GABA as solely anxiolytic. Notably, these manipulations did not affect short-term memory. Project II.I confirmed the presence of DAT-MRR neurons in mice and humans, revealing their specific involvement in modulating social behavior. Stimulating these neurons decreased social investigation, while inhibition increased prosocial social interactions, suggesting context-dependent social effects. Importantly, DAT-MRR manipulation did not impact locomotion, anxiety, or memory, indicating involvement of distinct pathways or brain regions compared to traditional dopaminergic circuits.

These findings underscore the complex, context-dependent roles of MRR neurons and the importance of cell-type-specific manipulations for unraveling their contributions. While chemogenetics provided this targeted approach, limitations like temporal resolution and potential off-target effects of CNO should be considered. The observed effects on reinforcement-based learning, social interaction, and anxiety point to the MRR as a critical node in related neural circuits. This research provides a foundation for understanding these behavioral processes and their dysregulation in neuropsychiatric disorders, suggesting the MRR as a potential target for future therapies. Further research incorporating optogenetics, electrophysiology, and detailed circuit mapping is warranted to fully elucidate the underlying mechanisms.

7 Summary

We investigated the roles of GABAergic and dopaminergic neurons in the MRR in modulating behaviors relevant to neuropsychiatric disorders. Using chemogenetics and behavioral testing, we dissected the specific contributions of these neuronal subtypes to reinforcement-based learning, social behavior, anxiety, and memory.

Project I. examined VGAT-MRR neurons in reinforcement-based learning (VGAT-Cre mice, DREADDs). Specific GABAergic neuron manipulation yielded more pronounced behavioral changes than nonspecific MRR stimulation, suggesting roles in response disinhibition and aversive learning.

Project II. focused on VGAT-MRR neurons in social behavior and anxiety (VGAT-Cre mice). Stimulation enhanced social investigation, while inhibition had no effect. A mild anxiogenic effect was observed with inhibition, but no effects on short-term social or working memory were found.

Project III. investigated DAT-MRR neuron function, confirming their presence in mice and humans. Chemogenetic manipulation revealed specific effects on social behavior: stimulation decreased social investigation, while inhibition increased prosocial interactions. No effects were seen on locomotion, anxiety, or memory. IHC confirmed viral expression, neuronal phenotype, and c-Fos activation.

These findings highlight distinct, context-dependent roles for VGAT-MRR and dopaminergic neurons. While chemogenetics allows cell-type specificity, limitations regarding temporal precision and off-target effects warrant consideration. The observed behavioral effects suggest the MRR is a critical node in relevant neural circuits, warranting further investigation using techniques like optogenetics and electrophysiology, combined with detailed anatomical and functional mapping.

8 References

aan het Rot, M., Moskowitz, D. S., Pinard, G., & Young, S. N. (2006). Social behaviour and mood in everyday life: the effects of tryptophan in quarrelsome individuals. *J Psychiatry Neurosci*, *31*(4), 253-262. https://www.ncbi.nlm.nih.gov/pubmed/16862243

https://www.jpn.ca/content/jpn/31/4/253.full.pdf

Abela, A. R., Browne, C. J., Sargin, D., Prevot, T. D., Ji, X. D., Li, Z., Lambe, E. K., & Fletcher, P. J. (2020). Median raphe serotonin neurons promote anxiety-like behavior via inputs to the dorsal hippocampus. *Neuropharmacology*, *168*, 107985. https://doi.org/10.1016/j.neuropharm.2020.107985

Ahmadlou, M., Shirazi, M. Y., Zhang, P., Rogers, I. L. M., Dziubek, J., Young, M., & Hofer, S. B. (2025). A subcortical switchboard for perseverative, exploratory and disengaged states. *Nature*. https://doi.org/10.1038/s41586-025-08672-1

Aliczki, M., Fodor, A., Balogh, Z., Haller, J., & Zelena, D. (2014). The effects of lactation on impulsive behavior in vasopressin-deficient Brattleboro rats. *Horm Behav*, *66*(3), 545-551. https://doi.org/10.1016/j.yhbeh.2014.08.002

Allan, A. M., & Harris, R. A. (1986). gamma-Aminobutyric acid agonists and antagonists alter chloride flux across brain membranes. *Mol Pharmacol*, *29*(5), 497-505. https://www.ncbi.nlm.nih.gov/pubmed/3010078

Amilhon, B., Lepicard, E., Renoir, T., Mongeau, R., Popa, D., Poirel, O., Miot, S., Gras, C., Gardier, A. M., Gallego, J., Hamon, M., Lanfumey, L., Gasnier, B., Giros, B., & El Mestikawy, S. (2010). VGLUT3 (vesicular glutamate transporter type 3) contribution to the regulation of serotonergic transmission and anxiety. *J Neurosci*, *30*(6), 2198-2210. https://doi.org/10.1523/JNEUROSCI.5196-09.2010

Andrade, R., & Haj-Dahmane, S. (2013). Serotonin neuron diversity in the dorsal raphe. *ACS Chem Neurosci*, *4*(1), 22-25. https://doi.org/10.1021/cn300224n

Andrade, T. G., & Graeff, F. G. (2001). Effect of electrolytic and neurotoxic lesions of the median raphe nucleus on anxiety and stress. *Pharmacol Biochem Behav*, *70*(1), 1-14. https://doi.org/10.1016/s0091-3057(01)00512-3

Andrade, T. G., Zangrossi, H., Jr., & Graeff, F. G. (2013). The median raphe nucleus in anxiety revisited. *J Psychopharmacol*, *27*(12), 1107-1115. https://doi.org/10.1177/0269881113499208

Andrews, N., File, S. E., Fernandes, C., Gonzalez, L. E., & Barnes, N. M. (1997). Evidence that the median raphe nucleus--dorsal hippocampal pathway mediates diazepam withdrawal-induced anxiety. *Psychopharmacology (Berl)*, *130*(3), 228-234. https://doi.org/10.1007/s002130050233

Anstey, M. L., Rogers, S. M., Ott, S. R., Burrows, M., & Simpson, S. J. (2009). Serotonin mediates behavioral gregarization underlying swarm formation in desert locusts. *Science*, *323*(5914), 627-630. https://doi.org/10.1126/science.1165939

Arakawa, H., Blanchard, D. C., & Blanchard, R. J. (2007). Colony formation of C57BL/6J mice in visible burrow system: identification of eusocial behaviors in a background strain for genetic animal models of autism. *Behav Brain Res*, *176*(1), 27-39. https://doi.org/10.1016/j.bbr.2006.07.027

Arias, D., Saxena, S., & Verguet, S. (2022). Quantifying the global burden of mental disorders and their economic value. *EClinicalMedicine*, *54*, 101675. https://doi.org/10.1016/j.eclinm.2022.101675

Armbruster, B. N., Li, X., Pausch, M. H., Herlitze, S., & Roth, B. L. (2007). Evolving the lock to fit the key to create a family of G protein-coupled receptors potently activated by an inert ligand. *Proc Natl Acad Sci U S A*, *104*(12), 5163-5168. https://doi.org/10.1073/pnas.0700293104

Asin, K. E., & Fibiger, H. C. (1983). An analysis of neuronal elements within the median nucleus of the raphe that mediate lesion-induced increases in locomotor activity. *Brain Res*, *268*(2), 211-223. https://doi.org/10.1016/0006-8993(83)90487-0

Atasoy, D., Aponte, Y., Su, H. H., & Sternson, S. M. (2008). A FLEX switch targets Channelrhodopsin-2 to multiple cell types for imaging and long-range circuit mapping. *J Neurosci*, *28*(28), 7025-7030. https://doi.org/10.1523/JNEUROSCI.1954-08.2008

Azmitia, E. C., & Segal, M. (1978). An autoradiographic analysis of the differential ascending projections of the dorsal and median raphe nuclei in the rat. *J Comp Neurol*, *179*(3), 641-667. https://doi.org/10.1002/cne.901790311

Backman, C. M., Malik, N., Zhang, Y., Shan, L., Grinberg, A., Hoffer, B. J., Westphal, H., & Tomac, A. C. (2006). Characterization of a mouse strain expressing Cre recombinase from the 3' untranslated region of the dopamine transporter locus. *Genesis*, *44*(8), 383-390. https://doi.org/10.1002/dvg.20228

Bahi, A., & Dreyer, J. L. (2019). Dopamine transporter (DAT) knockdown in the nucleus accumbens improves anxiety- and depression-related behaviors in adult mice. *Behav Brain Res*, *359*, 104-115. https://doi.org/10.1016/j.bbr.2018.10.028

Baik, J. H. (2020). Stress and the dopaminergic reward system. *Exp Mol Med*, *52*(12), 1879-1890. https://doi.org/10.1038/s12276-020-00532-4

Balazsfi, D., Zelena, D., Demeter, K., Miskolczi, C., Varga, Z. K., Nagyvaradi, A., Nyiri, G., Cserep, C., Baranyi, M., Sperlagh, B., & Haller, J. (2018). Differential Roles of the Two Raphe Nuclei in Amiable Social Behavior and Aggression - An Optogenetic Study. *Front Behav Neurosci*, *12*, 163. https://doi.org/10.3389/fnbeh.2018.00163

Balazsfi, D. G., Zelena, D., Farkas, L., Demeter, K., Barna, I., Cserep, C., Takacs, V. T., Nyiri, G., Goloncser, F., Sperlagh, B., Freund, T. F., & Haller, J. (2017). Median raphe region stimulation alone generates remote, but not recent fear memory traces. *PLoS One*, *12*(7), e0181264. https://doi.org/10.1371/journal.pone.0181264

Bariselli, S., Hornberg, H., Prevost-Solie, C., Musardo, S., Hatstatt-Burkle, L., Scheiffele, P., & Bellone, C. (2018). Role of VTA dopamine neurons and neuroligin 3 in sociability traits related to nonfamiliar conspecific interaction. *Nat Commun*, *9*(1), 3173. https://doi.org/10.1038/s41467-018-05382-3

Barnes, N. M., Ahern, G. P., Becamel, C., Bockaert, J., Camilleri, M., Chaumont-Dubel, S., Claeysen, S., Cunningham, K. A., Fone, K. C., Gershon, M., Di Giovanni, G., Goodfellow, N. M., Halberstadt, A. L., Hartley, R. M., Hassaine, G., Herrick-Davis, K., Hovius, R., Lacivita, E., Lambe, E. K., . . . Hoyer, D. (2021). International Union of Basic and Clinical Pharmacology. CX. Classification of Receptors for 5-hydroxytryptamine; Pharmacology and Function. *Pharmacol Rev*, *73*(1), 310-520. https://doi.org/10.1124/pr.118.015552

Barnes, N. M., & Sharp, T. (1999). A review of central 5-HT receptors and their function. *Neuropharmacology*, *38*(8), 1083-1152. https://doi.org/10.1016/s0028-3908(99)00010-6

Beck, S. G., Pan, Y. Z., Akanwa, A. C., & Kirby, L. G. (2004). Median and dorsal raphe neurons are not electrophysiologically identical. *J Neurophysiol*, *91*(2), 994-1005. https://doi.org/10.1152/jn.00744.2003

Becker, J. B., Arnold, A. P., Berkley, K. J., Blaustein, J. D., Eckel, L. A., Hampson, E., Herman, J. P., Marts, S., Sadee, W., Steiner, M., Taylor, J., & Young, E. (2005). Strategies and methods for research on sex differences in brain and behavior. *Endocrinology*, *146*(4), 1650-1673. https://doi.org/10.1210/en.2004-1142

Beery, A. K., & Zucker, I. (2011). Sex bias in neuroscience and biomedical research. *Neurosci Biobehav Rev*, *35*(3), 565-572. https://doi.org/10.1016/j.neubiorev.2010.07.002

Behzadi, G., Kalen, P., Parvopassu, F., & Wiklund, L. (1990). Afferents to the median raphe nucleus of the rat: retrograde cholera toxin and wheat germ conjugated horseradish peroxidase tracing, and selective D-[3H]aspartate labelling of possible excitatory amino acid inputs. *Neuroscience*, *37*(1), 77-100. https://doi.org/10.1016/0306-4522(90)90194-9

Beninger, R. J. (1983). The role of dopamine in locomotor activity and learning. *Brain Res*, *287*(2), 173-196. https://doi.org/10.1016/0165-0173(83)90038-3

Biro, L., Toth, M., Sipos, E., Bruzsik, B., Tulogdi, A., Bendahan, S., Sandi, C., & Haller, J. (2017). Structural and functional alterations in the prefrontal cortex after post-weaning social isolation: relationship with species-typical and deviant aggression. *Brain Struct Funct*, *222*(4), 1861-1875. https://doi.org/10.1007/s00429-016-1312-z

Bland, B. H., Bland, C. E., & MacIver, M. B. (2016). Median raphe stimulation-induced motor inhibition concurrent with suppression of type 1 and type 2 hippocampal theta. *Hippocampus*, *26*(3), 289-300. https://doi.org/10.1002/hipo.22521

Blier, P., de Montigny, C., & Chaput, Y. (1990). A role for the serotonin system in the mechanism of action of antidepressant treatments: preclinical evidence. *J Clin Psychiatry*, *51 Suppl*, 14-20; discussion 21. https://www.ncbi.nlm.nih.gov/pubmed/2157700

Bluthe, R. M., Gheusi, G., & Dantzer, R. (1993). Gonadal steroids influence the involvement of arginine vasopressin in social recognition in mice. *Psychoneuroendocrinology*, *18*(4), 323-335. https://doi.org/10.1016/0306-4530(93)90028-j

Bobillier, P., Pettijean, F., Salvert, D., Ligier, M., & Seguin, S. (1975). Differential projections of the nucleus raphe dorsalis and nucleus raphe centralis as revealed

by autoradiography. *Brain Res*, *85*(2), 205-210. https://doi.org/10.1016/0006-8993(75)90071-2

Bobillier, P., Seguin, S., Petitjean, F., Salvert, D., Touret, M., & Jouvet, M. (1976). The raphe nuclei of the cat brain stem: a topographical atlas of their efferent projections as revealed by autoradiography. *Brain Res*, *113*(3), 449-486. https://doi.org/10.1016/0006-8993(76)90050-0

Botterill, J. J., Khlaifia, A., Walters, B. J., Brimble, M. A., Scharfman, H. E., & Arruda-Carvalho, M. (2021). Off-Target Expression of Cre-Dependent Adeno-Associated Viruses in Wild-Type C57BL/6J Mice. *eNeuro*, *8*(6). https://doi.org/10.1523/ENEURO.0363-21.2021

Boyden, E. S., Zhang, F., Bamberg, E., Nagel, G., & Deisseroth, K. (2005). Millisecond-timescale, genetically targeted optical control of neural activity. *Nat Neurosci*, *8*(9), 1263-1268. https://doi.org/10.1038/nn1525

Brown, P., & Molliver, M. E. (2000). Dual serotonin (5-HT) projections to the nucleus accumbens core and shell: relation of the 5-HT transporter to amphetamine-induced neurotoxicity. *J Neurosci*, *20*(5), 1952-1963. https://doi.org/10.1523/JNEUROSCI.20-05-01952.2000

Burgess, N., Maguire, E. A., & O'Keefe, J. (2002). The human hippocampus and spatial and episodic memory. *Neuron*, *35*(4), 625-641. https://doi.org/10.1016/s0896-6273(02)00830-9

Buzsaki, G. (2002). Theta oscillations in the hippocampus. *Neuron*, *33*(3), 325-340. https://doi.org/10.1016/s0896-6273(02)00586-x

Camats Perna, J., & Engelmann, M. (2017). Recognizing Others: Rodent's Social Memories. *Curr Top Behav Neurosci*, *30*, 25-45. https://doi.org/10.1007/7854_2015_413

Castle, M. J., Turunen, H. T., Vandenberghe, L. H., & Wolfe, J. H. (2016). Controlling AAV Tropism in the Nervous System with Natural and Engineered Capsids. *Methods Mol Biol*, *1382*, 133-149. https://doi.org/10.1007/978-1-4939-3271-9_10

Celada, P., Puig, M. V., & Artigas, F. (2013). Serotonin modulation of cortical neurons and networks. *Front Integr Neurosci*, *7*, 25. https://doi.org/10.3389/fnint.2013.00025

Challis, C., Boulden, J., Veerakumar, A., Espallergues, J., Vassoler, F. M., Pierce, R. C., Beck, S. G., & Berton, O. (2013). Raphe GABAergic neurons mediate the acquisition of avoidance after social defeat. *J Neurosci*, *33*(35), 13978-13988, 13988a. https://doi.org/10.1523/JNEUROSCI.2383-13.2013

Challis, R. C., Ravindra Kumar, S., Chen, X., Goertsen, D., Coughlin, G. M., Hori, A. M., Chuapoco, M. R., Otis, T. S., Miles, T. F., & Gradinaru, V. (2022). Adeno-Associated Virus Toolkit to Target Diverse Brain Cells. *Annu Rev Neurosci*, *45*, 447-469. https://doi.org/10.1146/annurev-neuro-111020-100834

Chaves, T., Török, B., Fazekas, C., Correia, P., Karailiev, P., Oravcova, H., Sipos, E., Biró, L., Haller, J., Jezova, D., & Zelena, D. (2024). The role of the GABAergic cells of the median raphe region in reinforcement-based learning. Scientific reports, 14(1), 1175. https://doi.org/10.1038/s41598-024-51743-y

Chaves, T., Török, B., Fazekas, C. L., Correia, P., Sipos, E., Várkonyi, D., Hellinger, Á., Erk, D., & Zelena, D. (2022). Median raphe region GABAergic neurons contribute to social interest in mouse. Life sciences, 289, 120223. https://doi.org/10.1016/j.lfs.2021.12022

Chaves, T., Török, B., Fazekas, C. L., Correia, P., Sipos, E., Várkonyi, D., Tóth, Z. E., Dóra, F., Dobolyi, Á., & Zelena, D. (2024). The Dopaminergic Cells in the Median Raphe Region Regulate Social Behavior in Male Mice. *International journal of molecular sciences*, *25*(8), 4315. https://doi.org/10.3390/ijms25084315

Chen, P., & Hong, W. (2018). Neural Circuit Mechanisms of Social Behavior. *Neuron*, *98*(1), 16-30. https://doi.org/10.1016/j.neuron.2018.02.026

Chen, X., Choo, H., Huang, X. P., Yang, X., Stone, O., Roth, B. L., & Jin, J. (2015). The first structure-activity relationship studies for designer receptors exclusively activated by designer drugs. *ACS Chem Neurosci*, *6*(3), 476-484. https://doi.org/10.1021/cn500325v

Cho, J. R., Treweek, J. B., Robinson, J. E., Xiao, C., Bremner, L. R., Greenbaum, A., & Gradinaru, V. (2017). Dorsal Raphe Dopamine Neurons Modulate Arousal and Promote Wakefulness by Salient Stimuli. *Neuron*, *94*(6), 1205-1219 e1208. https://doi.org/10.1016/j.neuron.2017.05.020

Ciarleglio, C. M., Resuehr, H. E., & McMahon, D. G. (2011). Interactions of the serotonin and circadian systems: nature and nurture in rhythms and blues. *Neuroscience*, *197*, 8-16. https://doi.org/10.1016/j.neuroscience.2011.09.036

Ciliax, B. J., Heilman, C., Demchyshyn, L. L., Pristupa, Z. B., Ince, E., Hersch, S. M., Niznik, H. B., & Levey, A. I. (1995). The dopamine transporter: immunochemical characterization and localization in brain. *J Neurosci*, *15*(3 Pt 1), 1714-1723. https://doi.org/10.1523/JNEUROSCI.15-03-01714.1995

Collins, S. A., Stinson, H. E., Himes, A., & Ninan, I. (2023). Sex-specific modulation of the medial prefrontal cortex by glutamatergic median raphe neurons. bioRxiv : the preprint server for biology, 2023.08.30.555555. https://doi.org/10.1101/2023.08.30.555555

Commons, K. G. (2016). Ascending serotonin neuron diversity under two umbrellas. *Brain Struct Funct*, *221*(7), 3347-3360. https://doi.org/10.1007/s00429-015-1176-7

Commons, K. G., Connolley, K. R., & Valentino, R. J. (2003). A neurochemically distinct dorsal raphe-limbic circuit with a potential role in affective disorders. *Neuropsychopharmacology*, *28*(2), 206-215. https://doi.org/10.1038/sj.npp.1300045

Congiu, M., Trusel, M., Pistis, M., Mameli, M., & Lecca, S. (2019). Opposite responses to aversive stimuli in lateral habenula neurons. *Eur J Neurosci*, *50*(6), 2921-2930. https://doi.org/10.1111/ejn.14400

Cordero, M. E., Valenzuela, C. Y., Torres, R., & Rodriguez, A. (2000). Sexual dimorphism in number and proportion of neurons in the human median raphe nucleus. Brain research. Developmental brain research, 124(1-2), 43–52. https://doi.org/10.1016/s0165-3806(00)00104-8

Cowen, P. J. (2008). Serotonin and depression: pathophysiological mechanism or marketing myth? *Trends Pharmacol Sci*, *29*(9), 433-436. https://doi.org/10.1016/j.tips.2008.05.004

Creed, M. C., Ntamati, N. R., & Tan, K. R. (2014). VTA GABA neurons modulate specific learning behaviors through the control of dopamine and cholinergic systems. *Front Behav Neurosci*, *8*, 8. https://doi.org/10.3389/fnbeh.2014.00008

Crooks, R., Jackson, J., & Bland, B. H. (2012). Dissociable pathways facilitate theta and non-theta states in the median raphe--septohippocampal circuit. *Hippocampus*, *22*(7), 1567-1576. https://doi.org/10.1002/hipo.20999

Dahlstroem, A., & Fuxe, K. (1964). Evidence for the Existence of Monoamine-Containing Neurons in the Central Nervous System. I. Demonstration of Monoamines in the Cell Bodies of Brain Stem Neurons. *Acta Physiol Scand Suppl*, SUPPL 232:231-255. https://www.ncbi.nlm.nih.gov/pubmed/14229500

de Leon, A. S., & Tadi, P. (2025). Biochemistry, Gamma Aminobutyric Acid. In *StatPearls*. https://www.ncbi.nlm.nih.gov/pubmed/31869147

De Marco, M., & Venneri, A. (2018). Volume and Connectivity of the Ventral Tegmental Area are Linked to Neurocognitive Signatures of Alzheimer's Disease in Humans. *J Alzheimers Dis*, *63*(1), 167-180. https://doi.org/10.3233/JAD-171018

Deisseroth, K. (2015). Optogenetics: 10 years of microbial opsins in neuroscience. *Nat Neurosci*, *18*(9), 1213-1225. https://doi.org/10.1038/nn.4091

den Boer, J. A., Westenberg, H. G., Kamerbeek, W. D., Verhoeven, W. M., & Kahn, R. S. (1987). Effect of serotonin uptake inhibitors in anxiety disorders; a double-blind comparison of clomipramine and fluvoxamine. *Int Clin Psychopharmacol*, *2*(1), 21-32. https://doi.org/10.1097/00004850-198701000-00002

Deverman, B. E., Pravdo, P. L., Simpson, B. P., Kumar, S. R., Chan, K. Y., Banerjee, A., Wu, W. L., Yang, B., Huber, N., Pasca, S. P., & Gradinaru, V. (2016). Cre-dependent selection yields AAV variants for widespread gene transfer to the adult brain. *Nat Biotechnol*, *34*(2), 204-209. https://doi.org/10.1038/nbt.3440

Dolen, G., Darvishzadeh, A., Huang, K. W., & Malenka, R. C. (2013). Social reward requires coordinated activity of nucleus accumbens oxytocin and serotonin. *Nature*, *501*(7466), 179-184. https://doi.org/10.1038/nature12518

Domonkos, A., Nikitidou Ledri, L., Laszlovszky, T., Cserep, C., Borhegyi, Z., Papp, E., Nyiri, G., Freund, T. F., & Varga, V. (2016). Divergent in vivo activity of non-serotonergic and serotonergic VGluT3-neurones in the median raphe region. *J Physiol*, *594*(13), 3775-3790. https://doi.org/10.1113/JP272036

Dos Santos, L., de Andrade, T. G., & Zangrossi, H., Jr. (2005). Serotonergic neurons in the median raphe nucleus regulate inhibitory avoidance but not escape behavior

in the rat elevated T-maze test of anxiety. *Psychopharmacology (Berl)*, *179*(4), 733-741. https://doi.org/10.1007/s00213-004-2120-3

Engelmann, M., Wotjak, C. T., & Landgraf, R. (1995). Social discrimination procedure: an alternative method to investigate juvenile recognition abilities in rats. *Physiol Behav*, *58*(2), 315-321. https://doi.org/10.1016/0031-9384(95)00053-l

Fazekas, C. L., Balazsfi, D., Horvath, H. R., Balogh, Z., Aliczki, M., Puhova, A., Balagova, L., Chmelova, M., Jezova, D., Haller, J., & Zelena, D. (2019). Consequences of VGluT3 deficiency on learning and memory in mice. *Physiol Behav*, *212*, 112688. https://doi.org/10.1016/j.physbeh.2019.112688

Fazekas, C. L., Bellardie, M., Torok, B., Sipos, E., Toth, B., Baranyi, M., Sperlagh, B., Dobos-Kovacs, M., Chaillou, E., & Zelena, D. (2021). Pharmacogenetic excitation of the median raphe region affects social and depressive-like behavior and core body temperature in male mice. *Life Sci*, *286*, 120037. https://doi.org/10.1016/j.lfs.2021.120037

Fazekas, C. L., Torok, B., Correia, P., Chaves, T., Bellardie, M., Sipos, E., Horvath, H. R., Gaszner, B., Dora, F., Dobolyi, A., & Zelena, D. (2024). The Role of Vesicular Glutamate Transporter Type 3 in Social Behavior, with a Focus on the Median Raphe Region. *eNeuro*, *11*(6). https://doi.org/10.1523/ENEURO.0332-23.2024

File, S. E., & Gonzalez, L. E. (1996). Anxiolytic effects in the plus-maze of 5-HT1A-receptor ligands in dorsal raphe and ventral hippocampus. *Pharmacol Biochem Behav*, *54*(1), 123-128. https://doi.org/10.1016/0091-3057(95)02108-6

File, S. E., Hyde, J. R., & MacLeod, N. K. (1979). 5,7-dihydroxytryptamine lesions of dorsal and median raphe nuclei and performance in the social interaction test of anxiety and in a home-cage aggression test. *J Affect Disord*, *1*(2), 115-122. https://doi.org/10.1016/0165-0327(79)90030-2

Garrido Zinn, C., Clairis, N., Silva Cavalcante, L. E., Furini, C. R., de Carvalho Myskiw, J., & Izquierdo, I. (2016). Major neurotransmitter systems in dorsal hippocampus and basolateral amygdala control social recognition memory. *Proc Natl Acad Sci U S A*, *113*(33), E4914-4919. https://doi.org/10.1073/pnas.1609883113

Geyer, M. A., Puerto, A., Menkes, D. B., Segal, D. S., & Mandell, A. J. (1976). Behavioral studies following lesions of the mesolimbic and mesostriatal

serotonergic pathways. *Brain Res*, *106*(2), 257-269. https://doi.org/10.1016/0006-8993(76)91024-6

Giambalvo, C. T., & Snodgrass, S. R. (1978). Effect of p-chloroamphetamine and 5,7-dihydroxytryptamine on rotation and dopamine turnover. *Brain Res*, *149*(2), 453-467. https://doi.org/10.1016/0006-8993(78)90487-0

Gianni, G., & Pasqualetti, M. (2023). Wiring and Volume Transmission: An Overview of the Dual Modality for Serotonin Neurotransmission. *ACS Chem Neurosci*, *14*(23), 4093-4104. https://doi.org/10.1021/acschemneuro.3c00648

Glass, J. D., Grossman, G. H., Farnbauch, L., & DiNardo, L. (2003). Midbrain raphe modulation of nonphotic circadian clock resetting and 5-HT release in the mammalian suprachiasmatic nucleus. *J Neurosci*, *23*(20), 7451-7460. https://doi.org/10.1523/JNEUROSCI.23-20-07451.2003

Gothard, K. M., & Fuglevand, A. J. (2022). The role of the amygdala in processing social and affective touch. *Curr Opin Behav Sci*, *43*, 46-53. https://doi.org/10.1016/j.cobeha.2021.08.004

Graeff, F. G., Guimaraes, F. S., De Andrade, T. G., & Deakin, J. F. (1996). Role of 5-HT in stress, anxiety, and depression. *Pharmacol Biochem Behav*, *54*(1), 129-141. https://doi.org/10.1016/0091-3057(95)02135-3

Gray, J. A. (1982). The Neuropsychology of Anxiety - an Inquiry into the Functions of the Septo-Hippocampal System. *Behavioral and Brain Sciences*, *5*(3), 469-484. https://doi.org/Doi 10.1017/S0140525x00013066

Greenberg, A. S., & Coleman, M. (1976). Depressed 5-hydroxyindole levels associated with hyperactive and aggressive behavior. Relationship to drug response. *Arch Gen Psychiatry*, *33*(3), 331-336. https://doi.org/10.1001/archpsyc.1976.01770030045006

Grimm, V., Gottesfeld, Z., Wassermann, I., & Samuel, D. (1975). The level of GABA in the brain and locomotor behavior. *Pharmacol Biochem Behav*, *3*(4), 573-578. https://doi.org/10.1016/0091-3057(75)90175-6

Grogan, J., Bogacz, R., Tsivos, D., Whone, A., & Coulthard, E. (2015). Dopamine and Consolidation of Episodic Memory: Timing is Everything. *J Cogn Neurosci*, *27*(10), 2035-2050. https://doi.org/10.1162/jocn_a_00840

Guzman-Ramos, K., Moreno-Castilla, P., Castro-Cruz, M., McGaugh, J. L., Martinez-Coria, H., LaFerla, F. M., & Bermudez-Rattoni, F. (2012). Restoration of dopamine release deficits during object recognition memory acquisition attenuates cognitive impairment in a triple transgenic mice model of Alzheimer's disease. *Learn Mem*, *19*(10), 453-460. https://doi.org/10.1101/lm.026070.112

Haery, L., Deverman, B. E., Matho, K. S., Cetin, A., Woodard, K., Cepko, C., Guerin, K. I., Rego, M. A., Ersing, I., Bachle, S. M., Kamens, J., & Fan, M. (2019). Adeno-Associated Virus Technologies and Methods for Targeted Neuronal Manipulation. *Front Neuroanat*, *13*, 93. https://doi.org/10.3389/fnana.2019.00093

Haller, J., Aliczki, M., Pelczer, K. G., Spitzer, K., Balogh, Z., & Kantor, S. (2014). Effects of the fatty acid amide hydrolase inhibitor URB597 on coping behavior under challenging conditions in mice. *Psychopharmacology (Berl)*, *231*(3), 593-601. https://doi.org/10.1007/s00213-013-3273-8

Haller, J., Varga, B., Ledent, C., Barna, I., & Freund, T. F. (2004). Context-dependent effects of CB1 cannabinoid gene disruption on anxiety-like and social behaviour in mice. *Eur J Neurosci*, *19*(7), 1906-1912. https://doi.org/10.1111/j.1460-9568.2004.03293.x

Hashikawa, K., Hashikawa, Y., Lischinsky, J., & Lin, D. (2018). The Neural Mechanisms of Sexually Dimorphic Aggressive Behaviors. *Trends Genet*, *34*(10), 755-776. https://doi.org/10.1016/j.tig.2018.07.001

Heddle, C., & Mazaleyrat, S. L. (2007). Development of a screening platform for directed evolution using the reef coral fluorescent protein ZsGreen as a solubility reporter. *Protein Eng Des Sel*, *20*(7), 327-337. https://doi.org/10.1093/protein/gzm024

Hensler, J. G. (2006). Serotonergic modulation of the limbic system. *Neurosci Biobehav Rev*, *30*(2), 203-214. https://doi.org/10.1016/j.neubiorev.2005.06.007

Higley, J. D., Mehlman, P. T., Poland, R. E., Taub, D. M., Vickers, J., Suomi, S. J., & Linnoila, M. (1996). CSF testosterone and 5-HIAA correlate with different types of aggressive behaviors. *Biol Psychiatry*, *40*(11), 1067-1082. https://doi.org/10.1016/S0006-3223(95)00675-3

Hikosaka, O. (2010). The habenula: from stress evasion to value-based decision-making. *Nat Rev Neurosci*, *11*(7), 503-513. https://doi.org/10.1038/nrn2866

Hornung, J. P. (2003). The human raphe nuclei and the serotonergic system. *J Chem Neuroanat*, *26*(4), 331-343. https://doi.org/10.1016/j.jchemneu.2003.10.002

Huang, W., Ikemoto, S., & Wang, D. V. (2022). Median Raphe Nonserotonergic Neurons Modulate Hippocampal Theta Oscillations. *J Neurosci*, *42*(10), 1987-1998. https://doi.org/10.1523/JNEUROSCI.1536-21.2022

Hynes, T. J., Hrelja, K. M., Hathaway, B. A., Hounjet, C. D., Chernoff, C. S., Ebsary, S. A., Betts, G. D., Russell, B., Ma, L., Kaur, S., & Winstanley, C. A. (2021). Dopamine neurons gate the intersection of cocaine use, decision making, and impulsivity. *Addict Biol*, *26*(6), e13022. https://doi.org/10.1111/adb.13022

Jaber, M., Robinson, S. W., Missale, C., & Caron, M. G. (1996). Dopamine receptors and brain function. *Neuropharmacology*, *35*(11), 1503-1519. https://doi.org/10.1016/s0028-3908(96)00100-1

Jacobs, B. L., & Cohen, A. (1976). Differential behavioral effects of lesions of the median or dorsal raphe nuclei in rats: open field and pain-elicited aggression. *J Comp Physiol Psychol*, *90*(1), 102-108. https://doi.org/10.1037/h0077262

Jacobs, B. L., Wise, W. D., & Taylor, K. M. (1974). Differential behavioral and neurochemical effects following lesions of the dorsal or median raphe nuclei in rats. *Brain Res*, *79*(3), 353-361. https://doi.org/10.1016/0006-8993(74)90433-8

Jahanshahi, A., Steinbusch, H. W., & Temel, Y. (2013). Distribution of dopaminergic cell bodies in the median raphe nucleus of the rat brain. *J Chem Neuroanat*, *53*, 60-63. https://doi.org/10.1016/j.jchemneu.2013.09.002

Jelitai, M., Barth, A. M., Komlosi, F., Freund, T. F., & Varga, V. (2021). Activity and Coupling to Hippocampal Oscillations of Median Raphe GABAergic Cells in Awake Mice. *Front Neural Circuits*, *15*, 784034. https://doi.org/10.3389/fncir.2021.784034

Jones, D. L., Mogenson, G. J., & Wu, M. (1981). Injections of dopaminergic, cholinergic, serotoninergic and GABAergic drugs into the nucleus accumbens: effects on locomotor activity in the rat. *Neuropharmacology*, *20*(1), 29-37. https://doi.org/10.1016/0028-3908(81)90038-1

Kalisch, R., Gerlicher, A. M. V., & Duvarci, S. (2019). A Dopaminergic Basis for Fear Extinction. *Trends Cogn Sci*, *23*(4), 274-277. https://doi.org/10.1016/j.tics.2019.01.013

Kawai, H., Bouchekioua, Y., Nishitani, N., Niitani, K., Izumi, S., Morishita, H., Andoh, C., Nagai, Y., Koda, M., Hagiwara, M., Toda, K., Shirakawa, H., Nagayasu, K., Ohmura, Y., Kondo, M., Kaneda, K., Yoshioka, M., & Kaneko, S. (2022). Median raphe serotonergic neurons projecting to the interpeduncular nucleus control preference and aversion. *Nat Commun*, *13*(1), 7708. https://doi.org/10.1038/s41467-022-35346-7

Kim, E. J., Jacobs, M. W., Ito-Cole, T., & Callaway, E. M. (2016). Improved Monosynaptic Neural Circuit Tracing Using Engineered Rabies Virus Glycoproteins. *Cell Rep*, *15*(4), 692-699. https://doi.org/10.1016/j.celrep.2016.03.067

Kim, S., & Lee, D. (2011). Prefrontal cortex and impulsive decision making. *Biol Psychiatry*, *69*(12), 1140-1146. https://doi.org/10.1016/j.biopsych.2010.07.005

Kim, Y., Venkataraju, K. U., Pradhan, K., Mende, C., Taranda, J., Turaga, S. C., Arganda-Carreras, I., Ng, L., Hawrylycz, M. J., Rockland, K. S., Seung, H. S., & Osten, P. (2015). Mapping social behavior-induced brain activation at cellular resolution in the mouse. *Cell Rep*, *10*(2), 292-305. https://doi.org/10.1016/j.celrep.2014.12.014

Kiser, D., Steemers, B., Branchi, I., & Homberg, J. R. (2012). The reciprocal interaction between serotonin and social behaviour. *Neurosci Biobehav Rev*, *36*(2), 786-798. https://doi.org/10.1016/j.neubiorev.2011.12.009

Kitahama, K., Nagatsu, I., Geffard, M., & Maeda, T. (2000). Distribution of dopamine-immunoreactive fibers in the rat brainstem. *J Chem Neuroanat*, *18*(1-2), 1-9. https://doi.org/10.1016/s0891-0618(99)00047-2

Klein, M. O., Battagello, D. S., Cardoso, A. R., Hauser, D. N., Bittencourt, J. C., & Correa, R. G. (2019). Dopamine: Functions, Signaling, and Association with Neurological Diseases. *Cell Mol Neurobiol*, *39*(1), 31-59. https://doi.org/10.1007/s10571-018-0632-3

Kocabicak, E., Jahanshahi, A., Schonfeld, L., Hescham, S. A., Temel, Y., & Tan, S. (2015). Deep Brain Stimulation of the Rat Subthalamic Nucleus Induced Inhibition of Median Raphe Serotonergic and Dopaminergic Neurotransmission. *Turk Neurosurg*, *25*(5), 721-727. https://doi.org/10.5137/1019-5149.JTN.11230-14.0

Kogan, J. H., Frankland, P. W., & Silva, A. J. (2000). Long-term memory underlying hippocampus-dependent social recognition in mice. *Hippocampus*, *10*(1), 47-56. https://doi.org/10.1002/(SICI)1098-1063(2000)10:1<47::AID-HIPO5>3.0.CO;2-6

Koolhaas, J. M., Coppens, C. M., de Boer, S. F., Buwalda, B., Meerlo, P., & Timmermans, P. J. (2013). The resident-intruder paradigm: a standardized test for aggression, violence and social stress. *J Vis Exp*(77), e4367. https://doi.org/10.3791/4367

Kosofsky, B. E., & Molliver, M. E. (1987). The serotoninergic innervation of cerebral cortex: different classes of axon terminals arise from dorsal and median raphe nuclei. *Synapse*, *1*(2), 153-168. https://doi.org/10.1002/syn.890010204

Kostowski, W., Cxlonkowski, A., Markowdka, L., & Markiewicz, L. (1975). Intraspecific aggressiveness after lesions of midbrain raphe nuclei in rats. *Pharmacology*, *13*(1), 81-85. https://doi.org/10.1159/000136887

Krashes, M. J., Koda, S., Ye, C., Rogan, S. C., Adams, A. C., Cusher, D. S., Maratos-Flier, E., Roth, B. L., & Lowell, B. B. (2011). Rapid, reversible activation of AgRP neurons drives feeding behavior in mice. *J Clin Invest*, *121*(4), 1424-1428. https://doi.org/10.1172/JCI46229

Kroeze, W. K., & Roth, B. L. (1998). The molecular biology of serotonin receptors: therapeutic implications for the interface of mood and psychosis. *Biol Psychiatry*, *44*(11), 1128-1142. https://doi.org/10.1016/s0006-3223(98)00132-2

Kulikova, E. A., & Kulikov, A. V. (2019). Tryptophan hydroxylase 2 as a therapeutic target for psychiatric disorders: focus on animal models. *Expert Opin Ther Targets*, *23*(8), 655-667. https://doi.org/10.1080/14728222.2019.1634691

Lakso, M., Sauer, B., Mosinger, B., Jr., Lee, E. J., Manning, R. W., Yu, S. H., Mulder, K. L., & Westphal, H. (1992). Targeted oncogene activation by site-specific recombination in transgenic mice. *Proc Natl Acad Sci U S A*, *89*(14), 6232-6236. https://doi.org/10.1073/pnas.89.14.6232

Leander, P., Vrang, N., & Moller, M. (1998). Neuronal projections from the mesencephalic raphe nuclear complex to the suprachiasmatic nucleus and the deep pineal gland of the golden hamster (Mesocricetus auratus). *J Comp Neurol*, *399*(1), 73-93. https://www.ncbi.nlm.nih.gov/pubmed/9725702

Liesi, P., Paetau, A., Rechardt, L., & Dahl, D. (1981). Glial uptake of monoamines in primary cultures of rat median raphe nucleus and cerebellum. A combined monoamine fluorescence and glial fibrillary acidic protein immunofluorescence study. *Histochemistry*, *73*(2), 239-250. https://doi.org/10.1007/BF00493024

Liu, Q., Shi, J., Lin, R., & Wen, T. (2017). Dopamine and dopamine receptor D1 associated with decreased social interaction. *Behav Brain Res*, *324*, 51-57. https://doi.org/10.1016/j.bbr.2017.01.045

Lopez-Yrigoyen, M., Fidanza, A., Cassetta, L., Axton, R. A., Taylor, A. H., Meseguer-Ripolles, J., Tsakiridis, A., Wilson, V., Hay, D. C., Pollard, J. W., & Forrester, L. M. (2018). A human iPSC line capable of differentiating into functional macrophages expressing ZsGreen: a tool for the study and in vivo tracking of therapeutic cells. *Philos Trans R Soc Lond B Biol Sci*, *373*(1750). https://doi.org/10.1098/rstb.2017.0219

Lopez Hill, X., Pascovich, C., Urbanavicius, J., Torterolo, P., & Scorza, M. C. (2013). The median raphe nucleus participates in the depressive-like behavior induced by MCH: differences with the dorsal raphe nucleus. *Peptides*, *50*, 96-99. https://doi.org/10.1016/j.peptides.2013.10.002

Loullis, C. C., Felten, D. L., & Shea, P. A. (1979). HPLC determination of biogenic amines in discrete brain areas in food deprived rats. *Pharmacol Biochem Behav*, *11*(1), 89-93. https://doi.org/10.1016/0091-3057(79)90302-2

Luo, S. X., & Huang, E. J. (2016). Dopaminergic Neurons and Brain Reward Pathways: From Neurogenesis to Circuit Assembly. *Am J Pathol*, *186*(3), 478-488. https://doi.org/10.1016/j.ajpath.2015.09.023

Lydiard, R. B. (2003). The role of GABA in anxiety disorders. *J Clin Psychiatry*, *64 Suppl 3*, 21-27. https://www.ncbi.nlm.nih.gov/pubmed/12662130

Mahler, S. V., Vazey, E. M., Beckley, J. T., Keistler, C. R., McGlinchey, E. M., Kaufling, J., Wilson, S. P., Deisseroth, K., Woodward, J. J., & Aston-Jones, G. (2014). Designer receptors show role for ventral pallidum input to ventral tegmental area in cocaine seeking. *Nat Neurosci*, *17*(4), 577-585. https://doi.org/10.1038/nn.3664

Maier, S. F., Grahn, R. E., & Watkins, L. R. (1995). 8-OH-DPAT microinjected in the region of the dorsal raphe nucleus blocks and reverses the enhancement of fear

conditioning and interference with escape produced by exposure to inescapable shock. *Behav Neurosci*, *109*(3), 404-412. https://doi.org/10.1037//0735-7044.109.3.404

Mamounas, L. A., & Molliver, M. E. (1988). Evidence for dual serotonergic projections to neocortex: axons from the dorsal and median raphe nuclei are differentially vulnerable to the neurotoxin p-chloroamphetamine (PCA). *Exp Neurol*, *102*(1), 23-36. https://doi.org/10.1016/0014-4886(88)90075-1

Mamounas, L. A., Mullen, C. A., O'Hearn, E., & Molliver, M. E. (1991). Dual serotoninergic projections to forebrain in the rat: morphologically distinct 5-HT axon terminals exhibit differential vulnerability to neurotoxic amphetamine derivatives. *J Comp Neurol*, *314*(3), 558-586. https://doi.org/10.1002/cne.903140312

Mann, J. J. (2003). Neurobiology of suicidal behaviour. *Nat Rev Neurosci*, *4*(10), 819-828. https://doi.org/10.1038/nrn1220

Maru, E., Takahashi, L. K., & Iwahara, S. (1979). Effects of median raphe nucleus lesions on hippocampal EEG in the freely moving rat. *Brain Res*, *163*(2), 223-234. https://doi.org/10.1016/0006-8993(79)90351-2

Matthews GA, L. M., Brewer EM, Borio M, Miranda R, Keyes LR, Peroni E, Pereira GS, Moraga AL, Palle A, Lee CR, Kimchi EY, Padilla-Coreano N, Wichmann R, Tye KM. (2021). Separable Dorsal Raphe Dopamine Projections Mediate Sociability and Valence. *Research Square*. https://doi.org/doi: 10.21203/rs.3.rs-1025403/v1

Matthews, G. A., Nieh, E. H., Vander Weele, C. M., Halbert, S. A., Pradhan, R. V., Yosafat, A. S., Glober, G. F., Izadmehr, E. M., Thomas, R. E., Lacy, G. D., Wildes, C. P., Ungless, M. A., & Tye, K. M. (2016). Dorsal Raphe Dopamine Neurons Represent the Experience of Social Isolation. *Cell*, *164*(4), 617-631. https://doi.org/10.1016/j.cell.2015.12.040

McNaughton, N., & Gray, J. A. (2002). "The neuropsychology of anxiety" as it really is: A response to O'Mara (2001). *Neuropsychological Rehabilitation*, *12*(4), 363-367. https://doi.org/10.1080/09602010244000129a

Miczek, K. A., Altman, J. L., Appel, J. B., & Boggan, W. O. (1975). Para-chlorophenylalanine, serotonin and killing behavior. *Pharmacol Biochem Behav*, *3*(3), 355-361. https://doi.org/10.1016/0091-3057(75)90043-x

Miczek, K. A., Fish, E. W., & De Bold, J. F. (2003). Neurosteroids, GABAA receptors, and escalated aggressive behavior. *Horm Behav*, *44*(3), 242-257. https://doi.org/10.1016/j.yhbeh.2003.04.002

Mihaljevic, B., Benavides-Piccione, R., Bielza, C., Larranaga, P., & DeFelipe, J. (2019). Classification of GABAergic interneurons by leading neuroscientists. *Sci Data*, *6*(1), 221. https://doi.org/10.1038/s41597-019-0246-8

Molliver, M. E., Berger, U. V., Mamounas, L. A., Molliver, D. C., O'Hearn, E., & Wilson, M. A. (1990). Neurotoxicity of MDMA and related compounds: anatomic studies. *Ann N Y Acad Sci*, *600*, 649-661; discussion 661-644. https://doi.org/10.1111/j.1749-6632.1990.tb16916.x

Morin, L. P. (1999). Serotonin and the regulation of mammalian circadian rhythmicity. *Ann Med*, *31*(1), 12-33. https://doi.org/10.3109/07853899909019259

Morin, L. P. (2013). Neuroanatomy of the extended circadian rhythm system. *Exp Neurol*, *243*, 4-20. https://doi.org/10.1016/j.expneurol.2012.06.026

Moy, S. S., Nadler, J. J., Perez, A., Barbaro, R. P., Johns, J. M., Magnuson, T. R., Piven, J., & Crawley, J. N. (2004). Sociability and preference for social novelty in five inbred strains: an approach to assess autistic-like behavior in mice. *Genes Brain Behav*, *3*(5), 287-302. https://doi.org/10.1111/j.1601-1848.2004.00076.x

Nagai, Y., Miyakawa, N., Takuwa, H., Hori, Y., Oyama, K., Ji, B., Takahashi, M., Huang, X. P., Slocum, S. T., DiBerto, J. F., Xiong, Y., Urushihata, T., Hirabayashi, T., Fujimoto, A., Mimura, K., English, J. G., Liu, J., Inoue, K. I., Kumata, K., . . . Minamimoto, T. (2020). Deschloroclozapine, a potent and selective chemogenetic actuator enables rapid neuronal and behavioral modulations in mice and monkeys. *Nat Neurosci*, *23*(9), 1157-1167. https://doi.org/10.1038/s41593-020-0661-3

Narvaes, R., & Martins de Almeida, R. M. (2014). Aggressive behavior and three neurotransmitters: dopamine, GABA, and serotonin–a review of the last 10 years. *Psychology & Neuroscience*, *7*(4), 601-607. https://doi.org/10.3922/j.psns.2014.4.20

Niederkofler, V., Asher, T. E., & Dymecki, S. M. (2015). Functional Interplay between Dopaminergic and Serotonergic Neuronal Systems during Development and Adulthood. *ACS Chem Neurosci*, *6*(7), 1055-1070. https://doi.org/10.1021/acschemneuro.5b00021

Numasawa, Y., Hattori, T., Ishiai, S., Kobayashi, Z., Kamata, T., Kotera, M., Ishibashi, S., Sanjo, N., Mizusawa, H., & Yokota, T. (2017). Depressive disorder may be associated with raphe nuclei lesions in patients with brainstem infarction. *J Affect Disord*, *213*, 191-198. https://doi.org/10.1016/j.jad.2017.02.005

Nunes-de-Souza, R. L., Canto-de-Souza, A., da-Costa, M., Fornari, R. V., Graeff, F. G., & Pela, I. R. (2000). Anxiety-induced antinociception in mice: effects of systemic and intra-amygdala administration of 8-OH-DPAT and midazolam. *Psychopharmacology (Berl)*, *150*(3), 300-310. https://doi.org/10.1007/s002130000428

Nuss, P. (2015). Anxiety disorders and GABA neurotransmission: a disturbance of modulation. *Neuropsychiatr Dis Treat*, *11*, 165-175. https://doi.org/10.2147/NDT.S58841

Nutt, D. J. (2005). Overview of diagnosis and drug treatments of anxiety disorders. *CNS Spectr*, *10*(1), 49-56. https://doi.org/10.1017/s1092852900009901

Ochi, J., & Shimizu, K. (1978). Occurrence of dopamine-containing neurons in the midbrain raphe nuclei of the rat. *Neurosci Lett*, *8*(4), 317-320. https://doi.org/10.1016/0304-3940(78)90142-8

Ogawa, S. K., Cohen, J. Y., Hwang, D., Uchida, N., & Watabe-Uchida, M. (2014). Organization of monosynaptic inputs to the serotonin and dopamine neuromodulatory systems. *Cell Rep*, *8*(4), 1105-1118. https://doi.org/10.1016/j.celrep.2014.06.042

Ohmura, Y., Tanaka, K. F., Tsunematsu, T., Yamanaka, A., & Yoshioka, M. (2014). Optogenetic activation of serotonergic neurons enhances anxiety-like behaviour in mice. *Int J Neuropsychopharmacol*, *17*(11), 1777-1783. https://doi.org/10.1017/S1461145714000637

Ohmura, Y., Tsutsui-Kimura, I., Sasamori, H., Nebuka, M., Nishitani, N., Tanaka, K. F., Yamanaka, A., & Yoshioka, M. (2020). Different roles of distinct serotonergic pathways in anxiety-like behavior, antidepressant-like, and anti-impulsive effects. *Neuropharmacology*, *167*, 107703. https://doi.org/10.1016/j.neuropharm.2019.107703

Olsen, R. W., & Sieghart, W. (2009). GABA A receptors: subtypes provide diversity of function and pharmacology. *Neuropharmacology*, *56*(1), 141-148. https://doi.org/10.1016/j.neuropharm.2008.07.045

Otrokocsi, L., Kittel, A., & Sperlagh, B. (2017). P2X7 Receptors Drive Spine Synapse Plasticity in the Learned Helplessness Model of Depression. *Int J Neuropsychopharmacol*, *20*(10), 813-822. https://doi.org/10.1093/ijnp/pyx046

Ozcete, O. D., Banerjee, A., & Kaeser, P. S. (2024). Mechanisms of neuromodulatory volume transmission. *Mol Psychiatry*, *29*(11), 3680-3693. https://doi.org/10.1038/s41380-024-02608-3

Papathanou, M., Dumas, S., Pettersson, H., Olson, L., & Wallen-Mackenzie, A. (2019). Off-Target Effects in Transgenic Mice: Characterization of Dopamine Transporter (DAT)-Cre Transgenic Mouse Lines Exposes Multiple Non-Dopaminergic Neuronal Clusters Available for Selective Targeting within Limbic Neurocircuitry. *eNeuro*, *6*(5). https://doi.org/10.1523/ENEURO.0198-19.2019

Paquelet, G. E., Carrion, K., Lacefield, C. O., Zhou, P., Hen, R., & Miller, B. R. (2022). Single-cell activity and network properties of dorsal raphe nucleus serotonin neurons during emotionally salient behaviors. *Neuron*, *110*(16), 2664-2679 e2668. https://doi.org/10.1016/j.neuron.2022.05.015

Paul, E. D., & Lowry, C. A. (2013). Functional topography of serotonergic systems supports the Deakin/Graeff hypothesis of anxiety and affective disorders. *J Psychopharmacol*, *27*(12), 1090-1106. https://doi.org/10.1177/0269881113490328

Paula, J. R., Messias, J. P., Grutter, A. S., Bshary, R., & Soares, M. C. (2015). The role of serotonin in the modulation of cooperative behavior. *Behavioral Ecology*, *26*(4), 1005-1012. https://doi.org/10.1093/beheco/arv039

Paxinos G., W. C. (2007). *The Rat Brain in Stereotaxic Coordinates* (Vol. 6th Edn). Academic Press.

Pezzato, F. A., Can, A., Hoshino, K., Horta Jde, A., Jr., Mijares, M. G., & Gould, T. D. (2015). Effect of lithium on behavioral disinhibition induced by electrolytic lesion of the median raphe nucleus. *Psychopharmacology (Berl)*, *232*(8), 1441-1450. https://doi.org/10.1007/s00213-014-3775-z

Pollak Dorocic, I., Furth, D., Xuan, Y., Johansson, Y., Pozzi, L., Silberberg, G., Carlen, M., & Meletis, K. (2014). A whole-brain atlas of inputs to serotonergic neurons of the dorsal and median raphe nuclei. *Neuron*, *83*(3), 663-678. https://doi.org/10.1016/j.neuron.2014.07.002

Poller, W. C., Madai, V. I., Bernard, R., Laube, G., & Veh, R. W. (2013). A glutamatergic projection from the lateral hypothalamus targets VTA-projecting neurons in the lateral habenula of the rat. *Brain Res*, *1507*, 45-60. https://doi.org/10.1016/j.brainres.2013.01.029

Proulx, C. D., Hikosaka, O., & Malinow, R. (2014). Reward processing by the lateral habenula in normal and depressive behaviors. *Nat Neurosci*, *17*(9), 1146-1152. https://doi.org/10.1038/nn.3779

Pucilowski, O., & Kostowski, W. (1981). Effects of stimulation of the raphe nuclei on muricide behavior in rats. *Pharmacol Biochem Behav*, *14 Suppl 1*, 25-28. https://doi.org/10.1016/s0091-3057(81)80006-8

Pucilowski, O., & Kostowski, W. (1983). Aggressive behaviour and the central serotonergic systems. *Behav Brain Res*, *9*(1), 33-48. https://doi.org/10.1016/0166-4328(83)90012-8

Purves D., A. G. J., Fitzpatrick D., Hall W. C., Lamantia A.-S., White L. E. (2018). Neuroscience. In *Neuroscience* (6 ed., pp. 113-143). Oxford University Press Inc.

Ramos, A. (2008). Animal models of anxiety: do I need multiple tests? *Trends Pharmacol Sci*, *29*(10), 493-498. https://doi.org/10.1016/j.tips.2008.07.005

Roth, B. L. (2016). DREADDs for Neuroscientists. *Neuron*, *89*(4), 683-694. https://doi.org/10.1016/j.neuron.2016.01.040

Saavedra, J. M., Grobecker, H., & Zivin, J. (1976). Catecholamines in the raphe nuclei of the rat. *Brain Res*, *114*(2), 337-345. https://doi.org/10.1016/0006-8993(76)90677-6

Sauer, B., & Henderson, N. (1988). Site-specific DNA recombination in mammalian cells by the Cre recombinase of bacteriophage P1. *Proc Natl Acad Sci U S A*, *85*(14), 5166-5170. https://doi.org/10.1073/pnas.85.14.5166

Schwarz, L. A., Miyamichi, K., Gao, X. J., Beier, K. T., Weissbourd, B., DeLoach, K. E., Ren, J., Ibanes, S., Malenka, R. C., Kremer, E. J., & Luo, L. (2015). Viral-genetic

tracing of the input-output organization of a central noradrenaline circuit. *Nature*, *524*(7563), 88-92. https://doi.org/10.1038/nature14600

Sharma, P., & Pienaar, I. S. (2018). The Use of DREADDs for Dissecting the Contribution of Cellular and Neural Circuit Mechanisms in Models of Neurodegenerative Disease. *Molecular-Genetic and Statistical Techniques for Behavioral and Neural Research*, 565-596. https://doi.org/10.1016/B978-0-12-804078-2.00024-6

Sharma, P., Sharma, B. S., Raval, H., & Singh, V. (2023). Endocytosis of GABA receptor: Signaling in nervous system. *Prog Mol Biol Transl Sci*, *196*, 125-139. https://doi.org/10.1016/bs.pmbts.2022.06.032

Shemesh, Y., & Chen, A. (2023). A paradigm shift in translational psychiatry through rodent neuroethology. *Mol Psychiatry*, *28*(3), 993-1003. https://doi.org/10.1038/s41380-022-01913-z

Shim, I., Stratford, T. R., & Wirtshafter, D. (2014). Dopamine is differentially involved in the locomotor hyperactivity produced by manipulations of opioid, GABA and glutamate receptors in the median raphe nucleus. *Behav Brain Res*, *261*, 65-70. https://doi.org/10.1016/j.bbr.2013.12.004

Shimada, S., Kitayama, S., Walther, D., & Uhl, G. (1992). Dopamine transporter mRNA: dense expression in ventral midbrain neurons. *Brain Res Mol Brain Res*, *13*(4), 359-362. https://doi.org/10.1016/0169-328x(92)90220-6

Smith, K. S., Bucci, D. J., Luikart, B. W., & Mahler, S. V. (2016). DREADDS: Use and application in behavioral neuroscience. *Behav Neurosci*, *130*(2), 137-155. https://doi.org/10.1037/bne0000135

Sos, K. E., Mayer, M. I., Cserep, C., Takacs, F. S., Szonyi, A., Freund, T. F., & Nyiri, G. (2017). Cellular architecture and transmitter phenotypes of neurons of the mouse median raphe region. *Brain Struct Funct*, *222*(1), 287-299. https://doi.org/10.1007/s00429-016-1217-x

Srebro, B., & Lorens, S. A. (1975). Behavioral effects of selective midbrain raphe lesions in the rat. *Brain Res*, *89*(2), 303-325. https://doi.org/10.1016/0006-8993(75)90721-0

Stahl, S. M. (1998). Mechanism of action of serotonin selective reuptake inhibitors. Serotonin receptors and pathways mediate therapeutic effects and side effects. *J Affect Disord*, *51*(3), 215-235. https://doi.org/10.1016/s0165-0327(98)00221-3

Stamp, J. A., & Semba, K. (1995). Extent of colocalization of serotonin and GABA in the neurons of the rat raphe nuclei. *Brain Res*, *677*(1), 39-49. https://doi.org/10.1016/0006-8993(95)00119-b

Sternberg, N., & Hamilton, D. (1981). Bacteriophage P1 site-specific recombination. I. Recombination between loxP sites. *J Mol Biol*, *150*(4), 467-486. https://doi.org/10.1016/0022-2836(81)90375-2

Stiedl, O., Pappa, E., Konradsson-Geuken, A., & Ogren, S. O. (2015). The role of the serotonin receptor subtypes 5-HT1A and 5-HT7 and its interaction in emotional learning and memory. *Front Pharmacol*, *6*, 162. https://doi.org/10.3389/fphar.2015.00162

Stratford, T. R., & Wirtshafter, D. (1990). Ascending dopaminergic projections from the dorsal raphe nucleus in the rat. *Brain Res*, *511*(1), 173-176. https://doi.org/10.1016/0006-8993(90)90239-8

Szonyi, A., Mayer, M. I., Cserep, C., Takacs, V. T., Watanabe, M., Freund, T. F., & Nyiri, G. (2016). The ascending median raphe projections are mainly glutamatergic in the mouse forebrain. *Brain Struct Funct*, *221*(2), 735-751. https://doi.org/10.1007/s00429-014-0935-1

Szonyi, A., Zicho, K., Barth, A. M., Gonczi, R. T., Schlingloff, D., Torok, B., Sipos, E., Major, A., Bardoczi, Z., Sos, K. E., Gulyas, A. I., Varga, V., Zelena, D., Freund, T. F., & Nyiri, G. (2019). Median raphe controls acquisition of negative experience in the mouse. *Science*, *366*(6469). https://doi.org/10.1126/science.aay8746

Takahashi, A., Kwa, C., Debold, J. F., & Miczek, K. A. (2010). GABA(A) receptors in the dorsal raphe nucleus of mice: escalation of aggression after alcohol consumption. *Psychopharmacology (Berl)*, *211*(4), 467-477. https://doi.org/10.1007/s00213-010-1920-x

Takahashi, A., Shimamoto, A., Boyson, C. O., DeBold, J. F., & Miczek, K. A. (2010). GABA(B) receptor modulation of serotonin neurons in the dorsal raphe nucleus

and escalation of aggression in mice. *J Neurosci*, *30*(35), 11771-11780. https://doi.org/10.1523/JNEUROSCI.1814-10.2010

Teissier, A., Chemiakine, A., Inbar, B., Bagchi, S., Ray, R. S., Palmiter, R. D., Dymecki, S. M., Moore, H., & Ansorge, M. S. (2015). Activity of Raphe Serotonergic Neurons Controls Emotional Behaviors. *Cell Rep*, *13*(9), 1965-1976. https://doi.org/10.1016/j.celrep.2015.10.061

Teleanu, R. I., Niculescu, A. G., Roza, E., Vladacenco, O., Grumezescu, A. M., & Teleanu, D. M. (2022). Neurotransmitters-Key Factors in Neurological and Neurodegenerative Disorders of the Central Nervous System. *Int J Mol Sci*, *23*(11). https://doi.org/10.3390/ijms23115954

Thompson, K. J., Khajehali, E., Bradley, S. J., Navarrete, J. S., Huang, X. P., Slocum, S., Jin, J., Liu, J., Xiong, Y., Olsen, R. H. J., Diberto, J. F., Boyt, K. M., Pina, M. M., Pati, D., Molloy, C., Bundgaard, C., Sexton, P. M., Kash, T. L., Krashes, M. J., . . . Tobin, A. B. (2018). DREADD Agonist 21 Is an Effective Agonist for Muscarinic-Based DREADDs in Vitro and in Vivo. *ACS Pharmacol Transl Sci*, *1*(1), 61-72. https://doi.org/10.1021/acsptsci.8b00012

Thor, D. H., & Holloway, W. R. (1982). Social Memory of the Male Laboratory Rat. *Journal of Comparative and Physiological Psychology*, *96*(6), 1000-1006. https://doi.org/Doi 10.1037/0735-7036.96.6.1000

Tiana, M., Acosta-Iborra, B., Hernandez, R., Galiana, C., Fernandez-Moreno, M. A., Jimenez, B., & Del Peso, L. (2020). Metabolic labeling of RNA uncovers the contribution of transcription and decay rates on hypoxia-induced changes in RNA levels. *RNA*, *26*(8), 1006-1022. https://doi.org/10.1261/rna.072611.119

Tork, I. (1990). Anatomy of the serotonergic system. *Ann N Y Acad Sci*, *600*, 9-34; discussion 34-35. https://doi.org/10.1111/j.1749-6632.1990.tb16870.x

Treiman, D. M. (2001). GABAergic mechanisms in epilepsy. *Epilepsia*, *42 Suppl 3*, 8-12. https://doi.org/10.1046/j.1528-1157.2001.042suppl.3008.x

Trulson, M. E., Cannon, M. S., & Raese, J. D. (1985). Identification of dopamine-containing cell bodies in the dorsal and median raphe nuclei of the rat brain using tyrosine hydroxylase immunochemistry. *Brain Res Bull*, *15*(2), 229-234. https://doi.org/10.1016/0361-9230(85)90142-x

Tse, W. S., & Bond, A. J. (2002). Serotonergic intervention affects both social dominance and affiliative behaviour. *Psychopharmacology (Berl)*, *161*(3), 324-330. https://doi.org/10.1007/s00213-002-1049-7

Urban, D. J., & Roth, B. L. (2015). DREADDs (designer receptors exclusively activated by designer drugs): chemogenetic tools with therapeutic utility. *Annu Rev Pharmacol Toxicol*, *55*, 399-417. https://doi.org/10.1146/annurev-pharmtox-010814-124803

van der Veldt, S., Henderson, F., Pizzoccaro, L., Simard, A.-S., Perreault, F., Fortin-Houde, J., Ducharme, G., & Amilhon, B. (2025). Hyperexcitability of female serotonin neurons underlies sex-specific anxiety responses. bioRxiv. https://doi.org/10.1101/2025.08.17.670715

Vardy, E., Robinson, J. E., Li, C., Olsen, R. H. J., DiBerto, J. F., Giguere, P. M., Sassano, F. M., Huang, X. P., Zhu, H., Urban, D. J., White, K. L., Rittiner, J. E., Crowley, N. A., Pleil, K. E., Mazzone, C. M., Mosier, P. D., Song, J., Kash, T. L., Malanga, C. J., . . . Roth, B. L. (2015). A New DREADD Facilitates the Multiplexed Chemogenetic Interrogation of Behavior. *Neuron*, *86*(4), 936-946. https://doi.org/10.1016/j.neuron.2015.03.065

Varga, V., Losonczy, A., Zemelman, B. V., Borhegyi, Z., Nyiri, G., Domonkos, A., Hangya, B., Holderith, N., Magee, J. C., & Freund, T. F. (2009). Fast synaptic subcortical control of hippocampal circuits. *Science*, *326*(5951), 449-453. https://doi.org/10.1126/science.1178307

Varga, V., Sik, A., Freund, T. F., & Kocsis, B. (2002). GABA(B) receptors in the median raphe nucleus: distribution and role in the serotonergic control of hippocampal activity. *Neuroscience*, *109*(1), 119-132. https://doi.org/10.1016/s0306-4522(01)00448-1

Vertes, R. P., Fortin, W. J., & Crane, A. M. (1999). Projections of the median raphe nucleus in the rat. *J Comp Neurol*, *407*(4), 555-582. https://www.ncbi.nlm.nih.gov/pubmed/10235645

Vertes, R. P., & Kocsis, B. (1997). Brainstem-diencephalo-septohippocampal systems controlling the theta rhythm of the hippocampus. *Neuroscience*, *81*(4), 893-926. https://doi.org/10.1016/s0306-4522(97)00239-x

Vertes, R. P., & Linley, S. B. (2007). Comparison of projections of the dorsal and median raphe nuclei, with some functional considerations. *International Congress Series*, *1304*, 98-120. https://doi.org/10.1016/j.ics.2007.07.046

Vertes, R. P., & Martin, G. F. (1988). Autoradiographic analysis of ascending projections from the pontine and mesencephalic reticular formation and the median raphe nucleus in the rat. *J Comp Neurol*, *275*(4), 511-541. https://doi.org/10.1002/cne.902750404

Vinogradova, O. S., Kitchigina, V. F., Kudina, T. A., & Zenchenko, K. I. (1999). Spontaneous activity and sensory responses of hippocampal neurons during persistent theta-rhythm evoked by median raphe nucleus blockade in rabbit. *Neuroscience*, *94*(3), 745-753. https://doi.org/10.1016/s0306-4522(99)00253-5

Vong, L., Ye, C., Yang, Z., Choi, B., Chua, S., Jr., & Lowell, B. B. (2011). Leptin action on GABAergic neurons prevents obesity and reduces inhibitory tone to POMC neurons. *Neuron*, *71*(1), 142-154. https://doi.org/10.1016/j.neuron.2011.05.028

Wang, D. V., Yau, H. J., Broker, C. J., Tsou, J. H., Bonci, A., & Ikemoto, S. (2015). Mesopontine median raphe regulates hippocampal ripple oscillation and memory consolidation. *Nat Neurosci*, *18*(5), 728-735. https://doi.org/10.1038/nn.3998

Wang, J., Sun, J., Gao, L., Zhang, D., Chen, L., & Wu, T. (2023). Common and unique dysconnectivity profiles of dorsal and median raphe in Parkinson's disease. *Hum Brain Mapp*, *44*(3), 1070-1078. https://doi.org/10.1002/hbm.26139

Wang, X., & Zhan, Y. (2022). Regulation of Social Recognition Memory in the Hippocampal Circuits. *Front Neural Circuits*, *16*, 839931. https://doi.org/10.3389/fncir.2022.839931

Wenck, A., Pugieux, C., Turner, M., Dunn, M., Stacy, C., Tiozzo, A., Dunder, E., van Grinsven, E., Khan, R., Sigareva, M., Wang, W. C., Reed, J., Drayton, P., Oliver, D., Trafford, H., Legris, G., Rushton, H., Tayab, S., Launis, K., . . . Melchers, L. (2003). Reef-coral proteins as visual, non-destructive reporters for plant transformation. *Plant Cell Rep*, *22*(4), 244-251. https://doi.org/10.1007/s00299-003-0690-x

Wenger, G. R., Schmidt, C., & Davisson, M. T. (2004). Operant conditioning in the Ts65Dn mouse: learning. *Behav Genet*, *34*(1), 105-119. https://doi.org/10.1023/B:BEGE.0000009480.79586.ee

Wess, J., Nakajima, K., & Jain, S. (2013). Novel designer receptors to probe GPCR signaling and physiology. *Trends Pharmacol Sci*, *34*(7), 385-392. https://doi.org/10.1016/j.tips.2013.04.006

Wirtshafter, D., & Asin, K. E. (1982). Evidence that electrolytic median raphe lesions increase locomotion but not exploration. *Physiol Behav*, *28*(5), 749-754. https://doi.org/10.1016/0031-9384(82)90189-5

Wirtshafter, D., Klitenick, M. A., & Asin, K. E. (1988). Is dopamine involved in the hyperactivity produced by injections of muscimol into the median raphe nucleus? *Pharmacol Biochem Behav*, *30*(3), 577-583. https://doi.org/10.1016/0091-3057(88)90068-8

Wirtshafter, D., Montana, W., & Asin, K. E. (1986). Behavioral and biochemical studies of the substrates of median raphe lesion induced hyperactivity. *Physiol Behav*, *38*(6), 751-759. https://doi.org/10.1016/0031-9384(86)90039-9

Wirtshafter, D., & Sheppard, A. C. (2001). Localization of GABA(B) receptors in midbrain monoamine containing neurons in the rat. *Brain Res Bull*, *56*(1), 1-5. https://doi.org/10.1016/s0361-9230(01)00487-7

Wirtshafter, D., Stratford, T. R., & Pitzer, M. R. (1993). Studies on the behavioral activation produced by stimulation of GABAB receptors in the median raphe nucleus. *Behav Brain Res*, *59*(1-2), 83-93. https://doi.org/10.1016/0166-4328(93)90154-i

Wirtshafter, D., Trifunovic, R., & Krebs, J. C. (1989). Behavioral and biochemical evidence for a functional role of excitatory amino acids in the median raphe nucleus. *Brain Res*, *482*(2), 225-234. https://doi.org/10.1016/0006-8993(89)91185-2

Wong, C. G., Bottiglieri, T., & Snead, O. C., 3rd. (2003). GABA, gamma-hydroxybutyric acid, and neurological disease. *Ann Neurol*, *54 Suppl 6*, S3-12. https://doi.org/10.1002/ana.10696

Xu, Z., Feng, Z., Zhao, M., Sun, Q., Deng, L., Jia, X., Jiang, T., Luo, P., Chen, W., Tudi, A., Yuan, J., Li, X., Gong, H., Luo, Q., & Li, A. (2021). Whole-brain connectivity atlas of glutamatergic and GABAergic neurons in the mouse dorsal and median raphe nuclei. *Elife*, *10*. https://doi.org/10.7554/eLife.65502

Yamamoto, T., & Ueki, S. (1978). Effects of drugs on hyperactivity and aggression induced by raphe lesions in rats. *Pharmacol Biochem Behav*, *9*(6), 821-826. https://doi.org/10.1016/0091-3057(78)90362-3

Yang, M., Weber, M. D., & Crawley, J. N. (2008). Light phase testing of social behaviors: not a problem. *Front Neurosci*, *2*(2), 186-191. https://doi.org/10.3389/neuro.01.029.2008

Zhang, Y., Zhang, P., Shin, M., Chang, Y., Abbott, S. B. G., Venton, B. J., & Zhu, J. J. (2025). Coding principles and mechanisms of serotonergic transmission modes. *Mol Psychiatry*. https://doi.org/10.1038/s41380-025-02930-4

Zhao, L., Yang, Z., Zheng, M., Shi, L., Gu, M., Liu, G., Miao, F., Chang, Y., Huang, F., & Tang, N. (2024). Recombinant adeno-associated virus 8 vector in gene therapy: Opportunities and challenges. *Genes Dis*, *11*(1), 283-293. https://doi.org/10.1016/j.gendis.2023.02.010

9 Bibliography

9.1 Publications related to the thesis

Chaves, T., Török, B., Fazekas, C. L., Correia, P., Sipos, E., Várkonyi, D., Hellinger, Á., Erk, D., & Zelena, D. (2022). Median raphe region GABAergic neurons contribute to social interest in mouse. *Life sciences*, *289*, 120223. https://doi.org/10.1016/j.lfs.2021.120223

Chaves, T., Török, B., Fazekas, C., Correia, P., Karailiev, P., Oravcova, H., Sipos, E., Biró, L., Haller, J., Jezova, D., & Zelena, D. (2024). The role of the GABAergic cells of the median raphe region in reinforcement-based learning. *Scientific reports*, *14*(1), 1175. https://doi.org/10.1038/s41598-024-51743-y

Chaves, T., Török, B., Fazekas, C. L., Correia, P., Sipos, E., Várkonyi, D., Tóth, Z. E., Dóra, F., Dobolyi, Á., & Zelena, D. (2024). The Dopaminergic Cells in the Median Raphe Region Regulate Social Behavior in Male Mice. International journal of molecular sciences, 25(8), 4315. https://doi.org/10.3390/ijms25084315

9.2 Other publications

Fazekas, C. L., Török, B., Correia, P., Chaves, T., Bellardie, M., Sipos, E., Horváth, H. R., Gaszner, B., Dóra, F., Dobolyi, Á., & Zelena, D. (2024). The Role of Vesicular Glutamate Transporter Type 3 in Social Behavior, with a Focus on the Median Raphe Region. eNeuro, 11(6), ENEURO.0332-23.2024. https://doi.org/10.1523/ENEURO.0332-23.2024

Szabó, A., Farkas, S., Fazekas, C., Correia, P., Chaves, T., Sipos, E., Makkai, B., Török, B., & Zelena, D. (2023). Temporal Appearance of Enhanced Innate Anxiety in Alzheimer Model Mice. Biomedicines, 11(2), 262. https://doi.org/10.3390/biomedicines11020262

Fazekas, C. L., Szabó, A., Török, B., Bánrévi, K., Correia, P., Chaves, T., Daumas, S., & Zelena, D. (2022). A New Player in the Hippocampus: A Review on VGlut3+ Neurons and Their Role in the Regulation of Hippocampal Activity and Behaviour. International journal of molecular sciences, 23(2), 790. https://doi.org/10.3390/ijms23020790

Várkonyi, D., Török, B., Sipos, E., Fazekas, C. L., Bánrévi, K., Correia, P., Chaves, T., Farkas, S., Szabó, A., Martínez-Bellver, S., Hangya, B., & Zelena, D. (2022). Investigation of Anxiety- and Depressive-like Symptoms in 4- and 8-Month-Old Male Triple Transgenic Mouse Models of Alzheimer's Disease. International journal of molecular sciences, 23(18), 10816. https://doi.org/10.3390/ijms231810816

Farkas, S., Szabó, A., Török, B., Sólyomvári, C., Fazekas, C. L., Bánrévi, K., Correia, P., Chaves, T., & Zelena, D. (2022). Ovariectomy-induced hormone deprivation aggravates Aβ1-42 deposition in the basolateral amygdala and cholinergic fiber loss in the cortex but not cognitive behavioral symptoms in a triple transgenic mouse model of Alzheimer's disease. Frontiers in endocrinology, 13, 985424. https://doi.org/10.3389/fendo.2022.985424

Chaves, T., Fazekas, C. L., Horváth, K., Correia, P., Szabó, A., Török, B., Bánrévi, K., & Zelena, D. (2021). Stress Adaptation and the Brainstem with Focus on Corticotropin-Releasing Hormone. International journal of molecular sciences, 22(16), 9090. https://doi.org/10.3390/ijms22169090

Krisztina, B., Tiago, C., Pedro, C., Lea, F. C., Adrienn, S., Bibiána, T., & Dóra, Z. (2021). Brain corticotropin releasing hormone and stress reactivity. Интегративная физиология, 2(1), 6-14.

10 Acknowledgments

This PhD journey wasn't just my own; it was made possible by a fantastic group of mentors, colleagues, family, and friends. To everyone who helped me along the way, thank you from the bottom of my heart.

I want to begin by expressing my sincere gratitude to my supervisor, Dr. Dóra Zelena. Your guidance right from my undergraduate days was so important. You patiently taught me the basics of research, and that has been key to my growth. Thanks for always guiding me and giving me the freedom to learn and develop. I'm also incredibly grateful to Csilla Fazekas and Bibiana Török. I learned so much about behavioral science from both of you, and your willingness to share your knowledge meant a lot to me. Csilla, your advice and support, especially when I was deep in writing this thesis, were incredibly helpful and kept me going.

To my wonderful former co-workers in the Behavioral and Stress Studies Group at the Institute of Experimental Medicine (KOKI, Budapest, Hungary) – Krisztina G. Bánrévik, Adrienn Szabó, Pedro Correia, Dorottya Várkonyi, Dogu Erk, Eszter Sipos, and all the other members – thank you. I really appreciate all the help, the good discussions, and the friendly atmosphere you all created. You made the lab a place of both science and laughter (and sometimes, questionable playlists).

I also want to give a big thanks to my current supervisor in the subcortical modulation group, Viktor Varga. Viktor, your profound wisdom and your patience in always being open to explaining things have been truly beneficial to me. My thanks also go out to Márta Jelitai for always being so helpful and supportive, and to everyone in my current group: Gergő Nagy, Rita Nyilas, Kathrin Petrik, Péter Földi, Flóra Vásárhelyi-Nagy, Péter Barthó, and Kolos Németh. I've really appreciated working alongside you all and the positive environment we shared.

On a more personal note, I couldn't have done this without the amazing support of my loved ones. My heartfelt thanks go to my family, and especially to my mother, Maria da Consolação, in Brazil; your love and support, even from so far away, have meant the world to me. Thank you for always believing in me, no matter the distance.

To my incredible girlfriend, Elza, thank you for your endless patience, for understanding the crazy PhD life, and for being such a constant source of strength and support for me. Huge thanks to Elza's family too, for always being so warm and encouraging.

And to my awesome friends back in Brazil – Eliel, Jackson, and Jhonatan. Even with an ocean between us, your support and good vibes made a huge difference. Thanks for keeping my spirits up and cheering me on from so far away.